



Università  
degli Studi  
di Catania



*Università degli Studi di Catania*  
*Scuola Superiore di Catania*

---

*International PhD*  
*In*  
*Energy*  
*XXV cycle*

Title:

***Optimal Sizing of Power Generation Systems Based on  
Multi Criteria Decision Making (MCDM)***

Mohammed F. M. Alsayed

Tutor:  
Prof. Ing. Mario Cacciato

Coordinator of the PhD  
Prof. Ing. Luigi Marletta

December - 2012

## ***Abstract***

Distributed Power Generation Systems (PGSs) are believed to be the most promising sustainable power generation solutions in the near future. It has obvious economic, environmental, and technical benefits increasingly attract governments and policy makers.

Due to the technology development in the last two decades, distributed PGSs based on Hybrid Renewable Energy (HRE) became the most competitive in this field; its environmental friendly characteristics and resources inexhaustibility obviously dominate other alternatives in the long term. Among different configurations, hybrid Photovoltaic - Wind turbine (PV-WT) grid connected PGSs are the most adopted for their energy resources global distribution availability and good performance. However, the system design is characterized by significant complexity; where PV and WT power generation technologies suffer from intermittency and variability respectively. Thus, optimal balance between these two energy sources requires particular attention to achieve a good engineering solution.

Previous literature is full of contributions where suitable approaches were developed for defining optimal size and combination of hybrid PGSs. Different techniques and algorithms have been used to develop these approaches such as Particle Swarm Optimization, genetic algorithm, deterministic methods, iterative techniques, simple numeric algorithms, linear programming, analytic hierarchy processes, and other contributions focusing on optimizing hybrid PGS technical performance; the main goal of such methods is the reduction of system total costs applying economic-environment or techno-economic optimization. All of these approaches focus on optimizing a single criterion, mostly the total costs.

However, in real life applications, different criteria with conflicting performance are important in defining the optimal solution, and these criteria are not in the dimension (unit) or same importance to be directly summed in a single objective function. Moreover, social evaluation criteria are almost missing and not considered in previous approaches.

This research deals with the problem of optimal sizing and combination of PV-WT grid connected PGSs, where a Multi Criteria Decision Making (MCDM) approach has been developed for this purpose. Different MCDM algorithms were considered in building a suitable optimization approach; Weighted Sum Method (WSM), the Technique for Order Preference by Similarity to Ideal Solution method (TOPSIS), Preference Ranking Organization METHod for Enrichment Evaluation (PROMETHEE II), and Multi Objective Genetic Algorithm (MOGA) algorithms have been used.

The developed approach takes into consideration technical, environmental, economic, and social criteria to define the optimal solution. The social criteria were modeled and implemented using fuzzy logic. Moreover, the proposed approach enables the user to include

different importance values to the considered criteria. It has been comprehensively tested with different real solar, wind, and load demand profiles. In addition, its robustness has been proved by implementing input data sensitivity and stochastic uncertainty tests. At the end, it could be assumed as a powerful tool for designers, decision makers, analysts, and policy makers in designing PV-WT PGSs that enhance energy sustainable development.

## *Acknowledgments*

I am grateful to acknowledge and thank all people assisted and encouraged me during my PhD study.

The research activity was carried out under the supervision of Prof. Ing. Mario Cacciato. My deepest gratitude goes to Prof. Cacciato for his patience, encouragement and kind support during the elaboration of my PhD thesis.

I would like to express my thanks to Dott.ssa Maria Sanfilippo and Dott.ssa Bice Immè from Scuola Superiore di Catania for their professional support, which made my living abroad experience comfortable and full of unforgettable memories.

During my PhD study, I met many colleagues and new friends, for whom I have great regards; especially I am obliged to thank Alberto Gaeta, Cristina Isaia, Aysar Yasin, France Marangolo, Lorida Anelli, and Moin Omar.

I wish to extend my warmest thanks to all colleagues and friends from Centro per la Promozione e il Trasferimento dell'innovazione e Informatica (CePTIT) for their encouragement and support. I am obliged to thank Dr. Eng. Giacomo Scelba, my honest mentor who supported me with a great patience.

Finally, as the Arabic quotation says ‘the last part is for the most beloved people’, I owe my loving thanks to my family, my father, mother, amazing wife Ola, my treasure Hamsa, my brother Razi, my sister Rawia and their families. They have lost a lot due to my research abroad. Without their encouragement and understanding it would have been impossible for me to finish this work.

*To the memory of Prof. Alfio Consoli. A great man who taught us how to fight until last breath, without considering giving up among our options.*

## ***Table of Contents***

	Page
Abstract	ii
Acknowledgments	iv
Dedication	v
Table of contents	vi
Nomenclature	ix
Chapter One: Introduction	1
1.1 Introduction	1
1.2 Sustainable energy Development	2
1.3 Problem Definition and Objective	4
1.4 State of the Art	4
1.5 Main Contribution	5
1.6 Thesis Outlines	6
Chapter Two: Power Generation systems	8
2.1 Introduction	8
2.2 Renewable Energy	8
2.3 Advantages vs. Disadvantages of Renewable Energy Sources	9
2.4 Economics of Using Renewable Energy Sources	9
2.5 Electric Power Generation	10
2.6 Distributed Generation	10
2.7 Power generators	11
2.7.1 Photovoltaic Cells	12
2.7.1.1 General Description of Photovoltaic Cell	13
2.7.1.2 Electrical Description of Solar Cell	15
2.7.1.3 Maximum Power Point (MPP)	16
2.7.1.4 Electrical Description of Photovoltaic Modules	17
2.7.2 Wind Turbines	19
2.7.2.1 Influence of Height	19
2.7.2.2 Utilization of Wind Energy	20
2.7.2.3 Types of Wind turbines	21
Chapter Three: Multi Criteria Decision Making	23
3.1 Introduction	23
3.2 Multi Attribute Decision Making	23
3.2.1 Criteria Weighting Methods	24
3.2.1.1 SMARTER	24
3.2.1.2 Entropy	25

3.2.1.3 Combined Weighting Methods	26
3.2.2 Weighted Sum Method (WSM)	26
3.2.3 Technique for Order Preference by Similarity to Ideal Solution (TOPSIS) Method	27
3.2.4 Preference Ranking Organization Method for Enrichment Evaluation (PROMETHEE) Method	29
3.3 Multi Objective Decision Making (MODM)	31
3.3.1 Genetic Algorithm (GA)	31
3.3.2 Representation of Design Variables	32
3.3.3 Representation of Objective Function and Constraints	32
3.3.4 Genetic Operators	33
3.3.5 Multi Objective Optimization	34
Chapter Four: Theory of Fuzzy Set	37
4.1 Introduction	37
4.2 Membership Functions	38
4.3 Fuzzy Process	39
Chapter Five: Optimal combination of PV-WT grid connected PG	41
5.1 Introduction	41
5.2 PV-WT Power Generation Systems Modeling	41
5.2.1 PV System Model	42
5.2.2 Wind Turbine System Model	43
5.3 Analysis Criteria Adopted in the Proposed Approach	43
5.4 Proposed optimization approach to a Case Study	47
5.5 Chapter Conclusion	56
Chapter Six: Multi Attribute Decision Making (MADM) Optimal Sizing and Combination of PV-WT grid connected Systems	57
6.1 Introduction	57
6.2 System Modeling and Design Constraints	57
6.3 Design Criteria	58
6.4 Multi Criteria Decision Analysis — MCDA	63
6.5 Proposed Optimal Sizing PV-WT grid connected PGSs Approach	63
6.6 Results of Applying the Proposed Approach to Case Study	65
6.7 Chapter Conclusions	73
Chapter Seven: Multi Criteria Decision Making (MCDM) Optimal Sizing and Combination of PV-WT grid connected Systems	74
7.1 Introduction	74
7.2 Problem Formulation	75
7.2.1 Analyzed PGS configuration	75

7.2.2 Load Model	76
7.2.3 PV System Mathematical Model	76
7.2.4 Wind Turbine System Mathematical Model	76
7.2.5 Design Criteria Objective Functions	76
7.2.6 Design constraint	77
7.3 Proposed Optimal Sizing of PV-WT grid connected PGSs Approach	77
7.4 Results of Applying the Proposed Approach to Case Studies	79
7.4.1 Scenario Number One.	82
7.4.2 Scenario Number Two.	94
7.5 Chapter Conclusions	106
Conclusions	107
References	108



## *Nomenclature*

### *List of abbreviations*

ASCWM	Additive Synthesis Combination Weighting Method
CF	Capacity Factor
CW	Combined Weighting
DG	Distributed Generation
GA	Genetic Algorithm
HP	Historical Profile
HRE	Hybrid Renewable Energy
LPGP	Loss in Power Generation Possibility
MADM	Multi Attribute Decision Making
MCDM	Multi Criteria Decision Making
MODM	Multi Objective Decision Making
MOGA	Multi Objective Genetic Algorithm
MSCWM	Multiplication Synthesis Combination Weighting Method
MPP	Maximum Power Point
PGS	Power Generation System
PROMETHEE	Preference Ranking Organization Method for Enrichment Evaluation
PV	Photovoltaic
RE	Renewable Energy
SD	Sustainable Development
SED	Sustainable Energy Development
TEL	Total energy Loss
TOPSIS	Technique for Order of Preference by Similarity to Ideal Solution
WMs	Weighting Methods
WSM	Weighted Sum Method
WT	Wind Turbine

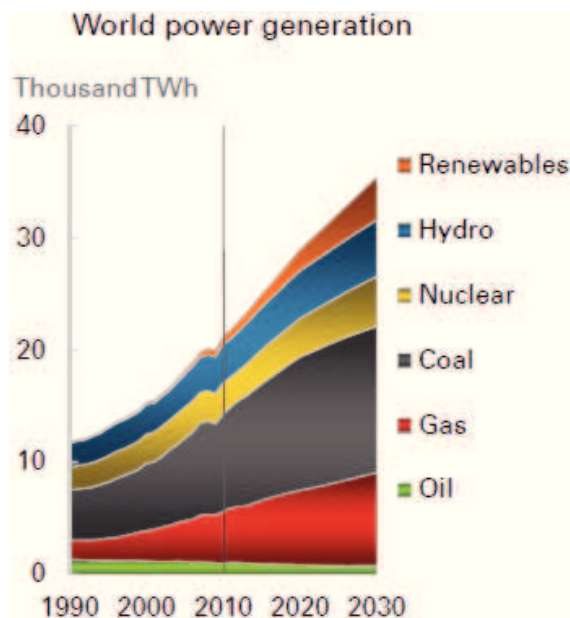
## Chapter One




### *Introduction*

#### 1.1 Introduction

Energy is deeply interrelated with humanity civilization and continuous development. It enters all aspects of humans life, including essential ones for existence such as agricultural, transportation, and medical, and also luxury ones such as tourism. All humans activities are related in somehow with one or more types of energy.

However, according to recent global population growth estimations, current global population is 6.7 billion and predicted to be 9.6 billion in 2050. As a result, energy demands are increasing rapidly, and, power generation is also increasing. Projections till 2030 shows that power generation will almost duplicate, moreover, renewable energy share will increase in order to compensate reduction in oil share. Figure -1.1- shows these projections. [1-3]



Share of fuel 1990-2030 (% shares of world energy use)		1990	2030
	Renewables*	0.4	6.3
	Nuclear	5.6	6.0
	Hydroelectric	6.0	6.8
	Coal	27.3	27.7
	Natural gas	21.8	25.9
	Oil	38.9	27.2

\*Renewable energy includes biofuels

Figure -1.1-: World power generation projections and share by fuel type (1990-2030). [4]

Basically, energy global challenges are clear and well defined, but unfortunately hard to solve. From one side, it comes mainly as a result of modern civilization heavy dependence on fossil fuels resources, where it's estimated that it fulfill about 84% of present global demand, and predicted to be like that till 2030. Moreover, fossil fuels reserves are limited and continually decreasing, where resources/production estimated ratios are 40, 60, and 120 for oil, gas, and coal respectively [2, 3, 5]. Humans living standards are directly affected by energy resources availability and consumption. Developing and undeveloped countries governments are ambitious to raise their living standards similar to developed countries, but if every human on the earth will use energy and resources the same way as in developed countries, at least three more earths are required, but unfortunately, there is only one [6, 7]. In addition to the depletion challenge, fossil fuels prices are fluctuating, unpredictable, and on average increasing due to political, technological, and availability factors [2].

In the last decades, global attention has been focused on energy consumption and its related consequences; environmental problems such as global warming, ozone depletion, and pre-mentioned consumption availability challenges are worldwide concerns for both of governments and scientific communities [1, 3, 6]. This led to unanimity of opinions that good energy management and planning practices are essential for civilization existence and continuous development.

However, managing and planning energy issues has its own privacy due to its high complexity, large number of variables, and in most situations, analysis and planning should be implemented under uncertain conditions [8-11]. To overcome these challenges, effective sustainable energy development (SED) models should be developed to improve the process of analyzing, managing and planning current and future energy systems [6].

## **1.2 Sustainable Energy Development (SED)**

The term sustainable development (SD) began to gain wide acceptance in the late 1980s. It has many definitions; the most common one is "the development that meets the needs of the present without compromising the ability of future generations to meet their own needs". It helps decision makers to think in a more comprehensive way through linking available technology with environment, economy, and society present and future issues [6, 12, 13].

From general point of view, SD aims to manage, plan, and take decisions after analyzing the interactions between environment, economy, and society. In this way, it can be assured that achieved advantages will not be unjustified because of some hidden disadvantages [6]. However, when applying SD on energy systems, some more focus is required, where the goal becomes to manage, plan, and take decisions after analysing the interactions between environment, energy, and socio-economy. In this context, more attention has been given to the energy issues, without losing the interactions between economic and social sectors [7, 11]. Figure -1.2- shows the definition of SD from both of general and energy point views.

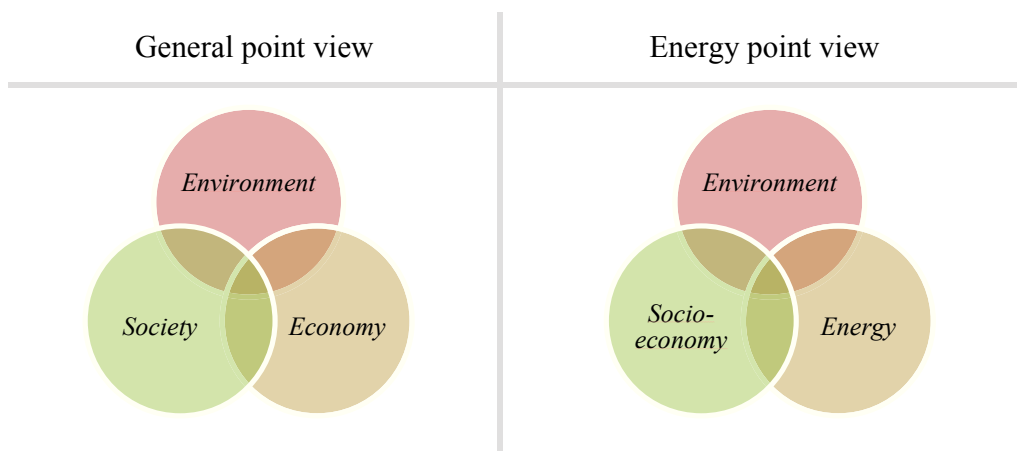


Figure 1.2: SD definitions illustration from general and energy point views

Adopting and applying SD models has many environmental, economic, and social advantages, these advantages are shown per SD sector bases in Table 1.1.

Table 1.1: Advantages of adopting and applying SD models.

Energy	Environment	Socio-economy
<ul style="list-style-type: none"> <li>• Ensure more comprehensive, precise, and easier planning practices [8-10].</li> <li>• Helps in building and assessing policies [1, 14].</li> <li>• Encourage energy efficiency improvement efforts [b].</li> <li>• Encourage global efforts in finding renewable alternatives [5].</li> </ul>	<ul style="list-style-type: none"> <li>• Manage, protect, and repair global environment [6, 7, 11].</li> </ul>	<ul style="list-style-type: none"> <li>• Enhance quality of life.</li> <li>• Avoid future conflicts.</li> <li>• Protect future generation rights.</li> <li>• Enhance national and international level planning.</li> <li>• Enhance international convention and corporation.</li> <li>• Support economic growth [6].</li> </ul>

### **1.3 Problem Definition and Objective**

Renewable energy (RE) sources are the most promising power generation solutions for the future. Among different sources, solar and wind are believed to have the highest potential. Its availability, global distribution, and zero emissions characteristics are attractive for facing global warming and conventional resources depletion challenges. However, solar energy suffers from intermittency while wind energy from variability, and both technologies still has its economic and social challenges.

Recently, grid connected distributed power generation systems based on RE sources became a well known solution. Designing hybrid solar-wind grid connected power generation system requires attention to be given for both of the system size and sources combination. Basically, available designing methods are devoted to optimize system total costs while fulfilling some technical requirements. Although these methods are practical, well defined, and feasible, in most cases, it does not take into consideration environmental and social issues efficiently. So, these methods suffer by not taking SED issues into consideration in the system designing process. In addition, previous methods does not support the analysis of multi conflicting criteria with different importance value, instead, a single global objective function is normally developed, and it aims to find the optimal solution based on minimizing costs or maximizing revenues for this objective function.

### **1.4 State of the Art**

Technical literature is rich in contributions proposing methods able to achieve the optimal sizing of hybrid power generation systems. Different approaches use optimization algorithms such as Particle Swarm Optimization [15-19], genetic algorithms [20-25], mixed integer nonlinear programming [26], hybrid simulated annealing Tabu search algorithm [27], fuzzy logic [28], HOMER optimization software [29], and other contributions focusing on optimizing hybrid PGS costs, maintaining specific technical performance [30-47]. The main goal of the presented methods is the reduction of system costs applying economic-environment and/or techno-economic optimization algorithms. Basically, a single objective function to be minimized is considered; mainly, this function is represented by the total system cost; the other technical-environmental requirements can be included in the optimization sizing process by following two

approaches: the first way is to consider such requirements as additional constraints, while the other approach is based on the conversion of the additional requirements units into costs to ensure unit consistency, and then add such variables to the objective function. The latter methods are not always practical since some of the system variables might not be easily unified into a single unit. Moreover, in both approaches it is assumed that all system requirements/variables have the same importance with respect to the final decision.

More insightful approaches have been presented in [48,49] where, by using a multi objective PSO or genetic algorithms, they are able to simultaneously optimize more objective functions (environment, economic, and technical) in order to find the Pareto set, which is considered the optimal solution set; hence, these methods provide different PV-WT configurations candidate as the best one, leaving the final decision to the decision maker preferences, which might not be a simple task; moreover, also in this case the same importance is assigned to all criteria.

Basically, most of the already proposed solutions could not be able to extract the best combination of PV-WT system, which is best compromise among different nature criteria, yielding to a suboptimal solution.

## **1.5 Main Contribution**

In this thesis, a MCDM approach has been developed for optimizing the size and sources combination of a hybrid solar-wind grid connected power generation system (PGS). In which, the user will be able to optimize the design of PV-WT PGSs taking into consideration multi conflicting criteria in a parallel manner, where each criteria has a specific importance in defining the optimal design. Different technical, environment, economic, and also social criteria (which is missing most of the time in previous contributions) have been considered in the applied case studies, in this way, the designed approach will enhance design process ability to move toward strategic SED solutions. In comparison to previous contributions in the same field, this approach is more realistic where the user can include all crucial evaluation criteria in the design process simultaneously, at the same time, each criteria has a specific weight in the process to meet designers preferences and main goals.

For this purpose, specific analysis strategies have been proposed to check the validity of these algorithms in such an application. Real photovoltaic cells (PV) and wind turbines (WTs)

commercial data have been used in the analysis. Also, different sensitivity analysis strategies have been proposed based on changing the importance factor for analysis criteria in order to define the risk behind implementing a specific solution from different analysis criteria point of view. Moreover, comprehensive stochastic analysis strategy has been proposed, its objective is to allow implementing uncertainty analysis for system main weather input data which are solar radiation profile, wind speed profile, and electric load profile. In this way, a comprehensive SED point of view has been considered by including technical, environmental, economic, and social criteria instead of assuming only economic feasibility.

To sum up, the proposed approach helps designers to have a deep understanding of their systems behavior under specific uncertainty and sensitivity scenarios. It helps to define and estimates advantages and drawbacks of their PGSs under different performance criteria consideration, and different sensitivity and uncertainty scenarios.

## **1.6 Thesis Outlines**

The remaining parts of the thesis have been organized as follows:

- Chapter two explains hybrid renewable energy PGSs with theoretical review regarding PV and WT technology.
- Chapter three provides a comprehensive review of MCDM applied algorithms.
- Chapter four illustrates the theory of fuzzy sets with a summary of previous contributions in evaluating social criteria using fuzzy logic.
- Chapter five presents results of applying TOPSIS-MCDM algorithm to define the optimal combination between PV-WT grid connected PGS, in addition, an analytical strategy for testing the validity of the results has been proposed in this chapter.
- Chapter six shows the results of applying different MCDM algorithms (WSM, TOPSIS, and PROMETHEE II), basically, in this chapter a MCDM based approach strategies to define the optimal size and combination of a PV-WT grid connected PGS has been proposed, in which the user defines nominated alternatives covering all possible PV-WT combinations. It has been tested with different sensitivity analysis scenarios based on changing considered criteria importance values. This approach is powerful and reliable

when assuming relatively small PGS when only PV-WT size and combination are the input variables.

- Chapter seven presents the results of applying a comprehensive MCDM algorithm based on MOGA and PROMETHEE II methods, it has been tested under sensitivity and uncertainty analysis strategies to define the optimal size and combination of a PV-WT grid connected PGS, the main basic idea of this chapter that the developed approach first generates alternatives using Pareto Set principle, then it is analyzed using PROMETHEE II algorithm to define the best solution among Pareto Set. Although this approach requires more calculations than previous one (chapter six), it allows considering more input variables in the optimization process, moreover, it is more reliable when assuming relatively large PGSs.



## Chapter Two

---

# *Power Generation Systems*

## **2.1 Introduction**

As mentioned before, energy is essential for both of an industrialized and developing society continues development. There are many different types of energy such as kinetic and potential, and a lot of examples like mechanical, electrical, thermal (heat), chemical, magnetic, nuclear, biological, tidal, geothermal, and so on. In reality, there are only four generalized interactions (forces between particles) in the universe which are nuclear, electromagnetic, weak, and gravitational. All the different types of energy in the universe can be traced back to one of these four interactions. In this chapter, RE PV-WT grid connected PGSs are described.

## **2.2 Renewable Energy**

RE resources are promising solutions for the future. All RE sources refer in somehow to the sun. Due to facts that the sun is available in the future, it is harmonic with the global environment and does not generate negative impacts, RE generated by the sun helps in enhancing SED.

Solar energy is referred to as *renewable* or *sustainable* energy because it will be available as long as the sun continues to shine. Estimates for the remaining life of the main stage of the sun are another 4 to 5 billion years. The energy from the sun, electromagnetic radiation, is referred to as *insolation*. The other main REs are wind, bio-energy, geothermal, hydro, tides, and waves. Wind energy is derived from the uneven heating of the surface of the earth due to more heat input at the equator with the accompanying transfer of water and thermal energy by evaporation and precipitation.

In contrast, fossil fuels are assumed as stored solar energy from past geological ages. Even though the quantities of oil, natural gas, and coal are large, they are finite, and for the long term of hundreds of years, they are not assumed as renewable or sustainable.

## 2.3 Advantages vs. Disadvantages of Renewable Energy Sources

The advantages of RE sources are: it is sustainable (non-depletable), ubiquitous (found everywhere across the world, in contrast to fossil fuels and minerals), and essentially non-polluting. Moreover, wind turbines and photovoltaic panels do not need water for the generation of electricity, which is not the case of steam plants fired by fossil fuels and nuclear power.

In contrast, disadvantages of RE are intermittency, variability, and low density, which in general results in higher initial cost. For different forms of RE, other disadvantages or perceived problems are visual pollution, odor from biomass, avian and bat mortality with wind turbines, and brine from geothermal energy. Wherever a large renewable facility is to be located, there will be perceived and real problems to the local people. For conventional power plants using fossil fuels, nuclear energy, and even RE, there is the problem of “not in my backyard.”

## 2.4 Economics of Using Renewable Energy Sources

Generally, economic feasibility of PGSs always plays an important role in the decision making process, there is always an argument says “We cannot have a clean environment because it is uneconomical.” The thought here is that RE is not economical in comparison to conventional energy sources, coal, oil, and natural gas.

The different types of economics to consider are pecuniary, social, and physical. *Pecuniary* is what everybody thinks of as economics, *money*. On that note, decisions should be based on life-cycle costs rather than ordinary way of doing business such as low initial costs. Life-cycle costs refer to all costs over the lifetime of the system. *Social economics* are those borne by everybody, and many businesses want the general public to pay for their environmental costs.

Physical economics are energy cost and efficiency of the process. There are fundamental limitations in nature due to physical laws. *Energetics*, which is the energy input versus energy in the final product for any source, should be positive. In other words, from economic feasibility point of view, applying RE solutions is still challenging [50].

## 2.5 Electric Power Generation

The role of electric power generation plants is to supply electric loads with adequate quantities of electric power. Therefore, it can be defined as “The large-scale production of electric power for industrial, residential, and rural use, generally in stationary plants designed for that purpose” [51].

Recently, these systems are shifting from centralized structure which is known as yesterday PGSs to distributed structure which is known as tomorrow PGs. Figure -2.1- below.

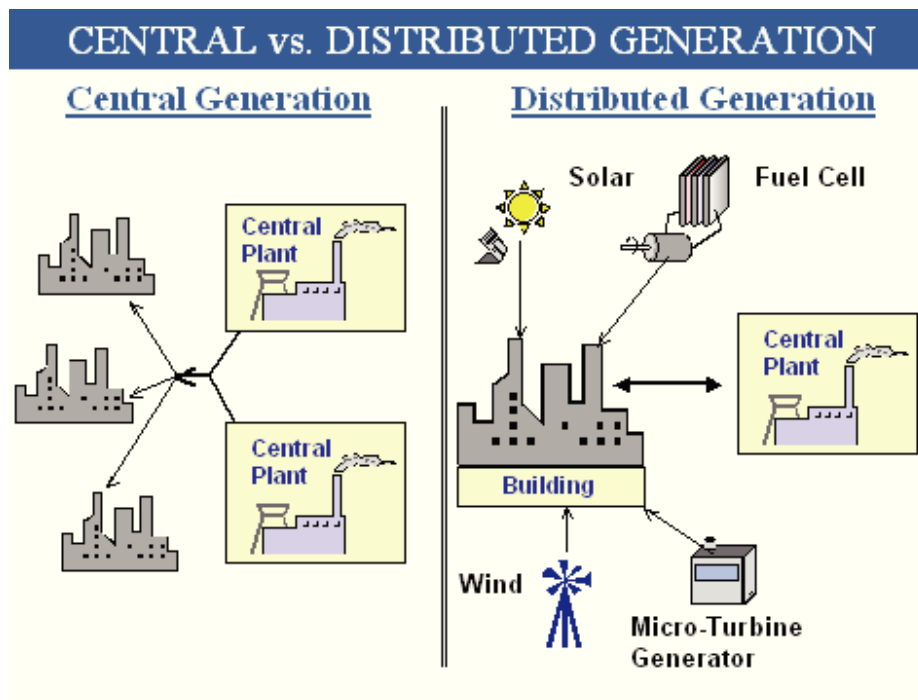


Figure 2.1: Central (yesterday) vs. distributed (tomorrow) power generation systems

## 2.6 Distributed Generation

Power Distributed Generation (DG) plants are defined as “small power plants at or near loads and scattered throughout the service area” [52]. It represents an alternative paradigm of generating electricity (and heat) at or close to the point of demand. The size range of DG technologies varies from few watts to approximately 50 MWe. It includes and not limited to fuel cells, micro-turbines, photovoltaic (PV), wind turbine (WT), and energy storage technologies.

Potential DG advantages include higher efficiency and lower cost through waste heat recovery and avoidance of transmission and distribution, reduced global and local air pollutants, enhanced flexibility of electricity grids, reduced investment uncertainty through modular increments of new capacity, and greater system and infrastructure reliability and security. In contrast, potential DG disadvantages include higher costs through loss of economies of scale, higher local air pollution near areas of population, and increased reliance on natural gas.

Generally, DG has been considered and studied in the context of niche applications, as emergency back-up power, or as limited to a small portion of grid-connected electricity supply. In many countries, the economies of scale of centralized generation, the low price of coal as a fuel for electricity generation, and regulatory barriers or disincentives to on-site generation have prevented the widespread adoption of DG. These institutional barriers have included lack of interconnection protocols, low electricity buy-back tariffs, and little consideration of the system's benefits of distributed resources.

However, changes in the relative economics of centralized versus distributed energy, the increasing use of natural gas, restrictions on new electricity transmission lines, recognition of the environmental benefits, and improved DG control technologies have resulted in the reconsideration of the widespread use of DG.

In this research, PVs and WTs technologies have been assumed. Each one has its strengths and weakness points when using in DG systems. Strengths of PVs and WTs are relatively low maintenance cost, fuel free, and no emissions. Weaknesses for PVs are intermittency and for WTs are power output variability and visual impacts, in addition, both PVs and WTs require high initial cost [53].

## **2.7 Power Generators**

A power generator is defined as “a device for producing electric energy, such as an ordinary electric generator or a magneto-hydrodynamic, thermo-ionic, or thermoelectric power generator” [51]. In this research, two RE power generators have been considered in the analysis, which are PVs and WTs.

## 2.7.1 Photovoltaic Cells

The word ‘photovoltaic’ consists of the two words, photo which stands for the Greek word means light and Volta (Italian physicist, 1745–1827) is the unit of the electrical voltage. Generally, PVs could be assumed as energy converters, it converts energy contained in sunlight directly into electricity [54, 55].

A PV or solar electric system is made up of several PV solar cells. An individual PV cell is usually small and typically producing about 1 or 2 watts of power. To increase PVs output power, they are connected together to form larger units called modules. Then, for larger outputs power, modules can be connected to form even larger units called arrays, which in turn, can be interconnected to produce more power, and so on. In this way, PV systems can be built to meet almost any electric power need, small or large. Figure -2.2- shows a solar cell, PV module, and PV array from left to right.

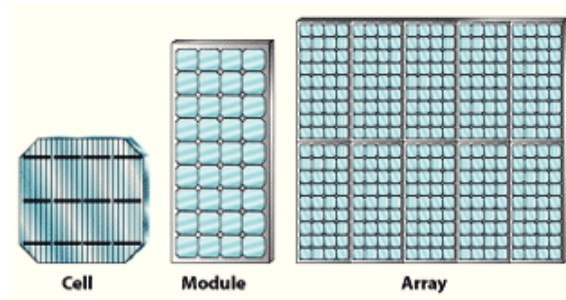


Figure 2.2: Solar cell, PV module, and PV array.

By themselves, modules or arrays do not represent an entire PV system. Normally, systems also include converters, structures to point them toward the sun, batteries ...etc. [56]

Due to many reasons, PV technology is believed to be the most promising RE in the future, extensive research activities over the past 25 years have led to significant cost reduction and efficiency improvement. With the current available technology, efficiency has reached as much as 14% in the most advanced prototype systems. However, although PVs cost has fallen down during recent decades, it is still four to six times the cost of power generation from fossil fuels [54, 55].

Some of the very attractive characteristics of PV technology are [54]:

1. Direct conversion of solar radiation into electricity.
2. No mechanical moving parts and no noise.
3. No high temperatures.
4. No pollution.
5. PV modules are very robust and have a long life.
6. The energy source (sun) is free and inexhaustible.
7. PV energy is a very flexible source; its power ranges from microwatts to megawatts.

Because of the PVs high costs and respectively low efficiency, Successful applications depend mainly on cost reduction of their power-generating systems. It is still not practical for large-scale power generation. With current available technology, about 10 m<sup>2</sup> of PVs are required to generate 1 kW of electricity in bright sunlight. Currently, problems for researchers in PVs technology are making it more reasonable in price and more efficient. Despite of the PV economic challenge, its applications are so wide, it could be small like powering a water pump, medium like meeting appliances and lights demands for isolated or grid connected home/s, where the distance from plants tends to cause a voltage reduction which is costly to fix, or large like meeting the demand of all electrical requirements of a community [54, 56].

### **2.7.1.1 General Description of Photovoltaic Cell**

Basically, PV cell consists of a junction between two thin layers (positive, p, and negative, n) of dissimilar semiconducting materials such as Silicon. When a photon of light strikes the PV surface, it is absorbed by a valance electron of an atom; as a result, the energy of the electron is increased by the amount of energy of the photon. If the energy of the photon is equal to or more than the band gap of the semiconductor, the electron with the excess energy will jump into the conduction band where it can move freely, while if the electron does not have sufficient energy to jump into the conduction band, the excess energy of the electron is converted to excess kinetic energy of the electron, which appears as an increase in temperature. In contrast, if the absorbed photon has more energy than the band gap, the excess energy over the band gap

simply increases the kinetic energy of the electron. It is important to mention that one photon can free up only one electron even if the photon energy is greater than the gap band. Figure -2.3- shows a simple PV module schematic.

As free electrons are generated in the n layer by the photon action, they can either pass through an external circuit or recombine with positive holes in the lateral direction, or move toward the p-type semiconductor. However, the negative charges in the p-type semiconductor at the p-n junction restrict their movement in that direction. If the n-type semiconductor is made extremely thin, the movement of electrons and their probability of recombination within the n-type semiconductor are greatly reduced unless the external circuit is open. In this case the electrons recombine with the holes and an increase in the PV temperature is observed.

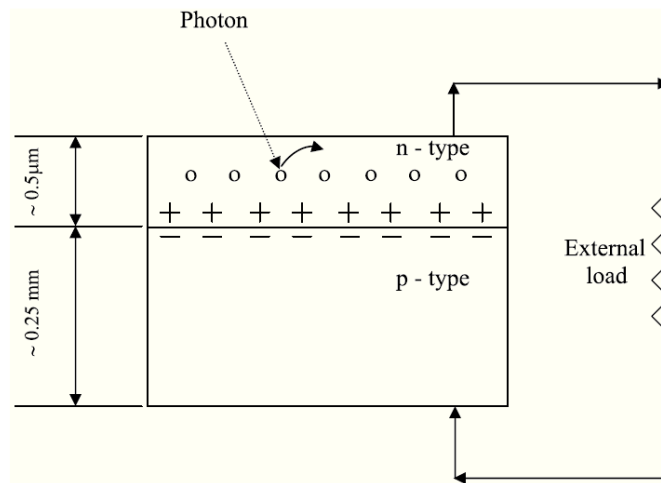


Figure -2.3-: Simple PV cell and resistive load

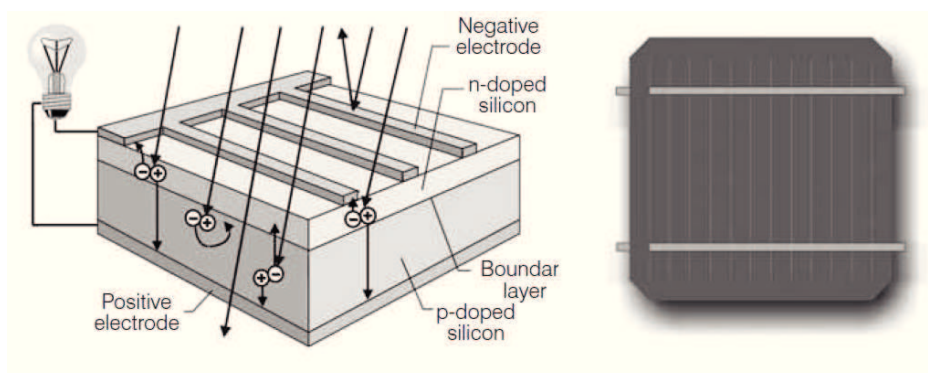


Figure -2.4- Solar cell structure and front view of a Crystalline Silicon solar cell

Although many semiconductor materials can be used in manufacturing PV cells, they are usually manufactured from silicon. Basically, n-type semiconductors are made of crystalline silicon that has been “doped” with tiny quantities of an impurity (usually phosphorous) in such a way that the doped material possesses a surplus of free electrons. Oppositely, p-type semiconductors are also made from crystalline silicon, but they are doped with very small amounts of a different impurity (usually boron) which causes the material to have a deficit of free electrons. Combination of these two dissimilar semiconductors produces an n-p junction, which sets up an electric field in the region of the junction (Fig. 2.4). This set up will cause negatively (positively) charged particles to move in one direction (in the opposite direction) [54].

### 2.7.1.2 Electrical Description of Solar cells

In order to describe a simple equivalent circuit for a PV cell, it is important to define first the solar Irradiation, which is the amount of solar radiation, both direct and diffuse, received at any location. [57] Typically, a non-irradiated solar cell has nearly the same behavior as a diode. Therefore, a simple diode can describe the equivalent circuit.

The equation (2.1) of the cell current  $I$  depends on the cell voltage (here  $V = V_D$  where  $V_D$  is the diode voltage) with the saturation current  $I_S$  and the diode factor  $m$ :

$$I = -I_D = -I_S \left[ \exp\left(\frac{V_D}{mV_T}\right) - 1 \right] \quad (2.1)$$

The thermal voltage  $V_T$  at a temperature of 25°C equals to 25.7 mV. The magnitude of the saturation current  $I_S$  is of the order of  $10^{-10}$  to  $10^{-5}$  A. The diode factor  $m$  of an ideal diode is equal to 1; however, a diode factor between 1 and 5 allows a better description of the solar cell characteristics. A current source connected in parallel to the diode completes the simple equivalent circuit of an irradiated solar cell. The current source generates the *photocurrent*  $I_{ph}$ , which depends on the irradiance  $E$  and the coefficient  $c_0$  is calculated by (2.2):

$$I_{ph} = c_0 E \quad (2.2)$$

Kirchhoff’s first law provides the current–voltage ( $I$ - $V$ ) characteristics of the simple PV cell equivalent circuit illustrated in Figure -2.5- and Figure -2.6- shows the  $I$ - $V$  characteristic curves at different irradiances, and the cell current can be estimated using (2.3):



$$I = I_{Ph} - I_D = I_{Ph} - I_S \left[ \exp\left(\frac{V}{mV_T}\right) - 1 \right] \quad (2.3)$$

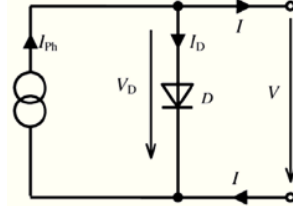


Figure 2.5: Simple equivalent circuit of a solar cell

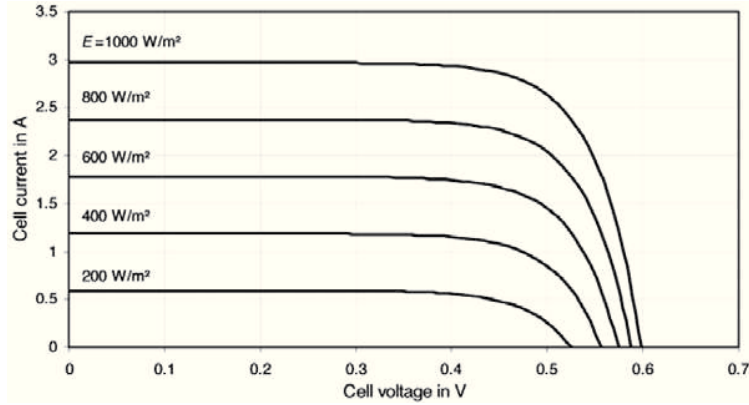


Figure 2.6: Influence of the Irradiance  $E$  on the I-V Characteristics of a Solar Cell

### 2.7.1.3 Maximum Power Point (MPP)

When assuming a short-circuited solar cell, the voltage is equal to zero, in which case, the short circuit current  $I_{SC}$  approximately equals the photocurrent  $I_{Ph}$ , and since the  $I_{Ph}$  is proportional to the irradiance  $E$ , the  $I_{SC}$  also depends on the  $E$  as shown in (2.4):

$$I_{SC} \approx I_{Ph} = c_0 E \quad (2.4)$$

Also, if assuming open circuit analysis, the cell current  $I$  is equal to zero. The cell voltage becomes the *open circuit voltage*  $V_{OC}$ . And it can be calculated using (2.5):

$$V_{OC} = mV_T \ln\left(\frac{I_{SC}}{I_S} + 1\right) \quad (2.5)$$

Since the short circuit current  $I_{SC}$  is proportional to the irradiance  $E$ , the open circuit voltage dependence is:

$$V_{OC} \sim \ln(E)$$

Figure -2.7- shows the  $I-V$  as well as the power-voltage characteristic. It shows that the power curve has a point of maximal power which is called the *maximum power point (MPP)*.

The voltage at the MPP,  $V_{MPP}$ , is less than the open circuit voltage  $V_{OC}$ , and the current  $I_{MPP}$  is lower than the short circuit current  $I_{SC}$ . The MPP current and voltage have the same relation to irradiance and temperature as the short circuit current and open circuit voltage. So, the maximum power  $P_{MPP}$  is calculated using (2.6):

$$P_{MPP} = V_{MPP}I_{MPP} < V_{OC}I_{SC} \quad (2.6)$$

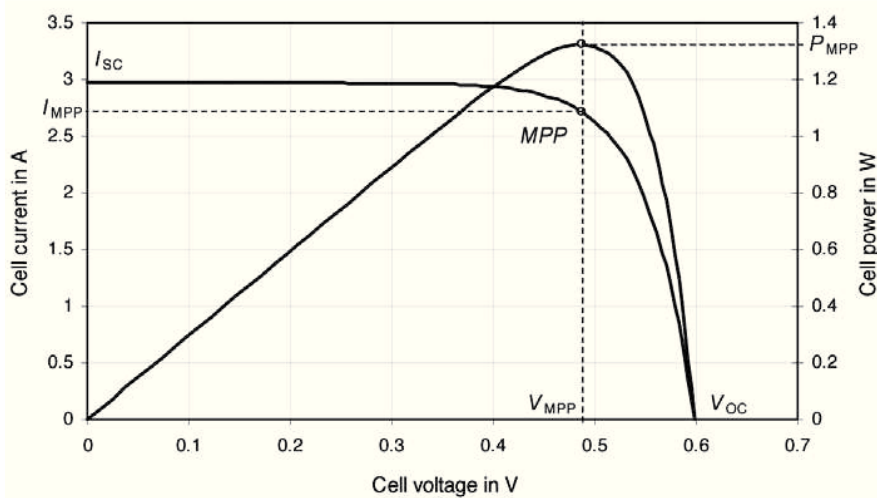
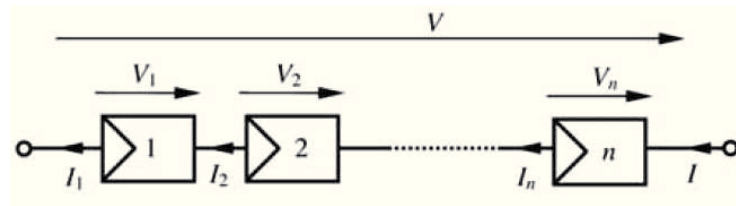


Figure -2.7- I-V and P-V Solar Cell Characteristics with Maximum Power Point (MPP)

### 2.7.1.4 Electrical Description of Photovoltaic Modules

Solar cells are normally not operated individually due to their low voltage. In photovoltaic modules, cells are mostly connected in series. A connection of these modules in series, parallel or series-parallel combinations builds up the photovoltaic system. Figure -2.8- shows structure and electrical description of possible connections.

Series connection



Parallel Connection

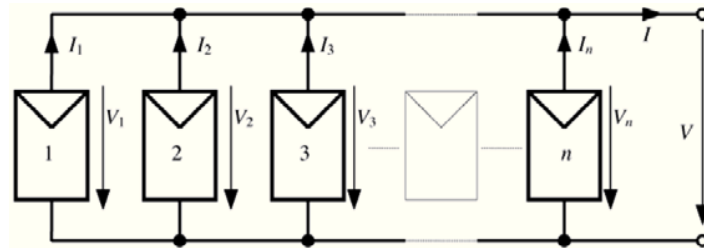


Figure -2.8-: PV cells series and parallel connections

In a series connection, according to Kirchhoff's law, the current  $I_i$  through all cells  $i$  of  $n$  cells is identical. The cell voltages  $V_i$  are added to obtain the overall module voltage  $V$ . Equations (2.7) and (2.8):

$$I = I_1 = I_2 = \dots = I_n \quad (2.7)$$

$$V = \sum_{i=1}^n V_i \quad (2.8)$$

Given that all cells are identical and experience the same irradiance and temperature, the total voltage is given as in (2.9):

$$V = nV_i \quad (2.9)$$

In a parallel connection, solar cells have the same voltage  $V$ , and the cell currents  $I_i$  are added to obtain the overall current  $I$ . Equations (2.10) and (2.11).

$$V = V_1 = V_2 = \dots = V_n \quad (2.10)$$

$$I = \sum_{i=1}^n I_i \quad (2.11)$$

## **2.7.2 Wind Turbines**

Wind energy is an indirect form of solar energy. Solar irradiation causes temperature differences on Earth and these are the origin of winds. Wind can reach much higher power densities than solar irradiance:  $10 \text{ kW/m}^2$  during a violent storm and over  $25 \text{ kW/m}^2$  during a hurricane, compared with the maximum terrestrial solar irradiance of about  $1 \text{ kW/m}^2$ . However, a gentle breeze of  $5 \text{ m/s}$  has a power density of only  $0.075 \text{ kW/m}^2$ .

The history of wind power goes back many centuries. It was used for irrigation systems 3000 years ago. Historical sources give evidence for the use of wind power for grain milling in Afghanistan in the 7th century. In Europe, it became important from the 12<sup>th</sup> century onwards. In contrast to the mechanical wind power systems of past centuries, modern wind converters almost exclusively generate electricity. State of the art wind generators have reached a high technical standard and now have powers exceeding 4 MW. The high growth rate of the wind power industry indicates that it will reach a significant share of the electricity supply within the next two decades.

Some environmental organizations protest against new WT installations. Their reasons are conservation nature or noise protection; indeed, some of their arguments are justifiable. On the other hand, wind power is one of the most important technologies for stopping global warming.

The discussions of wind power make clear that a social consensus about future energy policy does not exist. This leads to give more attention on raising social consensus or searching for compromised solutions with local communities before installing new WTs.

### **2.7.2.1 Influence of Height**

Wind speed is usually recorded at a height of 10 m. The wind speed increases with the height from ground because the wind is slowed down by the roughness of the ground. WTs usually have hub heights of more than 10 m. For the estimation of the wind potential, additional wind speed measurements at other heights are necessary. However, if the type of ground cover is known, the wind speed at other heights can be estimated using (2.12).

$$\frac{v(h_2)}{v(h_1)} = \left(\frac{h_2}{h_1}\right)^a \quad (2.12)$$

Where  $v(h_2)$  is the wind speed at height  $h_2$ ,  $v(h_1)$  is the wind speed at height  $h_1$ ,  $a$  is the power law coefficient which equals 1/7 for open areas.

### 2.7.2.2 Utilization of Wind Energy

The power content of a mass of air with density  $\rho$  (varies with the air pressure and temperature) flows through an area  $A$  with speed  $v$  is calculated by (2.13):

$$P = \frac{1}{2} \rho A v^3 \quad (2.13)$$

For the utilization of wind power, a technical system such as a WT should take as much power from the wind as possible. This turbine slows the wind from speed  $v_1$  to speed  $v_2$  and uses the corresponding power difference. In other words, the turbine has an efficiency which called in this case the coefficient of performance  $C_p$ . In 1926, Betz has calculated the maximum  $C_p$  possible, which is called the ideal or Betz power coefficient and equals to 0.593. Practically, real wind generators do not reach this theoretical optimum; however, good systems have power coefficients  $C_p$  between 0.4 and 0.5 [55, 56]. Therefore, power output from wind turbines can be estimated by (2.14):

$$P = \frac{1}{2} \rho A v^3 C_p \quad (2.14)$$

It is usually considered that there are four distinct wind speed regions of operation as shown in figure 2.9, these four regions affects the power output from the WT, hence, WT power output can be estimated using 2.15:

$$P_{WT.out} = \begin{cases} 0 & v(t) < v_{ci} \\ P_{WT.max} & v_{ci} \leq v(t) < v_{ra} \\ P_r & v_{ra} \leq v(t) \leq v_{co} \\ 0 & v_{co} < v(t) \end{cases} \quad (2.15)$$

where  $P_{WT.max}$  and  $P_{WT.out}$  are the maximum available output WT power and the actual output power respectively.  $v_{ci}$ ,  $v_{ra}$ , and  $v_{co}$  are, respectively, the cut in, the rated, and the cut out wind speed [58].

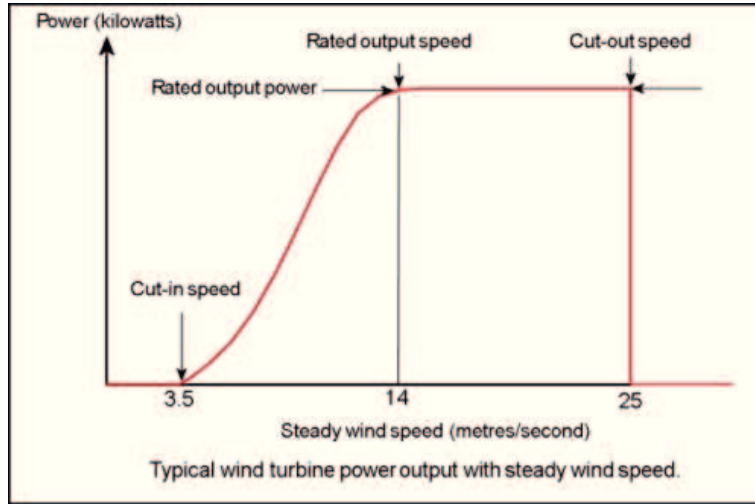


Figure 2.9: Wind turbine operating regions and power performance.

### 2.7.2.3 Types of Wind Turbines

WTs are mainly classified into two types, vertical and horizontal axis as shown in figure - 2.10- below.

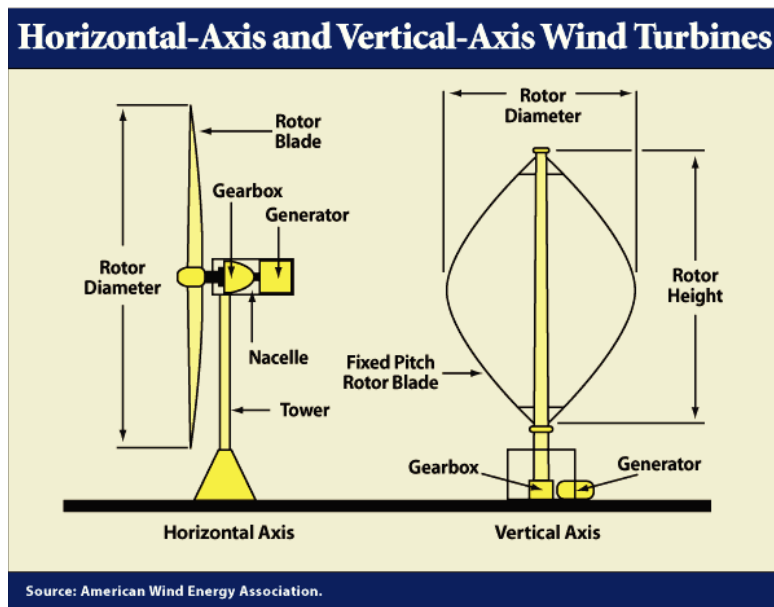


Figure -2.10- WTs main classifications on axis type bases

Advantages of vertical axis WT are simple design that includes the possibility of housing mechanical and electrical components, gearbox and generator at ground level, and there is no

yaw system. This is countered by disadvantages such as its low tip-speed ratio, its inability to self-start and not being able to control power output or speed by pitching the rotor blades.

However, horizontal axis wind turbines still have its undisputed superiority to date. In propeller designs, rotor speed and power output can be controlled by pitching the rotor blades about their longitudinal axis (blade pitch control). Moreover, rotor blade pitching is the most effective protection against over speed and extreme wind speeds, especially in large WTs. In addition, the rotor blade shape can be aerodynamically optimized [55, 56].

## Chapter Three

---

### *Multi Criteria Decision Making*

#### **3.1 Introduction**

Energy planning using multi-criteria analysis has attracted the attention of decision makers for a long time. It can provide solutions to complex energy management problems. Multi-criteria decision making (MCDM) methods deal with the process of making decisions in the presence of multiple objectives. A decision-maker is required to choose among multiple criteria. The objectives are usually conflicting and therefore, the solution is highly dependent on the preferences of the decision-maker and must be a compromise.

MCDM is a well known class of operations research. This class is further divided into multi objective decision making (MODM) and multi-attribute decision making (MADM).

These methodologies share common characteristics of conflict among criteria, incomparable units, and difficulties in selection of alternatives. In MODM, the alternatives are not predetermined but instead a set of objective functions is optimized subject to a set of constraints. The most satisfactory and efficient solution is sought. In this identified efficient solution it is not possible to improve the performance of any objective without degrading the performance of at least one other objective. However, in MADM a small number of alternatives are to be evaluated against a set of attributes which are often hard to quantify. The best alternative is usually selected by making comparisons between alternatives with respect to each attribute [59].

#### **3.2 Multi-attribute Decision Making**

MADM methods perform the comparison of two or more *alternatives* against two or more criteria, where each criterion has a defined importance (weight) in the final decision. The problem can be formulated as in (3.1):



$$\begin{aligned}
\text{Criteria} &= [C_1 \quad C_2 \quad \dots \quad C_n] \\
\text{Weights} &= [w_1 \quad w_2 \quad \dots \quad w_n] \\
X &= \begin{matrix} A_1 \\ A_2 \\ \vdots \\ A_m \end{matrix} = \begin{bmatrix} X_{11} & X_{12} & \dots & X_{1n} \\ X_{21} & X_{22} & \dots & X_{2n} \\ \vdots & \vdots & \ddots & \vdots \\ X_{m1} & X_{m2} & \dots & X_{mn} \end{bmatrix}_{m \times n}
\end{aligned} \tag{3.1}$$

where  $A_i$  are the *alternatives*,  $X$  is the performance matrix with  $X_{ij}$  expressing the performance of the  $i$ -th *alternative* against the  $j$ -th criteria,  $n$  is the number of criteria and  $m$  is the number of *alternatives*. In this research,  $X_{ij}$  are determined through simulation of the different *alternatives*.

Basically, MADM methods are divided into three categories [59]: elementary methods, methods in unique synthesizing criteria and outranking methods. In this research, one algorithm from each category has been applied. The weighted Sum Method (WSM) from the elementary methods, the The Technique for Order of Preference by Similarity to Ideal Solution (TOPSIS) from the unique synthesizing criteria methods, and the Preference Ranking Organization Method for Enrichment Evaluation (PROMETHEE) from the outranking methods have been considered in this research.

### 3.2.1 Criteria Weighting Methods (WMs)

One of the most important characteristics of MCDM algorithms that it is possible to define specific weight for each criteria to distinguish the importance between analysis criteria.

*WMs* are classified into subjective, objective, and Combined Weighting (CW) methods [59]. In this study, an additional synthesis combination of SMARTER [60] (subjective) and Entropy [61] (objective) weighting methods is applied to increase the credibility of the criteria weights.

#### 3.2.1.1 SMARTER

SMARTER is a Multi-Attribute Choice scoring model technique depending on the judgment of decision makers, by which a consultant or group of consultants define the criteria importance according to their experience and preference. Each consultant associates a position to the considered criteria, thus defining a criteria ranking (1 is associated to the most important

criterion). Then, all consultants scores are summed up, and in the resultant criteria ranking, the lowest score (indicated with 1) means the most important criteria, while the least important criterion is indicated with n, where n is the number of criteria.

According to such a ranking, the weight of the criterion ranked to be *i-th* is calculated using (3.1):

$$w_{is} = \frac{1}{n} \sum_{k=i}^n \frac{1}{k} \quad (3.1)$$

where *w<sub>is</sub>* is the criterion weight, and *k* is the final score of each criterion according to the consultants judgment.

### 3.2.1.2 Entropy

Entropy is a measure of uncertainty in the information formulated using probability theory. It indicates that a broad distribution represents more uncertainty than does a sharply peaked one. It is an objective weighting method depending only on the decision matrix, where the importance of each criterion is related to the variation between alternative values. Entropy method can be applied using the following steps:

- i. Calculation of the index *P<sub>ij</sub>* using (3.2), where *i* = 1, 2...*m*, and *j* = 1, 2...*n*:

$$P_{ij} = \frac{X_{ij}}{\sum_{i=1}^m X_{ij}} \quad (3.2)$$

*X<sub>ij</sub>* being the performance of the *i*th alternative with respect to the *j*th criteria.

- ii. Calculation of the output entropy *E<sub>j</sub>* of index *j* using (3.3)-(3.4):

$$E_j = -k \sum_{i=1}^m P_{ij} \ln(P_{ij}) \quad (3.3)$$

$$k = \frac{1}{\ln(m)} \quad (3.4)$$

Note that:  $0 \leq P_{ij} \leq 1$  and  $m > 1$  then

$$0 \leq - \sum_{i=1}^m P_{ij} \ln(P_{ij}) \leq \ln(m)$$

Hence  $0 \leq E_j \leq 1$ ,  $j = 1, 2, \dots, n$ .

- iii. Calculation of the entropy variation *d<sub>j</sub>* for the index *j* using (3.5):

$$d_j = 1 - E_j \quad (3.5)$$

Calculation of the Entropy weight  $w_{ei}$  of index  $j$  using (3.6):

$$w_{ei} = \frac{d_j}{\sum_{j=1}^n d_j} \quad (3.6)$$

Where  $0 \leq w_{ei} \leq 1$  and  $\sum w_{ei} = 1$ .

### 3.2.1.3 Combined weighting methods

The two aforementioned weighting methods (SMARTER and Entropy) can be suitable combined by using two different approaches: the Additive Synthesis Combination Weighting Method ASCWM and the Multiplication Synthesis Combination Weighting Method MSCWM.

ASCWM is calculated using (3.7):

$$ASCWM = (q \times w_j^s) + ((1 - q) \times w_j^b) \quad (3.7)$$

For calculating MSCWM, equation (3.8) is used:

$$MSCWM = \frac{w_j^s \cdot w_j^b}{\sum_{j=1}^n w_j^s \cdot w_j^b} \quad (3.8)$$

Where  $w_j^s$  and  $w_j^b$  are the subjective and objective weights for criteria  $j$  respectively,  $q$  ( $0 < q < 1$ ) is a linear combination coefficient defining the importance of the subjective weights in determining the ASCWM combined weights [59].

### 3.2.2 Weighted Sum Method (WSM)

WSM is the most commonly used MADM method in energy systems, it has been considered in different energy engineering sustainable development applications previous contributions [62-65]. In order to apply WSM, the performance matrix needs to be normalized to convert it into a dimensionless matrix and overcome the scaling unit effect; this task is achieved by applying (3.9):

$$r_{ij} = \begin{cases} \left( \frac{x_{ij} - Min_i}{Max_i - Min_i} \right) & \forall j \in J \\ \left( \frac{x_{ij} - Min_i}{Max_i - Min_i} \right) & \forall j \in J' \end{cases} \quad (3.9)$$

where  $r_{ij}$  is the generic element of the normalized performance matrix,  $J$  is the performance evaluation vector where the criteria is considered a benefit (the higher value, the better performance) and  $J'$  is the performance evaluation vector where the criteria is considered a cost (the lower value, the better performance). In our analysis  $J$  consists of  $C_1$  and  $C_3$ , while  $J'$  is composed by only  $C_2$ .

After that, WSM scores are calculated using (3.10):

$$WSM_{score} = \sum_{j=1}^n w_j \cdot r_{ij} \quad (3.10)$$

where  $w_j$  is the weight of criteria  $j$ .  $WSM_{score}$  equals the final score for the alternative  $i$ ; the higher score alternative means the better one.

### 3.2.3 Technique for Order Preference by Similarity to Ideal Solution (TOPSIS) Method

TOPSIS method was developed by Hwang and Yoon (1981). This method is based on the concept that the chosen alternative should have the shortest Euclidean distance from the ideal solution, and the farthest from the negative ideal solution. The ideal solution is hypothetical for which all attribute values correspond to the maximum performance attribute values in the database comprising the satisfying solutions; the negative ideal solution is the hypothetical solution for which all attribute values correspond to the minimum performance attribute values in the database. TOPSIS thus gives a solution that is not only closest to the hypothetically best, that is also the farthest from the hypothetically worst. TOPSIS has been applied in various energy engineering applications previous contributions such as [66, 67].

First step to apply TOPSIS is the normalization of performance components of  $X$  by using (3.11):

$$r_{ij} = X_{ij} / \left( \sum_{i=1}^m X_{ij}^2 \right)^{\frac{1}{2}} \quad (3.11)$$

where  $r_{ij}$  is the generic element of the normalized performance matrix. The second step is to obtain weighted normalized decision matrix by using (3.12):

$$v_{ij} = w_j \cdot r_{ij} \quad (3.12)$$

where  $v_{ij}$  is the generic element of the weighted normalized performance matrix and  $w_j$  is the combined weights vector. The third step is the calculation of the positive ideal solution  $A^+$  and the negative ideal solution  $A^-$  by using (3.13) and (3.14):

$$A^+ = \{v_1^+, v_2^+, \dots, v_n^+\} = \begin{cases} \left( \text{Max}_i v_{ij} \mid j \in J \right) \\ \left( \text{Min}_i v_{ij} \mid j \in J' \right) \end{cases} \quad (3.13)$$

$$A^- = \{v_1^-, v_2^-, \dots, v_n^-\} = \begin{cases} \left( \text{Min}_i v_{ij} \mid j \in J \right) \\ \left( \text{Max}_i v_{ij} \mid j \in J' \right) \end{cases} \quad (3.14)$$

where  $v_j^+$  and  $v_j^-$  are the positive ideal and negative ideal criteria performance among all alternatives.

The positive distance  $s_i^+$  and the negative distance  $s_i^-$  between alternative  $A_i$  and positive and negative ideal solutions  $A^+$  and  $A^-$  are calculated by (3.15) and (3.16) as follows:

$$s_i^+ = \sqrt{\sum_{j=1}^n (v_{ij} - A_j^+)^2} \quad (3.15)$$

$$s_i^- = \sqrt{\sum_{j=1}^n (v_{ij} - A_j^-)^2} \quad (3.16)$$

where  $A_i^+$  is the ideal performance of the  $j$ th criteria,  $A_i^-$  is the worst performance of the  $j$ th criteria. Finally, relative closeness degree of alternative  $A_i$  to  $A^+$   $TOPSIS_{score}$  is calculated by (3.17):

$$TOPSIS_{score} = s_i^- / (s_i^- + s_i^+) \quad (3.17)$$

The best alternative has the maximum closeness degree among all alternatives, meaning the shortest distance from the ideal solution and the longest distance from the nadir solution.

### 3.2.4 Preference Ranking Organization Method for Enrichment Evaluation (PROMETHEE) Method

A different MCDA method is the complete outranking PROMETHEE II, where alternatives are compared against each other in a pair wise approach according to preference function. PROMETHEE methods have been used in different sustainable energy application [69-73]. PROMETHEE II scores are calculated using the following steps:

Performance differences between each single alternative and all other alternatives are calculated in pair wise bases using (3.18):

$$d_j(a,b) = x_{aj} - x_{bj} \quad \forall a, b \in A \quad (3.18)$$

where  $d_j(a, b)$  is the difference between alternatives  $a$  and  $b$  with respect to criteria  $j$ .

After that, preference value  $P_j$  is calculated using (3.19):

$$P_j(a,b) = \begin{cases} F_j[d_j(a,b)] & \forall j \in J \\ F_j[-d_j(a,b)] & \forall j \in J' \end{cases} \quad (3.19)$$

where  $F_j$  is the preference function; in the following, a V-shape criterion preference function is applied as shown in (3.20) and Fig. 3.1:

$$F_j(d) = \begin{cases} 0 & \text{if } d \leq 0 \\ \frac{d}{p} & \text{if } 0 \leq d \leq p \\ 1 & \text{if } d > p \end{cases} \quad (3.20)$$

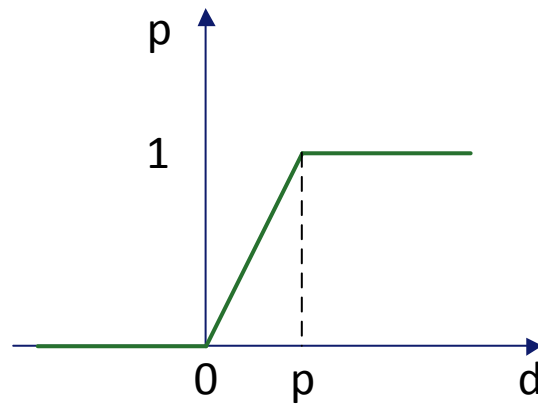


Fig. 3.1 V-shape criterion preference function

where  $p$  is the threshold of strict preference; different values of  $p$  can be applied for each criteria, defining a vector  $P_{value}$ :

$$P_{value} = [p_1 \quad p_2 \quad p_3 \quad \dots \quad p_j]$$

Then aggregated preference indices are calculated using (3.21) and (3.22):

$$\Pi(a,b) = \sum_{j=1}^n P_j(a,b) \cdot w_j \quad (3.21)$$

$$\Pi(b,a) = \sum_{j=1}^n P_j(b,a) \cdot w_j \quad (3.22)$$

where  $\Pi(a,b)$  represents the preference degree of alternative  $a$  with respect the  $b$  one; similar consideration are valid for  $\Pi(b,a)$ .

The outranking flow can be calculated now using (3.23) and (3.24):

$$\phi^+(a) = \frac{1}{m-1} \sum_{x \in A} \Pi(a,x) \quad (3.23)$$

$$\phi^-(a) = \frac{1}{m-1} \sum_{x \in A} \Pi(x,a) \quad (3.24)$$

where  $\phi^+$  and  $\phi^-$  are the positive and negative outranking flows respectively;  $(m-1)$  is the number of possible alternatives facing in a pair wise comparison with alternative  $a$ . Finally the complete ranking for each alternative is calculated using (3.25):

$$PROM_{score} = \phi^+(a) - \phi^-(a) \quad (3.25)$$

where  $PROM_{score}$  is the complete ranking for alternative  $a$ . The latter quantity is the balance between the positive and the negative outranking flows. The higher the net flow means better alternative. When  $PROM_{score}$  is positive, alternative  $a$  is more outranking all other alternatives on all the criteria, and when  $PROM_{score}$  is negative, alternative  $a$  is more outranked by other alternatives.

### **3.3 Multi Objective Decision Making (MODM)**

In recent years, some complex engineering optimization methods that are conceptually different from the traditional mathematical programming techniques have been developed. These methods are labeled as modern or nontraditional methods of optimization. Multi objective optimization algorithms are among these methods. In this research, a multi objective genetic algorithm (MOGA) optimization method has been applied.

#### **3.3.1 Genetic algorithm (GA)**

GA is a probabilistic search technique that has been inspired by Darwin theory regarding survival and fitness. The beginning of GAs is credited to John Holland, who developed the basic ideas in the late 1960s and early 1970s. Since its conception, GAs have been used widely as a tool in computer programming and artificial intelligence, optimization, neural network training, and many other areas [73, 74].

Many practical optimum design problems are characterized by mixed continuous discrete variables, and discontinuous and non-convex design spaces. If standard non-linear programming techniques are used for this type of problem they will be inefficient, computationally expensive, and, in most cases, find a relative optimum that is closest to the starting point. GA is well suited for solving such problems, and in most cases they can find the global optimum solution with a high probability.

As mentioned before, GA is based on Darwin natural selection theory. The basic elements of natural genetics reproduction, crossover, and mutation are used in the genetic search procedure. GA differs from the traditional methods of optimization in the following respects:

1. A population of points (trial design vectors) is used for starting the procedure instead of a single design point.
2. GA uses only the values of the objective function. The derivatives are not used in the search procedure.
3. In GA, the design variables are represented as strings of binary variables that correspond to the chromosomes in natural genetics. Thus the search method is naturally applicable



for solving discrete and integer programming problems. For continuous design variables, the string length can be varied to achieve any desired resolution.

4. The objective function value corresponding to a design vector plays the role of fitness in natural genetics.
5. In every new generation, a new set of strings is produced by using randomized parents selection and crossover from the old generation (old set of strings) [75].

### 3.3.2 Representation of Design Variables

In GA, the design variables are represented as strings of binary numbers, 0 and 1. If each design variable  $x_i$ ,  $i = 1, 2, \dots, n$  is coded in a string of length  $q$ , a design vector is represented using a string of total length  $nq$ .

### 3.3.3 Representation of Objective Function and Constraints

Basically, GA maximizes a function called the fitness function. Thus it is naturally suitable for solving unconstrained maximization problems. The fitness function,  $F(X)$ , can be taken to be same as the objective function  $f(X)$  of an unconstrained maximization problem so that  $F(X) = f(X)$ . A minimization problem can be transformed into a maximization problem before applying the GAs. Usually the fitness function is chosen to be nonnegative. The commonly used transformation to convert an unconstrained minimization problem to a fitness function is given by (3.26)

$$F(X) = \frac{1}{1+f(x)} \quad (3.26)$$

It can be seen that Eq. (3.26) does not alter the location of the minimum of  $f(X)$  but converts the minimization problem into an equivalent maximization problem. A general constrained minimization problem can be stated as (3.27 – 3.29):

$$\text{Minimize } f(X) \quad (3.27)$$

Subject to

$$g_i(X) \leq 0, i = 1, 2, \dots, m \quad (3.28)$$

And

$$h_j(X) = 0, j = 1, 2, \dots, p \quad (3.29)$$

Where  $g_i(X)$  and  $h_i(X)$  are inequalities and equalities constraints respectively.

### 3.3.4 Genetic Operators

GA optimization algorithm starts with the selection of an initial population of random strings denoting several (population of) design vectors. The population size ( $n$ ) is usually fixed. Each string (or design vector) is evaluated to find its fitness value. The population (of designs) is operated by three operators — reproduction, crossover, and mutation — to produce a new population of points (designs). The new population is further evaluated to find the fitness values and tested for the convergence of the process. One cycle of reproduction, crossover, and mutation and the evaluation of the fitness values are known as a generation in GAs. If the convergence criterion is not satisfied, the population is iteratively operated by the three operators and the resulting new population is evaluated for the fitness values. The procedure is continued through several generations until the convergence criterion is satisfied and the process is terminated. The details of the three operations of GAs are given below. [75]

The algorithm can be summarized as [73, 74]:

1. Set generation number  $k = 0$ ; and form initial population Pop(0);
2. Evaluate objective function (fitness value) for Pop(k) elements;
3. If stopping criterion satisfied, then stop;
4. Else, set  $k = k+1$ , form Pop(k) using reproduction, mutation, and crossover operators;
5. Go to step 2.

These steps are described in figure 3.2.

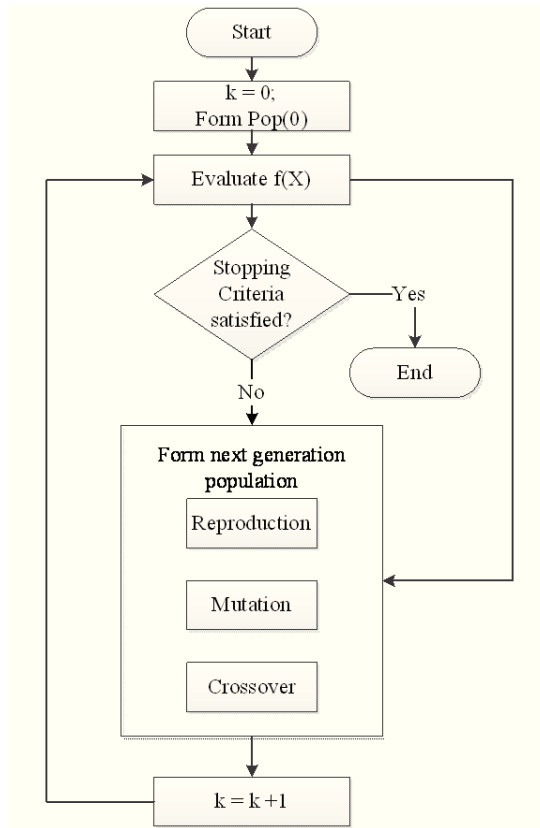


Figure 3.2: Steps of applying genetic algorithm optimization technique

### 3.3.5 Multi Objective Optimization

In practical applications, not only one but several features or performance criteria are typically important in the optimal decision making process. In power systems, the efficiency, emissions, and costs are common quantities that are of interest. Thus, any of these could be chosen individually as the objective function, though interest clearly lies in dealing with more than one objective function, in this case the optimization problem becomes a multi objective one.

A common approach to multiple objective functions is to combine them to yield a single objective function that is minimized or maximized. However, the various quantities that compose the objective function should be scaled and normalized in order to include it in one objective function. Equal or different weights can similarly be used to increase or decrease the importance of a given criteria compared to the others. Although this approach can lead to good solutions in different applications, it is not guaranteed to achieve a good compromise between all objectives

of interest, instead, the optimizer deals with all objectives included in the fitness function as a single value.

Another approach, which has gained interest in recent years, is that of multi objective optimization. In this case, two or more objective functions that are of interest in a given problem are considered and a strategy is developed to solve the conflict between these objective functions.

A multi objective optimization problem with inequality and equality constraints can be stated as (3.30-9.32):

$$\text{Find } X = \begin{Bmatrix} x_1 \\ x_2 \\ \vdots \\ x_n \end{Bmatrix} \quad (3.30)$$

Which minimizes  $f_1(X), f_2(X), \dots, f_k(X)$

Subject to

$$g_i(X) \leq 0, i = 1, 2, \dots, m \quad (3.31)$$

And

$$h_j(X) = 0, j = 1, 2, \dots, p \quad (3.32)$$

Where  $g_i(X)$  and  $h_j(X)$  are inequalities and equalities constraints respectively.  $k$  denotes the number of objective functions to be minimized. Any or all of the functions  $f_i(X)$  and  $g_j(X)$  may be nonlinear.

In general, no solution vector  $X$  exists that minimizes all the  $k$  objective functions simultaneously. Hence, a new concept, known as the Pareto optimum solution is introduced. A feasible solution  $X$  is called Pareto optimal if there exists no other feasible solution  $Y$  such that  $f_i(Y) \leq f_i(X)$  for  $i = 1, 2, \dots, k$  with  $f_j(Y) < f_j(X)$  for at least one  $j$ . In other words, a feasible vector  $X$  is called Pareto optimal if there is no other feasible solution  $Y$  that would reduce some objective function without causing a simultaneous increase in at least one other objective function [73, 76].

In this research, Multi Objective Genetic Algorithm (MOGA) optimization method has been applied using Matlab program, where this algorithm provides the Pareto Set of equal value optimal solutions.

## Chapter Four

---

### *Theory of Fuzzy Sets*

#### **4.1 Introduction**

In the conventional sets theory, an element is either belongs or does not belong to a set. However, this essential concept does not take into account common and simple real life situations when an element is partially belongs to a set. To deal with these situations, the concept of a fuzzy set was created. Its theory is based on the concept of partial membership: each element belongs partially or gradually to the fuzzy sets that have been defined. The boundaries of each fuzzy set are not “crisp”, but “fuzzy” or “gradual”. In this research, fuzzy sets have been used to model and evaluate social performance criteria.

Modeling and evaluating energy systems social performance criteria have been proposed in previous contributions. [77] and [78] proposed social acceptability criteria for evaluating wind energy plants in an Italian island and comparing different power generation plants respectively, while [79] performed sustainability assessment for the Croatian co-generation sector future development.

Other researchers included social benefits as a social criteria in their analysis, [80] applied it to evaluate domestic solar water heating in comparison to other water heating alternatives. [81] applied fuzzy sets programming approach to perform solar water heating systems comparison for various applications, in which social benefits was included as a social criteria.

Land use also has been included as a crucial social criteria, [82] and [83] performed fuzzy multi-criteria decision making and improved grey incidence approach respectively for selecting and evaluating tri-generation systems where land use was one of the applied social criteria. [63] and [78] compared different power generation plants taking into consideration the land use as an important social criteria to enhance sustainability. Also, [84] used land use social indicator in evaluating several combined heat and power CHP systems.

Moreover, job creation which is the number of job opportunities will be established by applying specific alternative has also been included as a social criteria, [71] applied this criteria for evaluating geothermal energy projects. [85] used it in performing Electre MADM approach to assess an action plan for the diffusion of renewable energy technologies at regional scale. [86] presented a fuzzy multi-criteria decision making approach using linguistic variables to assist policy makers in formulating sustainable technological energy priorities taking new direct and indirect employment opportunities as one of the social analysis criteria. [87] proposed group decision-making framework for assisting with multi-criteria analysis in evaluating renewable energy projects where job creation has been taken into consideration. [64] included job creation as a social criteria in analysing hydrogen energy systems using multi-criteria assessment. [88] assumed workers hours as a social indicator in analysing different power generation systems using multi-criteria sustainability assessment.

Other social criteria has been also included in previous studies, [77] performed fuzzy based visual impact, acoustic noise in (dB), and fuzzy based impact on eco-systems where birds could collide with rotor blades. Accident fatalities depends on global statistics between 1970-1992 were performed in [78]. In [79], health social indicator was defined as the cost of the health care due to the specific impact of the cogeneration plants nitrogen oxides emissions. [85] performed qualitative based market maturity and compatibility with political, legislative and administrative situation social criteria. [86] included linguistic based contribution to regional development indicators in his social criteria, in this context, fuzzy logic has been used to perform the analysis.

## 4.2 Membership functions

A fuzzy set is defined by its “membership function” which corresponds to the concept of a “characteristic function” in classical logic. In the conventional set theory, the degree of membership of an element to a set is ruled by strict values [0; 1]. Figure 4.1 show the difference between a characteristic and membership functions, in the characteristic function,  $X_1$  and  $X_2$  are the boundaries of the set, if  $X_n < X_1$  it is not a member even if the difference is very small, and the same if  $X_n > X_2$ . In real life applications this is not practical. In contrast, the membership

function is able to solve this problem efficiently where the degree of membership varies between [0; 1].

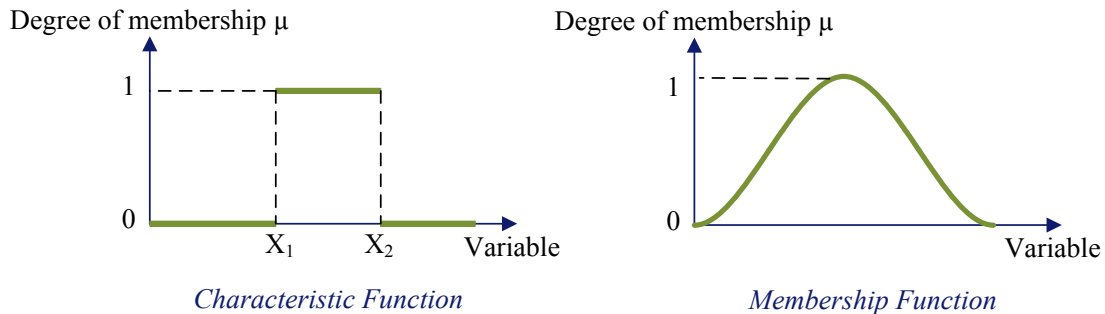


Figure 4.1: Characteristic function vs. membership function.

A number of fuzzy sets can be defined on the same variable to meet practical needs, for example the sets “high”, “medium” and “low”.

Moreover, membership functions can assume any shape. However they are often defined by straight segments. Benefits of using such a membership functions are its simplicity, and that they contain points allowing definition of areas where the variable belongs to the fuzzy set and areas where it does not, thereby simplifying the analysis.

### 4.3 Fuzzy Process

Fuzzy process consists of three main steps, fuzzification, inference, and defuzzification. Figure 4.2 illustrate the relation between it.

Fuzzification is the process of converting a real variable value into a fuzzy one. It consists of determining the degree of membership of a value to a fuzzy set. In this way, qualitative information such as expertise can be modeled and analyzed.

Fuzzy rules which are applied in the inference phase are classed in the field of artificial intelligence because its general purpose is to formalize and implement a human being’s method of reasoning, and normally it is derived from human expertise. The most commonly used inference mechanism is the “Mamdani” one. A fuzzy rule is of the type:

*IF “statement/s” THEN “conclusion”.*



Where a statement/s can be a combination of AND, OR, NOT operators.



Figure 4.2: fuzzy process description.

At the end of inference, the output fuzzy set is determined, but cannot be directly used. Defuzzification step is needed to move from the “fuzzy world” to the “real world”. A number of defuzzification methods can be used, the most common of which is calculation of the “centre of gravity” [89, 90].

## Chapter Five

---

### *Optimal combination of PV-WT grid connected PGS*

#### **5.1 Introduction**

This chapter proposes a simple MCDM approach based on TOPSIS method to define the optimal combination between PV-WT grid connected PGS for a specific predefined installed power, in the following case study, it equals the average load plus one standard deviation. However, real commercial data for PV-WT equipment have been used in the analysis, where two PV modules (150 W and 250 W) and three WT's (10 kW, 30 kW, and 50 kW) have been considered. For the number of installed WT's, a simple algorithm has been developed to choose suitable equipment capacity and number among available ones, where installed power of WT's should be equal or a little bit more than required WT capacity share, taking into account that the lower the number of installed WT equipment is better from social criteria point of view.

For PV modules, it is not common in PV-PGSs to use different modules in the same PGS, however, each PV module (150 W and 250 W) has been assumed in a separate configuration.

In other words, this chapter presents the analysis results of two assumed configurations, where in both, installed WT's numbers and technical specifications are identical and the only difference is in the PV module, one configuration considers the 150 W PV modules while the other considers the 250 W PV modules. The required power to install has been assumed to be fixed (average load + 1 standard deviation), and the proposed algorithm aims to find the best combination between PV and WT's to fulfill the required power for each configuration.

#### **5.2 PV-WT Power Generation Systems Modeling**

A schematic diagram of the basic hybrid PV-WT PGS used in this chapter is shown in Figure 5.1. The energy management strategy works as follows: PV and WT power plants work together to satisfy the load demand. When energy sources (solar and wind energy) are abundant, after satisfying the load demand, the extra generated power is provided to the grid, in this case, extra generated power will be sold and profit will be gained. On the contrary, with reduced

energy sources any energy shortage is supplied by the grid, and in this case, extra costs of buying required energy will be added.

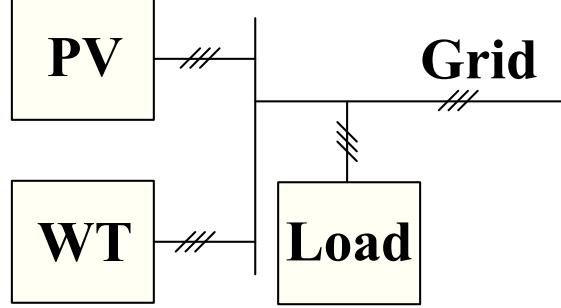


Figure 5.1: Basic configuration of a PV-WT generation system.

### 5.2.1 PV System Model

The mathematical representation of the PV system is given by (5.1)-(5.4), where the output power  $P_{PV}$  delivered by the PV plant at the instant  $t$  is calculated through the global solar radiation on the PV module surface, the PV module temperature, and the PV array power [91]:

$$T_C(t) = T_A(t) + \frac{NCOT - 20}{800} \cdot G(t) \quad (5.1)$$

$$I_{SC}(t) = \left\{ I_{SC.STC} + K_I [T_C(t) - 25] \right\} \frac{G(t)}{1000} \quad (5.2)$$

$$V_{OC}(t) = V_{OC.STC} + K_V (T_C(t) - 25) \quad (5.3)$$

$$P_{PV}(t) = N_{PV} V_{OC}(t) I_{SC}(t) FF \eta_{PVinv} \quad (5.4)$$

Where  $P_{PV}$  is the output power under standard test conditions (STC),  $N_{PV}$  is the number of PV modules,  $G(t)$  is the global irradiance,  $T_A(t)$  is the ambient temperature,  $T_C(t)$  is the cell operating temperature,  $I_{SC}$  is the short-circuit current,  $I_{SC.STC}$  is the short-circuit current under STC,  $V_{OC}$  is the open-circuit voltage,  $V_{OC.STC}$  is the open-circuit voltage under STC,  $K_I$  is the short-circuit current coefficient,  $K_V$  is the open-circuit voltage coefficient, and  $\eta_{PVinv}$  is the power inverter efficiency, FF is the fill factor. Some of the previous values can be determined from the parameters of the PV module which is provided by the manufacturer sheet.

## 5.2.2 Wind Turbine System Model

The power output of a WT is determined from the wind speed distribution has been calculated using equations 2.12 and 2.14, the only difference that equation 2.14 has been modified to include conversion efficiency as shown in 5.5 [58]:

$$P_{WT\max}(t) = \frac{1}{2} \rho A v(t)^3 C_p \eta_{Inv} \eta_{Mech}. \quad (5.5)$$

where  $\rho$  is the air density,  $A$  is the swept area of the rotor,  $v$  is the wind speed,  $C_p$  is the efficiency of the wind turbine,  $\eta_{Inv}$  is the power inverter efficiency, and  $\eta_{Mech}$  is the efficiency of the mechanical components. Power calculation achieved by (5.5) must take into account also the wind speed range operability of the turbine.

The aforementioned PV and WT mathematical models are used to predict and simulate the PV-WT electrical power production associated to different PV-WT share combinations (defined in the following as *alternatives*).

## 5.3 Analysis Criteria Adopted in the Proposed Approach

The proposed optimization approach aims to enhance SED in hybrid PGSSs, including technical, environmental, economic, and social criteria.

The technical evaluation criteria used in this paper are the Loss in Power Generation Possibility (*LPGP*) and the Capacity Factor *CF*. *LPGP* measures the possibility that the hybrid system will not be able to cover the required demand and the shortage will be compensated by the grid [40]. *LPGP* is calculated as:

$$LPGP = \sum_{t=0}^T failure\_time / T \quad (5.6)$$

where  $T$  is equal to the one year operating time of the plants, while the failure time is equal to the time in which the hybrid PV-WT system is not able to fulfill the demand and the shortage will be covered by the grid.

The *CF* shows the average utilized power from the rated power installed and is calculated using (5.7) [50]:

$$CF = \left( \frac{\text{mean}(P_{\text{output}})}{P_{\text{rated}}} \right) 100\% \quad (5.7)$$

where  $P_{\text{output}}$  is the total produced power from the hybrid PV-WT system per year, and  $P_{\text{rated}}$  is the installed PV-WT rated power.

The environmental evaluation criteria chosen in the proposed analysis are kilograms [kg] of reduced emissions and the renewable energy share. This indicator has become more and more important for governments and policy makers in the last decade. Emissions reduction is calculated through (5.8):

$$\text{Emissions} = \sum_{t=0}^T E_{\text{gen.}} \times (NOx_{kWh} \times CO_{2-kWh} \times SO_{2-kWh}) \quad (5.8)$$

where  $\text{Emissions}$  is kg of emissions not released to environment,  $NOx_{kWh}$ ,  $CO_{2-kWh}$ , and  $SO_{2-kWh}$  are kg of emissions generated by producing one kWh from the grid using fossil fuel,  $E_{\text{gen.}}$  is kWh generated by the hybrid system at time  $t$ .

$RE$  share is calculated by dividing the number of kWh generated from the hybrid PV/WT system over the total demand required during a specified period of time  $T$ .  $RE$  is calculated using (5.9):

$$RE_{\text{Share}} = \frac{\sum_{t=0}^T E_{\text{gen.}}}{\sum_{t=0}^T \text{Demand}_{kWh}} \quad (5.9)$$

where  $\text{Demand}_{kWh}$  is the required energy in kWh at time  $t$ .

For economic criteria, the initial investment calculated directly from the number of the adopted PV modules and WTs, and the cost of the required land has been chosen as economic evaluation criteria. The initial investments calculated using (5.10):

$$C_{\text{Inv.}} = N_{PV} \cdot PV_{RP} \cdot PV_{kW \text{ cost}} + \dots \\ N_{WT} \cdot WT_{RP} \cdot WT_{kW \text{ cost}} + (L_{PV} + L_{WT}) \cdot C_L \quad (5.10)$$

where  $C_{\text{Inv.}}$  is the total investment cost,  $N_{PV}$  and  $N_{WT}$  are the numbers of installed PV modules and WTs,  $PV_{RP}$  and  $WT_{RP}$  are the entire rated power respectively to the PV and WTs power systems,  $PV_{kW \text{ cost}}$  and  $WT_{kW \text{ cost}}$  are the costs of one kW power installed from PV modules and WTs,  $L_{PV}$  and  $L_{WT}$  are the required lands for PV modules and WT, and  $C_L$  is the cost of one

square meter of land. Another economic evaluation criterion is the maintenance cost which is calculated by (5.11):

$$C_{main}(y) = \sum_{y=1}^{20} C_{main}(1) \cdot (1+f)^y \quad (5.11)$$

where  $C_{main}(y)$  is the maintenance cost of the  $y$ -th year and  $f$  is the inflation rate [23]. The maintenance costs are calculated for 20 years lifetime of the project. The last economic cost assumed is the running cost of the grid. As aforementioned, power generation shortage of the PV-WT systems implies that energy is bought from the grid, while extra energy exceeding the demand allows us to sell such energy to the grid. This economic criteria is calculated by (5.12):

$$C_{Grid} = \sum_{t=0}^T E_B \cdot kWh_{B,price} - E_S \cdot kWh_{S,price} \quad (5.12)$$

where  $C_{Grid}$  is the grid cost,  $E_B$  is the amount of energy required from the grid in order to compensate the hybrid system production shortage,  $kWh_{B,price}$  is the cost of buying one kWh from the grid,  $E_S$  is the amount of extra energy sold to the grid,  $kWh_{S,price}$  is the revenue of selling one kWh to the grid.

Finally, social evaluation criteria Land Use (LU) and Social Acceptability (SA) are considered. LU and SA of the *alternatives* are evaluated by using a fuzzy logic approach. In particular, LU is calculated directly from the required area of the PV modules and WTs, where it is expected that local community will show resistance against occupying large area for installing the PGS especially if we are talking about limited available area, while SA takes into consideration the social resistance against using WTs. Obviously, a high number of installed WTs leads to a lower SA value due to local community resistance against negative WTs impacts such as acoustic noise, ecological disturbance, shading effects... etc.

In particular, no fuzzy logic model can be designed to fit social criteria performance evaluation in all areas, this system should be designed specifically for the area of study, local community response against HRE PGSs varies a lot if the area is natural reserve, historical, agricultural, rural, or urban. For the analysis of this chapter, a simple model has been proposed assuming that the available land for installing the required PGS is natural one, so local community will show obvious resistance against disturbing the view.

In both criteria, Gaussian curve Membership Functions (MFs) are applied, considering six LU which are acceptable, almost acceptable, neutral, almost rejected, and rejected MFs and three SA levels which are acceptable, neutral, and rejected MFs. Figures 5.2 and 5.3 show fuzzy surfaces for both LU and SA criteria respectively, while tables 5.1 and 5.2 show applied fuzzy rules for LU and SA criteria respectively.

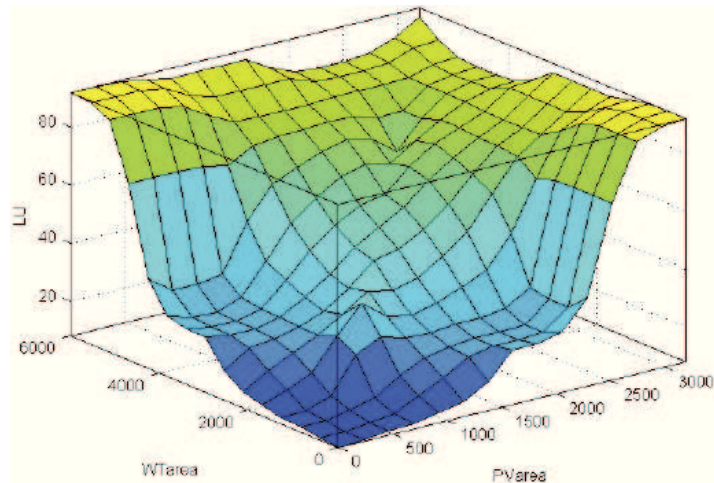


Figure 5.2: Fuzzy surface for LU social criteria

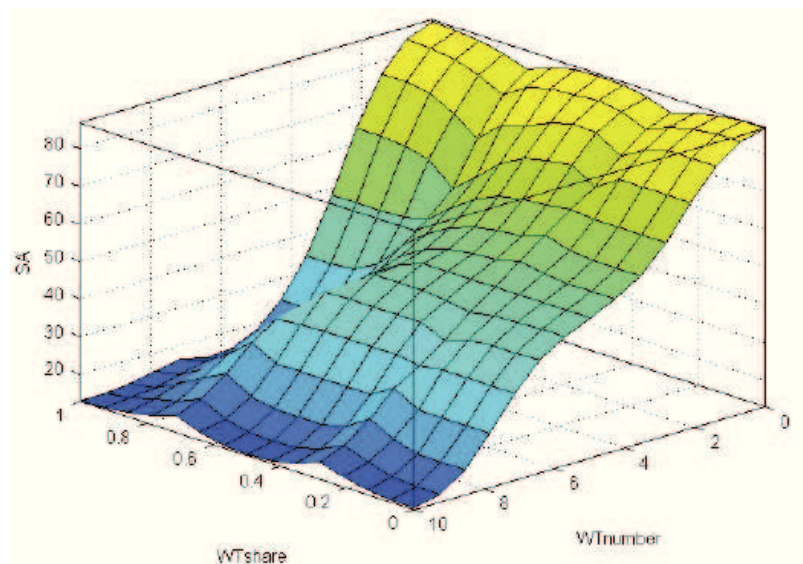


Figure 5.3: fuzzy surface for SA social criteria

Table 5.1: Applied fuzzy rules for LU social criteria

$PV_{area}$ / $WT_{area}$	Accepted	Almost accepted	neutral	Almost rejected	rejected
Accepted	Accepted	Accepted	Almost accepted	Almost rejected	Rejected
Almost accepted	Accepted	Almost accepted	Almost accepted	neutral	Rejected
neutral	Almost accepted	Almost accepted	Neutral	Almost rejected	Rejected
Almost rejected	neutral	neutral	Almost rejected	Almost rejected	Almost rejected
rejected	Rejected	Rejected	Rejected	Rejected	Rejected

Table 5.2: Applied fuzzy rules for SA social criteria

$WT_{share}$ / $WT_{number}$	Low	Moderate	High
Low	Accepted	Accepted	Accepted
Moderate	Fair	Fair	Resist
High	Resist	Resist	Resist

The output of the LU is an indicator ( $LU$ ) measured as percent that show the resistance against the PGS, while the output of the SA criteria is a percent scale indicator ( $SA$ ) that estimates the social acceptance of installing a HRE PGS.

## 5.4 Proposed optimization approach to a Case Study

In this chapter, the proposed approach exploits the applicability of MCDM algorithms for optimizing PV-WT PGS combinations. It allows users to systematically simulate different combinations of grid-connected PV-WT power systems to fulfill energy demand for a specific area and at the same time to satisfy the several technical, environmental, economic, and social aforementioned conflicting design criteria by defining the best compromise.

Application of the proposed optimal sizing approach can be summarized as in Fig. 5.4, where decision criteria and environmental conditions are given as inputs; the PV-WT models are exploited to generate and simulate different *alternatives*, which are evaluated by means of



TOPSIS MCDA method in order to achieve the optimal one. Criteria importance weights were calculated using ASMCW (equation 3.7) where  $q = 0.7$  factor has been applied, meaning that 30% of importance has been given to Entropy weights in forming ASMCW.

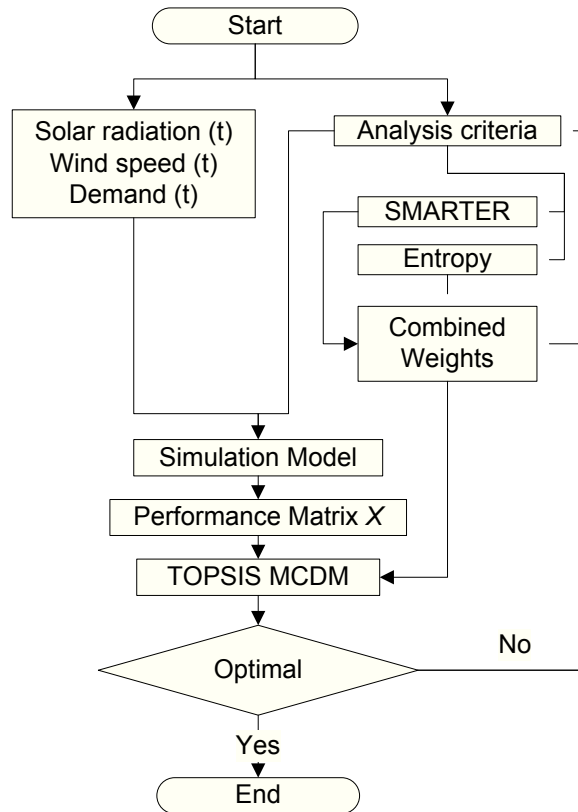


Fig. 5.4. Flowchart of the proposed optimal sizing method.

The optimal sizing approach has been applied to a real case. In particular, the hybrid power system is assumed to be located close to Messina (Italy) harbor, with the goal to satisfy part of the user load profile depicted in figure 5.5; solar radiation and wind speed profiles measured in that area are also indicated in the same figure.

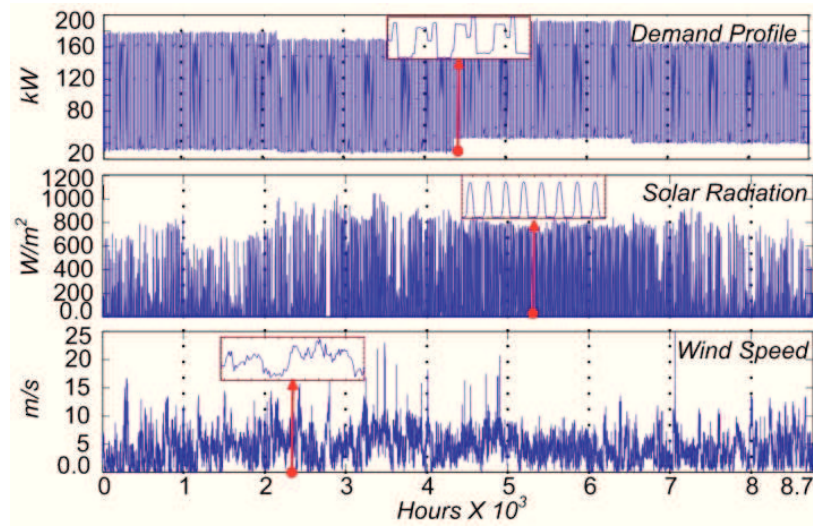


Figure 5.5: Messina harbor solar radiation, wind speed and load profiles per year.

PV modules, WT specifications and technical characteristics are shown in Table 5.3. Grid-related and environmental data used in the following analysis are presented in Table 5.4.

Table 5.3: WTs and PV modules technical specifications

Wind Turbines			
Specifications	10 kW	30 kW	50 kW
Prated	10kW	30kW	50kW
Pmaximum	15kW	45kW	75kW
Rotor blade diameter	8m	10m	12m
Cp	0.42	0.42	0.42
Tower height	12m	18m	18m
$\eta_{Inv}$	0.97	0.97	0.97
$\eta_{Mech}$	0.94	0.94	0.94
PV modules			
Specifications	PV 150 W	PV 250 W	
Pmax	150 W	250 W	
Voc	43.5 V	37.6 V	
Vpm	34.5 V	30.3 V	
Isc	4.75 A	8.9 A	
Ipm	4.35 A	8.26 A	
NOCT	47 °C	47.5 °C	
Temp. coefficient (Voc)	-0.0016 / °C	-0.00351 / °C	
Temp. coefficient (Isc)	0.00065 / °C	0.0053 / °C	
$\eta_{PV,Inv}$	0.94	0.94	

Table 5.4: Environmental and economic data

Buy kWh	Sell kWh	PV cost	WT cost
0.2 euro	0.3 euro	4350 euro/kW	1250 euro/kW
PV maint.	WT maint.	Inflation rate	NO <sub>x</sub> g/kWh
10 euro/kW	32 euro/ kW	1.5 %	1.34
CO <sub>2</sub> g/kWh	SO <sub>2</sub> g/kWh	Land Cost	
632	2.74	10 euro/ m <sup>2</sup>	

The simulation model calculates the required PGS power to be installed as average power demand or average power demand plus/minus specific number of standard deviations. However, in the following analysis +1 standard deviation is assumed with respect to the mean demand value. Moreover, alternatives have been generated by assuming in the first alternative that all required installed power will be fulfilled by PVs and it has been indicated as PV100WT0 alternative which means 100% of the required installed power will be fulfilled with PV modules and 0.0% with WTs, in the next alternative, the PV-WT combination has been changed by assuming a step size, where the second alternative PV modules share equals to (100% - step size) and the WTs share equals (0.0% + step size). The model continue in the same procedure until generating the last alternative which is PV0WT100 (0.0% of required installed power will be covered by PVs and 100% by WTs). In this chapter, a step size of 10% is used to generate different *alternatives* of PV and WTs systems.

In addition, two possible configurations are considered which are:

- G<sub>1</sub>: The hybrid system is built with 250 W PV modules and combining 10, 30, and 50 kW WTs.
- G<sub>2</sub>: The hybrid system is built with 150 W PV modules and combining 10, 30, and 50 kW WTs.

The reason behind defining and analyzing two configurations is to test the approach reliability. In MCDM field, no one knows the optimal answer in advance; it depends strongly on the analysis criteria and its weights. The two PV modules have been simulated separately, and it was clear that the 250 W modules have better performance and lower cost (due to less area required) than the 150 W. So, it should be expected that under the same environmental and

economic conditions, reliable results will show that in configuration G1, the optimal alternative will contain higher PV modules share.

Table (5.5) shows the number of required PV modules and WTs for each *alternative* and configuration.

Table 5.5: PV modules and WTs required for each *alternative* and configuration

		G1	G2	G1 & G2		
Alternative		PV 250W	PV 150W	WT 50 kW	WT 30 kW	WT 10 kW
A	PV100WT0	632	1053	0	0	0
B	PV90WT10	569	948	0	0	2
C	PV80WT20	506	842	0	1	1
D	PV70WT30	443	737	0	1	2
E	PV60WT40	379	632	1	0	2
F	PV50WT50	316	527	1	1	0
G	PV40WT60	253	421	1	1	2
H	PV30WT70	190	316	2	0	2
I	PV20WT80	127	211	2	1	0
J	PV10WT90	64	106	2	1	2
K	PV0WT100	0	0	3	0	1

For each configuration, the simulation results of the generated *alternatives* are used to formulate the Performance matrix  $X$  (equation 3.1) shown in Table 5.6 for G1 and Table 5.7 for G2, while the applied SMARTER weights are shown in Table 5.8.

TABLE –5.6-: Performance matrices associated to G1 configuration

G1	LPGP %	CF %	Emissions $\times 10^3$	RE %	Int. Inv. $\times 10^3$	Maint. $\times 10^3$	GridCost $\times 10^3$	LU %	SA %
A	89,4	15,0	132	23,7	711	37	129	45	87
B	89,0	17,2	156	27,9	678	48	122	30	75
C	87,5	17,3	161	28,8	636	60	121	34	75
D	86,5	18,5	166	29,7	584	64	120	42	63
E	85,9	18,5	170	30,4	541	75	118	45	62
F	85,4	19,7	175	31,3	489	79	117	44	53
G	85,8	19,7	180	32,2	447	90	115	39	50
H	85,9	19,7	184	32,9	405	101	113	33	43
I	85,7	20,9	189	33,8	353	105	110	76	27
J	85,2	20,9	194	34,7	311	116	108	88	19
K	86,2	20,1	179	32,1	250	120	113	84	28

TABLE –5.7-: Performance matrices associated to G2 configuration

G2	LPGP %	CF %	Emissions $\times 10^3$	RE %	Int. Inv. $\times 10^3$	Maint. $\times 10^3$	GridCost $\times 10^3$	LU %	SA %
A	89,7	14,4	127	22,8	1176	37	132	92	87
B	89,3	16,7	151	27,1	1096	48	124	87	75
C	87,7	16,9	156	28,0	1006	60	123	61	75
D	86,7	18,1	162	29,0	908	64	121	56	63
E	86,0	18,1	166	29,8	820	75	120	52	62
F	85,7	19,4	172	30,9	722	79	118	53	53
G	86,3	19,5	177	31,8	632	90	115	50	50
H	86,2	19,5	182	32,6	545	101	113	47	43
I	85,8	20,8	188	33,6	446	105	111	75	27
J	85,2	20,9	193	34,6	358	116	108	88	19
K	86,2	20,1	179	32,1	250	120	113	84	28

TABLE -5.8-: Smarter criteria weights used in the analysis

Criteria	C1: PLPG	C2: CF	C3: Emissions	C4: RE%	
Weight	9	4	1	7	
Criteria	C5: Ini. Inv.	C6: Maint. Cost	C7: Grid cost	C8: LU	C9: SA
Weight	3	2	5	8	6

The economic criterion is a key point to decide about the optimal *alternative*. In this study, three economic criteria are included C5, C6 and C7, whose sum is shown in Fig. 5.6 for each *alternative* and configuration.

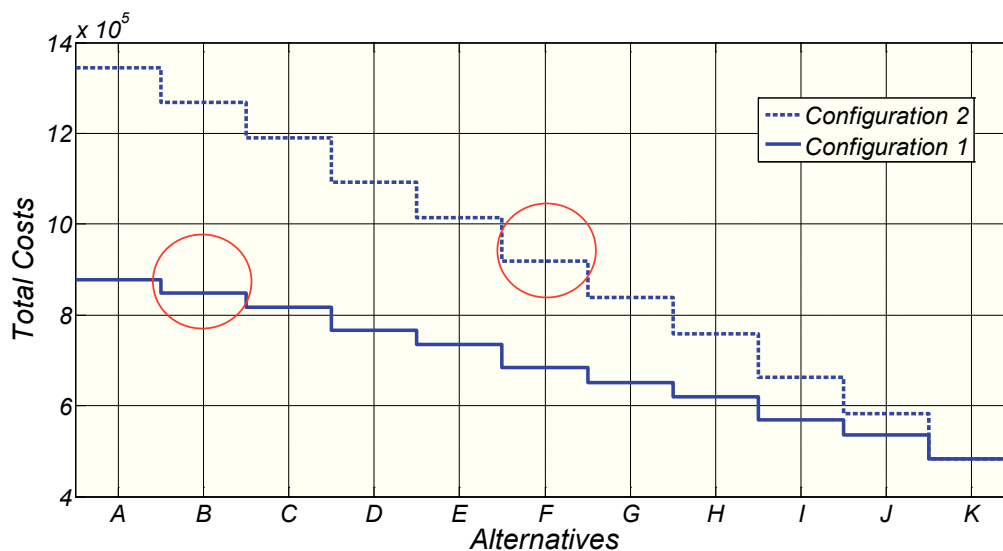


Fig. 5.6:- Economic criteria simulation results

Applying TOPSIS MCDA, the optimal combination of PV/WT power generation system in  $G_1$  is given by the *alternative B* (PV90WT10), while in  $G_2$ , the optimal *alternative* is F (PV50WT50) as shown in Fig. 5.7.

The results of Tables 5.6 and 5.7, Figure 5.6 and Figure 5.7 highlight that the optimal *alternatives* not always the cheapest one, instead, it is the best compromise among the different criteria.

Comparing the results of Tables 5.6 and 5.7, it is possible to observe that the configuration adopting PV250 W modules allows us to achieve superior performances than using PV 150 W modules. In fact, according to the *alternative A* (PV100WT0), where only the PhotoVoltaic system is used, it can be noted that configuration  $G_1$  is better than configuration  $G_2$  in almost all criteria (except maintenance and SA that are the same). Due to this consideration, it is expected that in configuration  $G_2$  the optimal *alternative* will include more wind energy share, and this is confirmed in Figure 5.7, giving a good indication about the validity and reliability of the proposed approach.

This method can be considered a powerful guide for decision makers, by which they can define the optimal or other compatible *alternatives*, such as A and C in  $G_1$ , and G in  $G_2$ ; in fact, according to the criteria weights, even if alternative A in  $G_1$  allows to achieve a higher SA degree and reduced maintenance cost, this advantage is paid in terms of all other criteria. Similar consideration can be made for *alternative C* in  $G_1$  and G in  $G_2$ . The *alternative K* in  $G_2$  has a compatible index compared to the optimal one because this solution allows to achieve very high performance in almost all criteria except to social criteria and maintenance costs, where very low performance are provided.

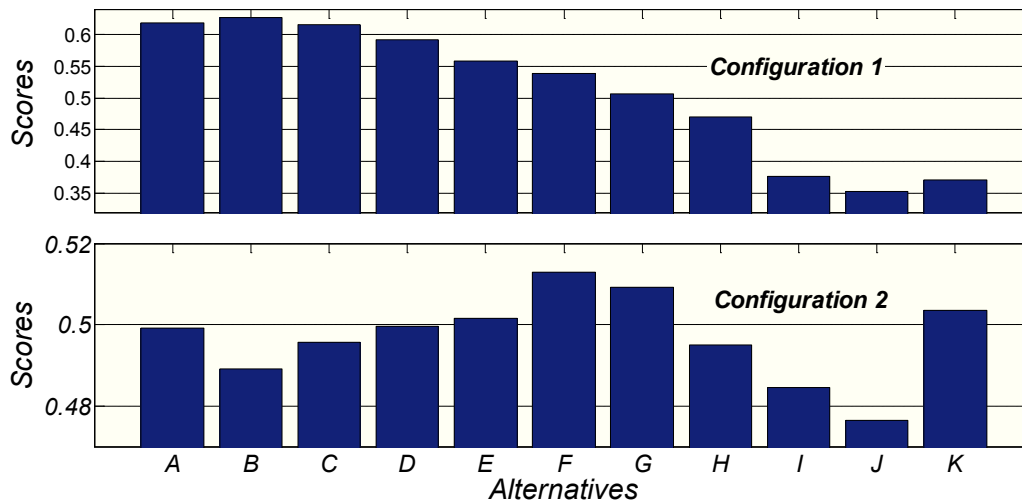


Fig. 5.7:- Final score of alternatives using TOPSIS method

In general, the decision maker can refer to Tables 5.6 and 5.7 in order to focus with more details on the differences between compatible *alternatives* and decide the best solution. Another more efficient way to show detailed results and how the MCDM algorithms define the optimal compromise is to use the statistical percentile principle. With respect to each performance criteria, alternatives are sorted from the worst performance to the best one, then, each alternative position is divided on the total number of alternatives, as an example, the worst alternatives which position equals to one is divided on the total number of alternatives which is eleven, the result is 9%, this number means that 9% of the alternatives are with equal performance or lower than this alternative, while for the best alternative which has position number eleven in the sorting process, dividing eleven by eleven which is the total number of alternatives results 100%, this value means that 100% of the alternatives performance with respect to this criteria are with equal performance or lower than this alternative (the best one). Applying this principle to Table 5.6 G1 configuration and Table 5.7 G2 configuration data, results are shown in figures 5.8 and 5.9 respectively.

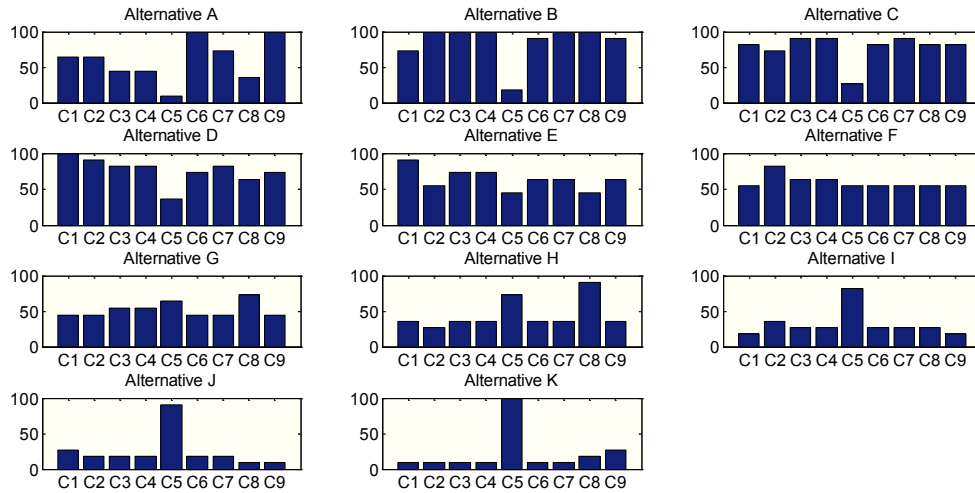


Figure -5.8-: Percentile analysis results for G1 configuration.

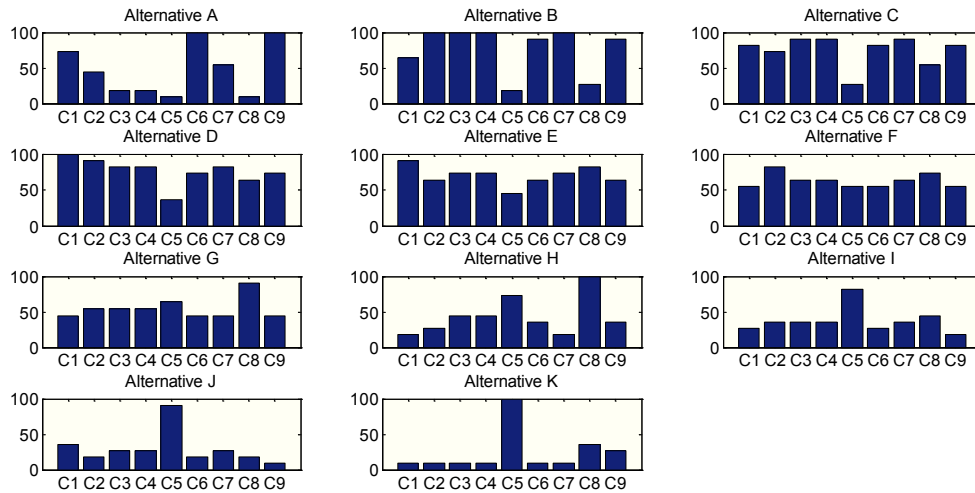


Figure -5.9-: Percentile analysis results for G2 configuration.

Looking at figure 5.8, alternative B which the optimal in this configuration (G1) achieved the best possible performance C2, C3, C4, C7, and C8, in addition, its performance in C6 and C9 are higher than or equal to 90% of all other alternatives, while C5 performance is one among the worst. However, looking at C5 performance in all alternatives presented in figure 5.8, it is obvious that this criteria improves when shifting to use more wind power in the alternatives, where all other criteria performances decrease. Figure 5.9 presents the same results but for G2 configuration, in this case, it can be noticed that alternative F which is the optimal in this



configuration did not scores 100% percentile on all its criteria, instead, it provides a very good compromise among all criteria.

## **5.5 Chapter Conclusion**

Combination optimization of PV-WT grid connected PGSs can be solved using MCDA methods. The advantage of the proposed approach is that it enables users to apply different conflicting criteria with different weights, thus leading to more realistic and practical solutions of the problem.

The proposed model is reliable and simple to be adapted according to user needs while guaranteeing the dynamic behavior of PV/WT systems and keeping into account the effects of the environment variable nature. However, this model is valid only when the amount of required power to install is fixed and predefined, more comprehensive approach is still required to optimize both of the size and sources combination of PV-WT grid connected PGSs.

## Chapter Six

# *MADM Optimal Sizing and Combination of PV-WT grid connected Systems*

## **6.1 Introduction**

This chapter deals with the optimal sizing and combination of grid connected PV-WT PGSs by considering different Multi Attribute Decision Making (MADM) optimization methods, which are WSM, TOPSIS, and PROMETHEE II.

The main differences between the developed approach in this chapter in comparison to the previous one presented in chapter five are: installed power of the required PGS is not fixed and or predefined, instead, it is determined through a specific power generation constraint. Moreover, three MADM algorithms have been considered, results were compared, and sensitivity analysis has been performed.

Sensitivity analysis have been performed by considering different weighting criteria techniques and vectors, with different fluctuation scenarios of wind speed and solar radiation profiles.

The proposed approach could be assumed as a powerful roadmap for decision makers, analysts, and policy makers. It can be applied either during the design of a new hybrid PGS or during the evaluation of different expansion alternatives of an already existing system.

## **6.2 System Modeling and Design Constraints**

Here, the main goal of PGS is in part to satisfy the load demand and enhance a SED. When HRE sources are abundant, the extra generated power, after having satisfied the load demand, is dumped (dump load), or on other words, no economic value will be added as an income from selling extra energy. On the contrary, when energy sources are poor, the energy shortage is fulfilled by the grid. Hence, load demand profile is an important input to be taken into consideration in formulating the problem, and is considered as known data of the system. A simple schematic diagram for the PGS is shown in figure 6.1.

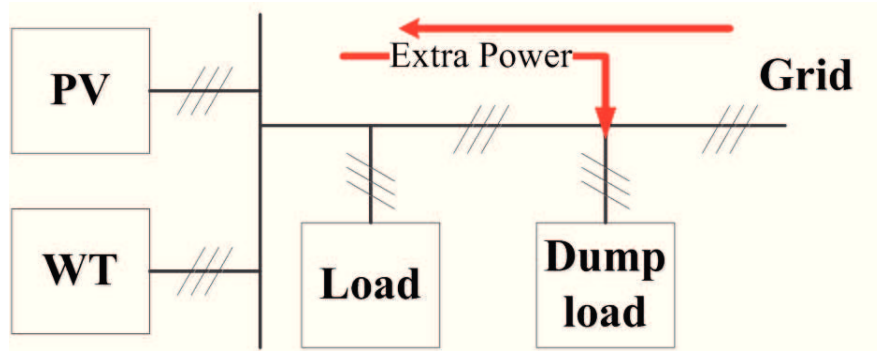


Figure 6.1: Basic configuration of a PV-WT generation system.

To simulate power output from PV and WTs, the same mathematical models described in sections 5.2.1 and 5.2.2 have been applied.

### 6.3 Design Criteria

In this chapter, different design criteria have been chosen to be optimized. Instead of using nine criteria as proposed in chapter five, the design criteria number have been reduced to three, it reflect environmental, economic, and social performance of the proposed PGS. In addition, one technical constraint has been considered to restrict the dump load annual quantity.

*Environmental criteria – emissions reduction ( $C_1$ ):*

The atmospheric pollutants such as sulphur dioxide ( $\text{SO}_2$ ) and nitrogen oxides ( $\text{NO}_x$ ) emissions reduction as a result of using HRE sources to fulfill the load instead of fossil-fueled thermal units is estimated in ton/h emission using (6.1) [48]:

$$Emss. = \alpha + \beta \sum_{t=1}^T P_{out}(t) + \gamma (\sum_{t=1}^T P_{out}(t))^2 \quad (6.1)$$

Where  $\alpha$ ,  $\beta$ , and  $\gamma$  are the coefficients approximating the generator emission characteristics,  $T$  is the analyzed period which equals 8760 hours (one year).

*Economic criteria – estimated costs (C<sub>2</sub>):*

This design criteria is calculated as the sum of initial investment, operational and maintenance, and energy bought from the grid costs minus the salvage value of the PVs and WTs. Calculation of this performance criteria, labeled in the following as EC, is achieved by using (6.2)-(6.10) [48]:

$$I_{inv.} = PV_P PV_C + WT_P WT_C \quad (6.2)$$

$$SV_{PV\_P} = PV_P PV_{SV} \left( \frac{1+\beta}{1+\gamma} \right)^{N_{PV}} \quad (6.3)$$

$$SV_{WT\_P} = WT_P WT_{SV} \left( \frac{1+\beta}{1+\gamma} \right)^{N_{WT}} \quad (6.4)$$

$$SV_{PGS\_P} = SV_{PV\_P} + SV_{WT\_P} \quad (6.5)$$

$$OM_{PV\_P} = PV_P PV_{OM} \sum_{i=1}^{N_{PV}} \left( \frac{1+\psi}{1+\gamma} \right)^i \quad (6.6)$$

$$OM_{WT\_P} = WT_P WT_{OM} \sum_{i=1}^{N_{WT}} \left( \frac{1+\psi}{1+\gamma} \right)^i \quad (6.7)$$

$$OM_{PGS\_P} = OM_{PV\_P} + OM_{WT\_P} \quad (6.8)$$

$$C_{grid} = E_{grid} E_{cost} \quad (6.9)$$

$$EC = \frac{I_{inv.} - SV_{PGS\_P} + OM_{PGS\_P}}{N_P} + C_{grid} \quad (6.10)$$

where  $I_{inv}$  is the initial investment,  $PV_C$  and  $WT_C$  are the investment costs of 1 kW power installed of PV modules and wind turbines respectively,  $SV_{PV\_P}$ ,  $SV_{WT\_P}$ ,  $SV_{PGS\_P}$  are the salvage present values of PV, WT and PSG;  $OM_{PV\_P}$ ,  $OM_{WT\_P}$ ,  $OM_{PGS\_P}$  are the operation and maintenance costs present value related to PV, WT and PGS, and  $C_{grid}$  is the cost of the required grid energy.  $PV_P$  is the PV installed power,  $PV_{SV}$  is the PV salvage value for each kW,  $PV_{OM}$  is the PV operation and maintenance costs for each kW,  $WT_P$  is the WT installed power,  $WT_{SV}$  is the WT salvage value for each kW, and  $WT_{OM}$  is the WT operation and maintenance costs for each kW.  $\beta$ ,  $\gamma$ , and  $\psi$  are inflation rate, interest rate, and escalation rate respectively.  $N_{PV}$ ,  $N_{WT}$ , and  $N_P$  are lifespan for PV, WT, and PGS project respectively.

*Social criteria – social acceptance (C<sub>3</sub>):*

Social acceptability (SA) is included as social performance evaluation criteria in order to take into consideration the social resistance as a result of estimated negative social effects related to the installation of hybrid PV-WT PGS. In this context, land use and visual impact have been included as social negative effects. Birds and bats fatality, electromagnetic interferences, acoustic noise, shadow flicker, and eco-system disturbance impact have been included as environmental negative impacts that create social resistance [92].

In this chapter, the social criteria is performed by using a fuzzy logic algorithm, where the land used area of PGS and the number of required WT are the input variables; hence, number of WTs takes into consideration the expected social and environmental negative impacts social resistance. The output of this algorithm is a social acceptance indicator measured as percentage (%), where the higher value means better performance of the PGS.

Membership functions applied to input and output system and the fuzzy surface are shown in Fig. 6.2 and Fig. 6.3 respectively, while applied fuzzy rules are shown in Tab. 6.1. Higher priority is given to PGS installation with the minimum number of WTs fitting the required power.

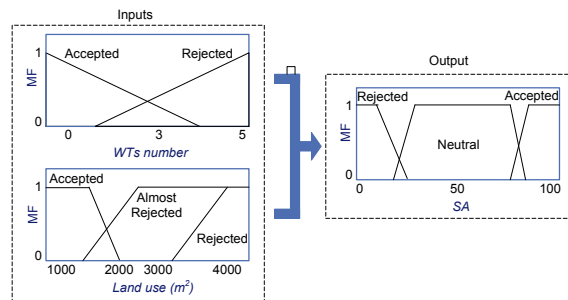


Fig. 6.2: Applied membership functions for Social Acceptance (SA).

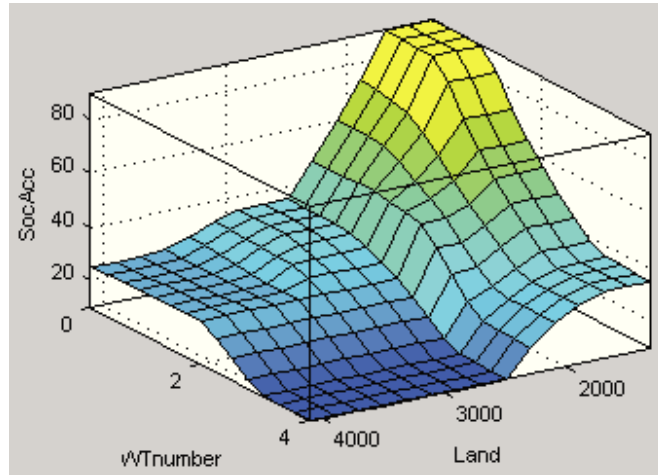


Figure 6.3: Social criteria fuzzy logic surface

Tab. 6.1: Applied rules for Social Acceptance (SA).

Rule	If (Land use)	And (WT number)	Then (SA)
1	Accepted	Accepted	Accepted
2	Almost rejected	Accepted	Neutral
3	Rejected	Accepted	Rejected
4	Accepted	Rejected	Neutral
5	Almost rejected	Rejected	Rejected
6	Rejected	Rejected	Rejected

The profiles displayed in Fig. 6.2 have been used in the proposed case study, where the maximum allowable installed WT power has been imposed to be equal to 200 kW; moreover, it is assumed to take into consideration wind turbine power systems whose power rated sizes are 10, 30, and 50 kW; as for all alternatives it is imposed the minimum number of WTs, the combination of the three wind turbine sizes with the maximum allowable installed WT power allows a maximum possible number of WTs equal to 5 (three 50 kW and two 10 kW WTs). For the land use calculation, it has been assumed that one kW of installed PV power requires 10 m<sup>2</sup> [54]. For WTs, as a rule of thumb, turbines in wind farms are usually spaced somewhere between 5 and 9 rotor diameters apart in the prevailing wind direction, and between 3 and 5 diameters apart in the direction perpendicular to the prevailing winds [93]. In this paper, due to relatively low number of installed WTs, it has been assumed that all turbines will be installed a line, thus, 7 rotor diameter has been considered between turbines, and 3 rotor diameter from each side of the

WT in the direction perpendicular to the prevailing winds. Total area required for the PGS is the sum of PV and WT required area.

However, social criteria analysis models will vary from site to site, and also from local community to another, the local community acceptance or resistance is different if the site is natural reserve, historic area, touristic site, urban, or rural. [92]. Thus, in this research, a simple social criteria model has been developed as an example of developing such models.

### *Design Constraint*

The total energy lost due to extra power generation from HRE system is minimized by imposing that such a quantity should not exceed a specific threshold THR over a defined analyzed period  $T$ , which is assumed here to be 8760 hours (1 year). Equations (6.11) and (6.12) impose this constraint:

$$TEL = \begin{cases} \sum_{t=1}^T (E_{PGS}(t) - LD(t)), & \text{if } LD(t) < E_{PGS}(t) \\ 0, & \text{else} \end{cases} \quad (6.11)$$

$$0 < TEL \leq THR \quad (6.12)$$

where TEL is the total energy lost due to extra generated power (dump load), which is provided to the grid free of charge according to the adopted system energy management strategy. Therefore, the proposed optimization approach deals with extra power as unjustified additional costs which also cause social acceptance penalty because of extra equipment installed, and so, it should be minimized.  $E_{PGS}$  is the energy generated by PGS, and  $LD$  is the load demand. Fig. 6.4 shows the graphical representation of TEL, where it is clearly visible the advantage of minimize TEL in order to reduce energy losses. The value of THR is strongly dependent on the PGS energy production and it has been considered in this study equal to 0.5% of  $E_{PGS}$ .

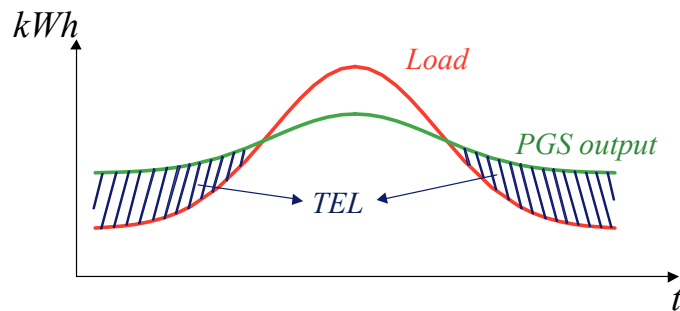


Fig. 6.4 — Graphical representation of TEL.

## 6.4 Multi Criteria Decision Making — MCDM

In this chapter, different MADM methods have been considered, WSM, TOPSIS, and PROMETHEE II algorithms were implemented through the proposed approach. In addition, SMARTER, Entropy, MSCWM, and ASCWM weighting techniques were used. All these algorithms mathematical formulation were described in section 3.2.

## 6.5 Proposed Optimal Sizing PV-WT grid connected PGSs Approach

The proposed approach allows to systematically evaluate different alternatives of grid-connected PV-WT PGSs in order to achieve the optimal design, satisfying as best as possible all criteria.

After having defined criteria and constraints that must be considered, solar radiation and wind speed, load demand and technical data regarding PV and WT power systems are needed.

Alternatives are generated, basing on a fixed step size variation of the shared power between PV and WT systems. Basically, PV-WT combinations sweep from the complete use of PV system till reaching 100% of the installed WT power system; starting from 100% dependence on PV system, the next alternative is generated by adding a certain step size to the WT power system and subtracting the same amount from PV plant, continuing on this procedure until reaching 100% dependence on WT technology. The step size value is chosen in order to achieve a suitable number of alternatives.



The next step of the design procedure is to detect the best power level associated to each PV-WT share (alternative); in fact, depending on the sharing factor,  $E_{PGS}$  profile able to better fit LD curve is different, since  $E_{PGS}$  is equal to the sum of the energy produced by the two generation plants. The initial installed power levels for each PV-WT share is assumed to be coincident to the average value of the annual load demand profile; after that, other power levels are determined considering fixed step size  $Z$  increments and decrements with respect to the initial power level. According to each power level, a simulation of the system is performed in order to determine the design constraint  $E_{PGS}$  and all criteria. Power level able to minimize TEL constraint, also satisfying the condition  $TEL < THR$ , is chosen as the optimal one for that PV-WT share. This operation is performed for each PV-WT share alternative and the results of these elaborations are transferred to the performance matrix  $X$ .

Starting from  $X$ , different weighting vectors can be defined to highlight the consistency of the optimal sizing PV-WT design solution.

In addition to SMARTER and ENTROPY weighting methods, the procedure can take into account also weighting vectors with one dominant criteria.

Known weighting vectors and performance matrix  $X$ , MCDA algorithms are applied in order to detect the optimal sizing PV-WT design configuration. The proposed procedure exploits the aforementioned MCDA algorithms in order to achieve higher confidence level of the optimal design solution.

Final step is the evaluation of the output results achieved by applying MCDA methods. Depending on the considered weighting method, different PV-WT alternatives could be candidate as the best one according to the decision makers preferences. Fig. 6.5 presents the flowchart of applying the proposed approach.

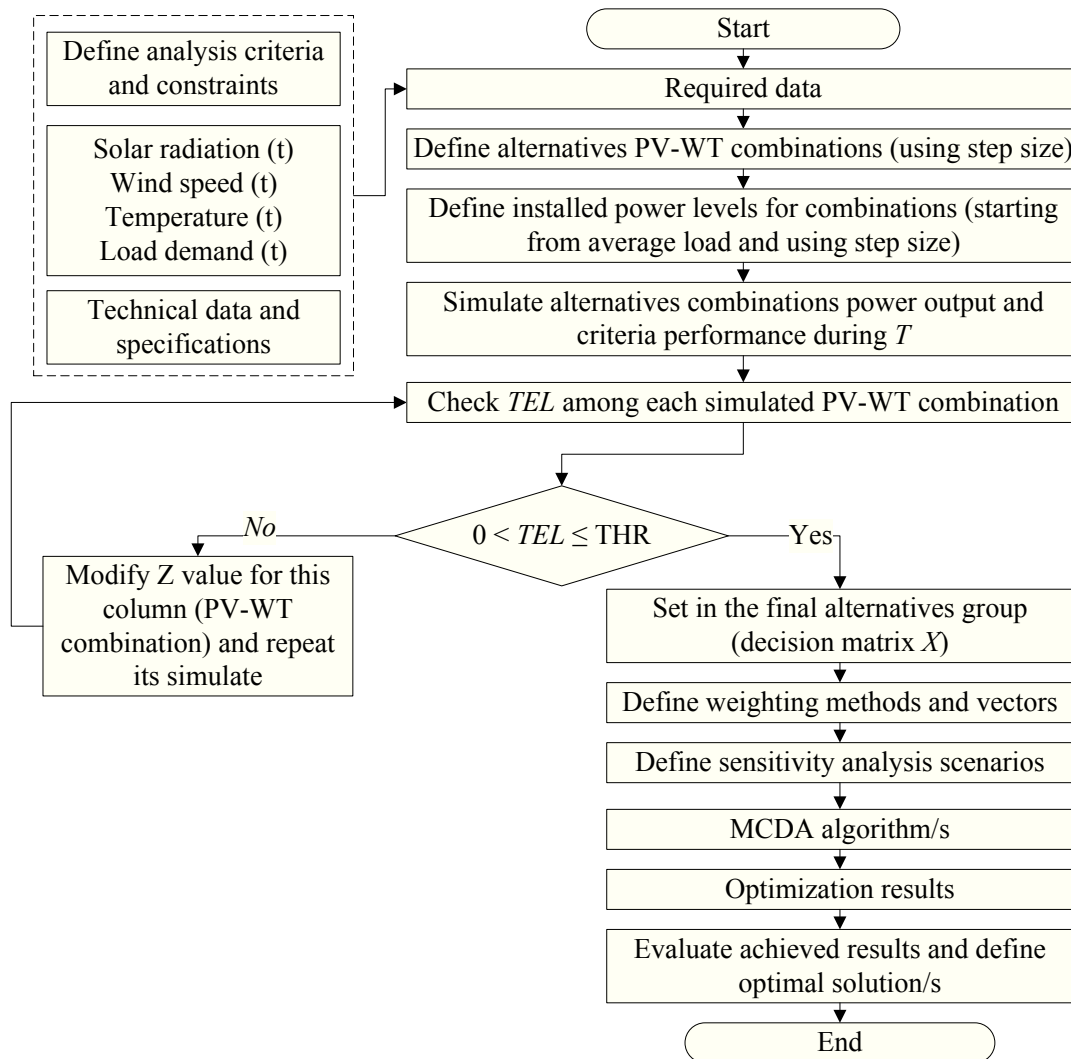


Fig. 6.5. Flowchart of the proposed optimal sizing method.

## 6.6 Results of Applying the Proposed Approach to Case Study

The proposed optimal sizing approach has been applied to real data. Wind speed, solar radiation, temperature, load demand profiles and technical data are shown in Table 6.2 and Fig. 6.6. The total annual electrical energy demand is equal to  $932.5MWh$ . PV modules and WT technical specifications are shown in Table 6.3, while other environmental and economic data used in the following study are presented in Table 6.4.

From solar radiation and wind speed profiles, it is also possible to calculate the capacity factor associated to PV modules and WTs. Capacity factor is determined by simulating the single equipment subjected to the input environmental profiles. In this case study, the capacity factor associated to PV modules is 12.6%, while that related to 10 kW, 30 kW and 50 kW WTs are 31%, 23%, and 20% respectively.

Table 6.2: Input data descriptive information

Load Profile	Peak load	base Load	Load factor
	200 kW	48 kW	55%
Weather Data	Peak value	Average value	
Wind speed	24 m/s	4.47 m/s	
Solar Radiation	955 W/m <sup>2</sup>	149.4 W/m <sup>2</sup>	

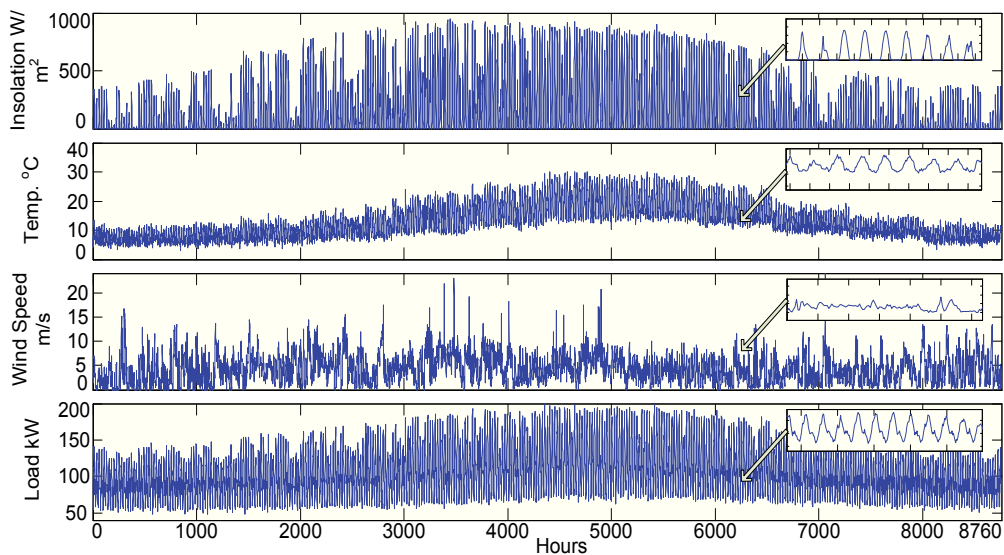


Fig. 6.6. Wind speed, solar radiation, temperature, and load demand profiles.

TABLE 6.3 WT and PV module Technical specifications

Wind Turbines			
$P_{rated} [kW]$	10	30	50
$P_{maximum} [kW]$	15	45	75
$Rotor\ diameter [m]$	8	10	12
$C_p$	0.42	0.42	0.42
$Tower\ height [m]$	12	18	18
PV modules			
$P_{max} [W]$	250		
$V_{oc} [V]$	37.6		
$V_{pm} [V]$	30.3		
$I_{sc} [A]$	8.9		
$I_{pm} [A]$	8.26		
$NOCT [^{\circ}C]$	47.5		
$K_V [1/^{\circ}C]$	-0.00351		
$K_I [1/^{\circ}C]$	0.0053		

TABLE 6.4 Technical, environmental and economic data

Grid $kWh$ price	0.12
PV $kW$ cost	3000
WT $kW$ cost	2500
PV maintenance cost per $kW$	10
WT maintenance cost per $kW$	30
Inflation rate	9%
Interest rate	12%
Escalation rate	12%
Salvage value from initial investment	10%
$\alpha$	4.091
$\beta$	-5.554
$\gamma$	6.49
$\eta_{Inv}$	0.97
$\eta_{Mech}$	0.94

Note: all costs included in this table are in Euro.

Eleven alternatives have been identified as indicated in Tab. 6.5; this number depends on the chosen step size to guarantee an acceptable resolution of the results; on the other hand, it has been experienced that a high number of alternatives could negatively affect the accuracy results, though, three MADM methods have been considered to help in detecting any inconsistency due to this phenomena.

After defining the PV-WT combinations, optimal power levels have been identified for each alternative, by simulating the PV-WT analytical models and considering a step size variations equal to 10% of the load standard deviation ( $32kW$ ).

TABLE 6.5 - Installed power of each PV-WT combinations and TEL.

Alternative		PV-WT kW	TEL kWh	E <sub>PGS</sub> MWh/year	N <sub>PV</sub>	Number of WT		
						50	30	10
A	PV100WT0	200	144	258.2	800	0	0	0
B	PV90WT10	200	497	289.6	720	0	0	2
C	PV80WT20	200	677	292.1	640	0	1	1
D	PV70WT30	170	203	237.8	476	1	0	0
E	PV60WT40	140	1046	220.5	336	1	0	1
F	PV50WT50	80	0,4	137.7	160	0	1	1
G	PV40WT60	80	188	125.4	128	1	0	0
H	PV30WT70	55	0,4	105.5	60	0	1	1
I	PV20WT80	50	0,4	99	40	0	1	1
J	PV10WT90	55	188	90.5	20	1	0	0
K	PV0WT100	50	188	84.1	0	1	0	0

Results of these simulations are transferred to the performance matrix  $X$  shown in Table 6.6. In particular, the terms listed below the column C3 indicate the social acceptance degree, while the other two columns report the emission reduction C1 and PGS costs C2.

It is interesting to note that comparing alternative A and alternative G, a considerable variation of the energy produced from the two different configurations is observed in Tab. 6.5; in fact, alternative A is able to produce almost double the annual energy of alternative G. Despite this advantage of alternative A, which will strongly improve its performance with respect to criteria C1 (table 6.6), note that G is still a nominated optimal solution due to its better performance with respect to C2 and C3. Hence, the optimal PV-WT combination can be strongly affected by criteria far from production interests, such as the social criteria.

The next step is to define the weighting vector. Choosing a suitable weighting vector is a critical issue due to its obvious effects on the optimal decision. In order to analyze the importance of weighting methods in the determination of the optimal solution, different weighting methods have been considered in this study and show in Table 6.7.

Table 6.6 - Performance matrix  $X$ .

Alternative	C1	C2	C3
A	240	124872	35
B	312	119523	26
C	331	116789	26
D	228	114970	31
E	203	110673	26
F	79	109005	46
G	70	109326	76
H	48	107384	48
I	43	107059	52
J	39	107575	89
K	34	107251	89

TABLE 6.7 - Weighting methods adopted in the case study.

Criteria	C1	C2	C3
Smarter	0.61	0.11	0.28
Entropy	0,73	0,00	0,27
ASCWM ( $q = 0.5$ )	0,67	0,06	0,27
MSCWM	0.86	0,00	0.14
Equal weights	0,33	0,33	0,33
C1 50%	0,50	0,25	0,25
C2 50%	0,25	0,50	0,25
C3 50%	0,25	0,25	0,50

It can be noticed that under some conditions where  $X$  has criteria with high performance variation and other criteria with relatively low variation, weights achieved for the later one by using *Entropy* might be almost equal to zero, like C2. This condition also affects the results achieved by applying combination weighting methods as MSCWM.

Different weighting methods of Tab. 6.7 have been purposely exploited by the MCDA algorithms treated in previous sections and the results of these elaborations are reported in Figs. 6.7 and 6.8. In particular, Fig. 6.7 shows the scores achieved applying the first four weighting methods listed in Tab. 6.7, where PROMETHEE II makes use of  $P_{value} = [20000, 1000, 25]$ .

From Fig. 6.7, the optimal alternative related to this four weighting vectors is C whenever MCDA algorithm is used, while alternatives A and B can be assumed as good solutions. Looking

at Tab. 6.7, it can be noticed that in all of the four weighting vectors, C1 is the most important criteria, very far from C2 and C3. Hence, Smarter and Entropy algorithms have given more importance to emission reduction, almost nullifying the influence of cost investment. This happen because investment cost variations among all alternatives is very limited compared to the other criteria, as clearly evident in Tab. 6.6.

Also weighting methods achieved as combination of the previous ones provide the same results.

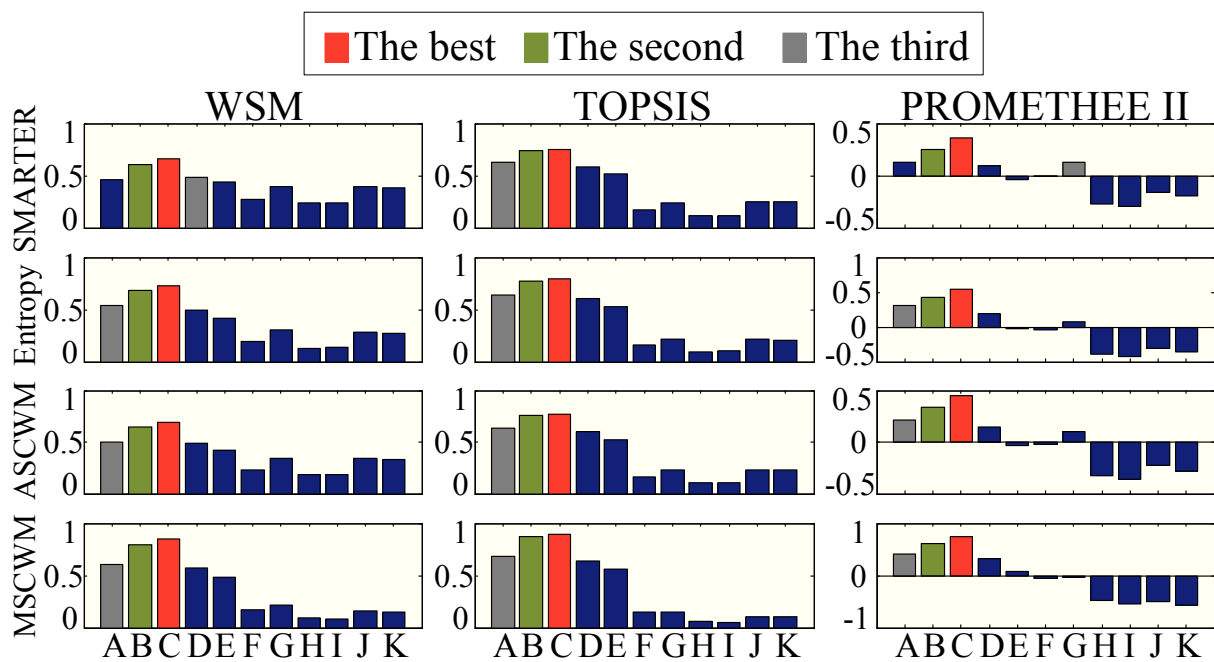


Fig. 6.7: Analysis results – subjective, objective, and combined weights.

Different results can be achieved when different weighting vectors are purposely considered in the MCDA algorithms. In particular, when higher variability weighting vectors, listed in the last four rows of Tab. 6.7 are adopted, the results of MCDA are that shown in Fig. 6.8; in this case, MCDA algorithms have been applied to  $X$  by assigning equally importance to all criteria and also considering the cases where in turn a weight of 50% is assigned to one criteria and the weights of the other two criteria is 25%. In this way, it is possible to highlight which alternatives are more affected by each selected criteria.

In this purposely created scenarios PROMETHEE and WSM provide different results compared to TOPSIS. In particular, when equal weights condition and PROMETHEE/or WSM are applied, alternatives G, J, and K can be considered as good candidate for the optimal design solution, while alternative C is the optimal PV-WT share only when weighting configuration is  $C_1$  (50%), while it is relatively weak with respect to economic and social criteria performance, as shown in  $C_2$  (50%) and  $C_3$  (50%) scenarios.

When investment cost is considered more relevant compared to the other criteria, the optimal PV-WT design solution achieved by WSM and PROMETHEE moves toward alternative K, as this is the combination minimizing PGS cost. The same alternative can be also considered the optimal one when  $C_3$  (50%) scenario is taken into consideration. In fact, PROMETHEE provides as good candidates alternative G, J and K, whose score is very close. Hence, comparing the two MCDA algorithms results, alternative K can be considered the best solution of scenario  $C_3$  (50%). Differently than WSM and PROMETHEE, TOPSIS continues to provide alternatives C as best PV-WT design configuration except when  $C_3$  (50%) is considered, showing less sensitivity to weighting coefficient variations. In the latter scenario, TOPSIS provides as best alternatives J and K, like the other two MCDA algorithms.

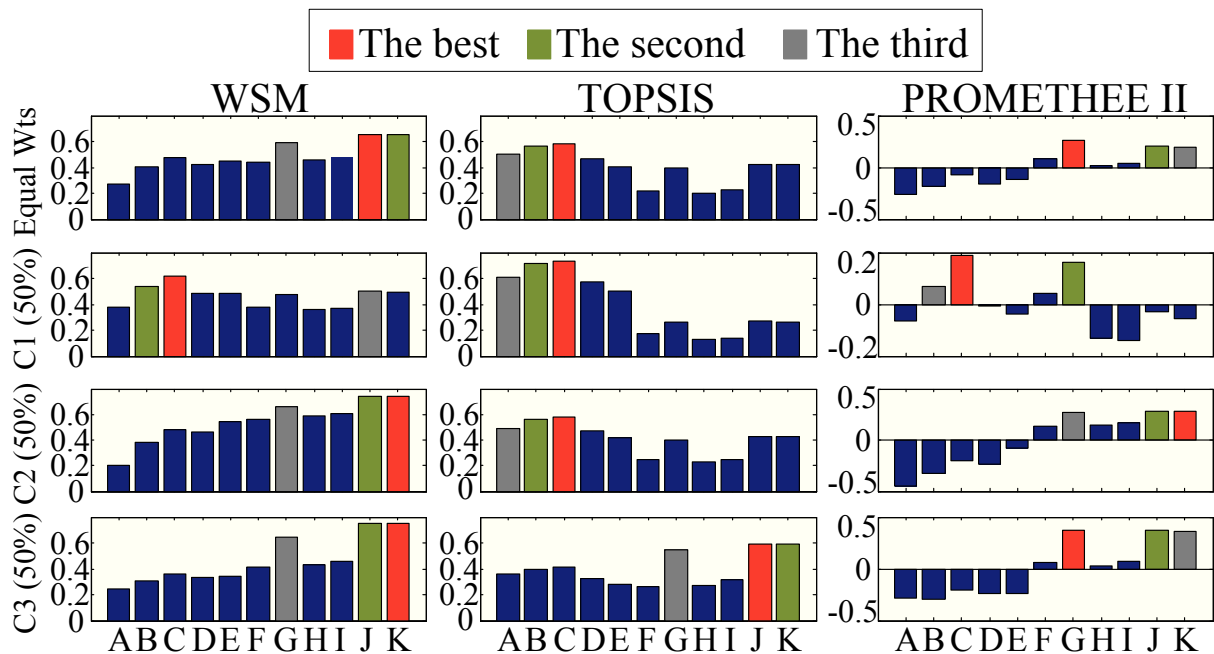


Fig. 6.8: Analysis results – equal, C1(50%), C2(50%), and C3(50%) weights.



The latter analysis can be considered as a powerful tool giving important information to the decision makers regarding how much benefits/sacrifice is gained/lost with respect to each criteria when choosing the final decision.

Finally, sensitivity analysis regarding input data has been performed by considering the effects of measured wind speed and solar radiation profiles variations; in particular, the profiles averages have been shifted by  $\pm 10\%$  assuming different weather input data combinations, as indicated in Tab. 6.8.

Tab. 6.8 - Variation of wind speed and solar radiation profiles.

Scenario	SR	WS
SH	SR + 10%	WS
SL	SR - 10%	WS
WH	SR	WS + 10%
WL	SR	WS - 10%
SH-WL	SR + 10%	WS - 10%
SL-WH	SR - 10%	WS + 10%

The results of this sensitivity analysis are shown in Fig. 6.9, considering the weighting method ASCWM. Note that, independently on MCDA algorithms and considered input data profile variations, alternative C is the best one, confirming the robustness of the solution to input data variations.

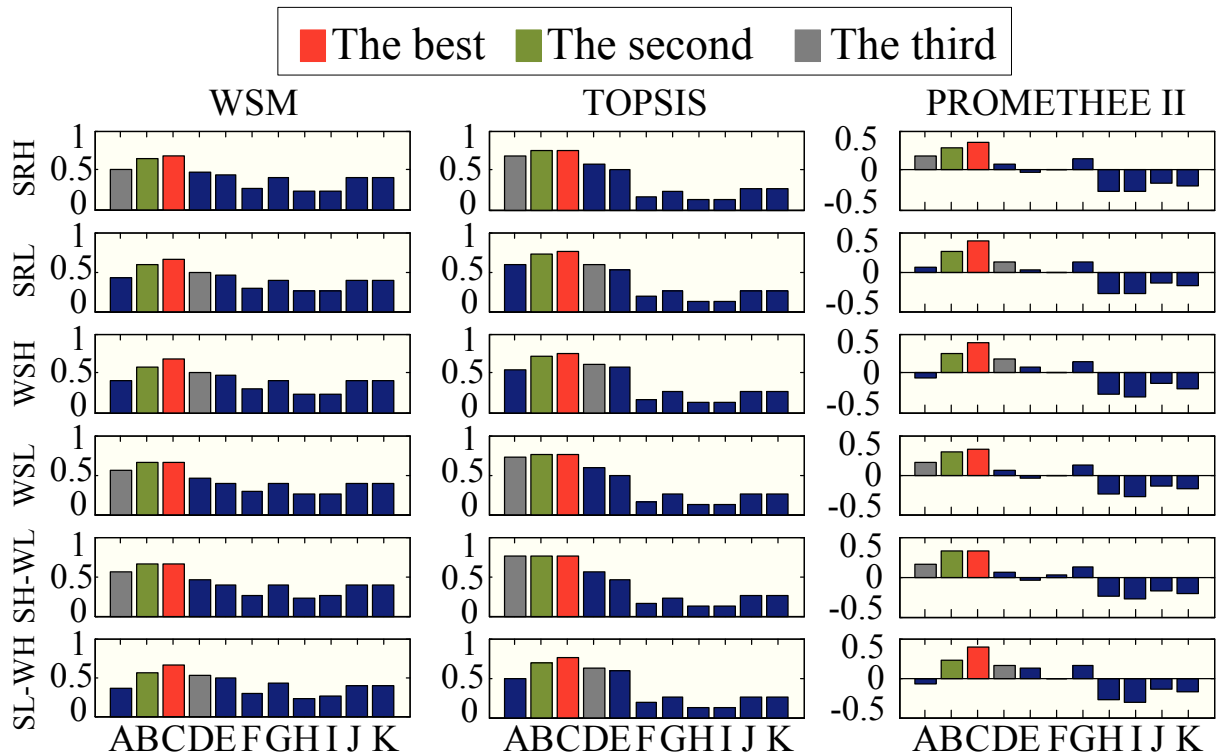


Fig. 6.9: Sensitivity analysis to wind speed and solar radiation profile variations.

## 6.7 Chapter Conclusions

Optimal sizing and combination (energy sources share) of PV-WT grid connected PGSs can be achieved by performing the proposed analysis, where different MADM algorithms exploiting different weighting methods have been applied. The proposed procedure gives decision maker flexibility to include any interesting criteria, and to test the effect of this criteria on the optimal solution under different weighting vectors and input data sensitivity scenarios. If an optimal design of hybrid power generation systems is required, it can be considered as a powerful guidance for the decision makers also to correctly justify the choice to the public opinion. Due to the simple algorithm used in defining nominated alternatives, this approach is simple, reliable, and valid for relatively small size PV-WT grid connected PGSs. However, if the PGS of interest needs to be designed with relatively higher installed power levels, or with higher number of input variable such as adding storage devices or diesel generators, a more comprehensive approach is required; which is proposed in chapter number seven.

## Chapter Seven

# *MCDM Optimal Sizing and Combination of PV-WT grid connected Systems*

## **7.1 Introduction**

This chapter deals with the optimal sizing and combination of grid connected PV-WT PGSs by considering a comprehensive Multi Criteria Decision Making (MCDM) optimization approach, in which Multi Objective Genetic Algorithm (MOGA) is used to define nominated alternatives by defining the Pareto set, then, PROMETHEE II method is applied to solve the conflict between design criteria and define the optimal solution taking into consideration decision maker preferences.

The main differences between the developed approach in this chapter in comparison to the previous one presented in chapter six are: nominated alternatives have been defined by applying Pareto Frontier principle, which is a superior method in comparison of the previous one in chapter six, especially when dealing with relatively large PGSs. In this case, there is no need to give attention to the step size or the amount of power above or below average load to be installed in the same time satisfying total energy loss constraint.

Two weather and load profiles input data scenarios have been considered, in each scenario, different solar radiation and wind speed profile were used, and for the load demand profile, in scenario number one it has been scaled to be with 200 kW maximum demand, while in scenario number two, the same load demand profile has been scaled up to be with 400 kW maximum demand. The main idea of applying two scenarios is to test proposed approach validity with relatively larger PGSs in comparison to all previous proposed case studies in chapter five and six. Another main advantage of the proposed approach in this chapter in comparison to the previous one is when higher number of input variables to be optimized ( $>2$ ), the mechanism of generating feasible solutions space more reliable, in chapter six, the input data to generate the feasible solutions are the PV and WT installed power, and it is very complicated to assume another variable such as storage devices, fuel cells, or even diesel generators. In this chapter, the feasible solutions are generated through Genetic algorithm searching mechanism, and it is easy to include more variable to the process of generating feasible solutions in addition to from PVs

and WTs, such as more power generation sources, or even more technical details with respect to the size of the power electronics equipment between the PGS and the grid.

Sensitivity analysis of MADM algorithms have been performed by considering different weighting criteria techniques with different fluctuation scenarios of wind speed and solar radiation profiles, in addition, uncertainty has been examined by applying stochastic analysis to the input weather and load profile data, thus highlighting advantages and drawbacks of the proposed optimal sizing approaches.

Similar to the previous approach, it could be assumed as a powerful roadmap for decision makers, analysts, and policy makers. It can be applied either during the design of a new hybrid PGS or during the evaluation of different expansion alternatives of an already existing system.

## **7.2 Problem Formulation**

In order to success in defining the optimal sizing and combination of PV-WT PGS, a detailed and accurate problem formulation is required, where PGS configuration must be provided as well as PV-WT analytical models, design criteria and technical constraints.

### **7.2.1 Analyzed PGS configuration**

Optimal sizing of Grid connected PGS needs to define the general power management strategy. In the following analysis, the same PGS configuration presented in section 6.2 has been assumed, where all generated power from PV-WT PGS is delivered to the grid in order to partially satisfy the daily average local load profile, and shortage will be covered from the grid. Whenever the energy produced from PV-WT is abundant with respect to that required from the load profile, extra generated energy is considered lost or with no economic value. The main goal of the design procedure is thus to fit, as much as possible the local energy load requirements.

## **7.2.2 Load Model**

In the following analysis, typical small community load profile has been assumed. It contains peak during the day and a global peak during summer. This load profile will be presented later with detailed information regarding stochastic uncertainty analysis applied on it.

## **7.2.3 PV System Mathematical Model**

To simulate power output from PV modules, the same mathematical model described in section 5.2.1 has been used.

## **7.2.4 Wind Turbine System Mathematical Model**

To simulate power output from WTs, the same mathematical model described in section 5.2.2 has been used.

## **7.2.5 Design Criteria Objective Functions**

The aforementioned models are exploited to simulate different PV-WT share combinations, indicated in the following as alternatives, starting from local historical data on solar radiation, wind speed and electrical load profiles; the selection of alternatives candidate to be the most favourable sizing solution is based on the evaluation of three objective functions which are emissions reduction, total estimated costs, and social acceptance, and it needs to be optimized simultaneously by the optimal PV-WT sharing combination. These objective functions are the same as the one described in section 6.3 before, the only difference is with the social acceptance criteria, where in this chapter, two scenarios were applied with load demand profile maximum power level equal to 200 and 400 kW, when applying the 200 kW maximum point load profile, the same social acceptance model described in section 6.3 has been used, while when considering the 400 kW maximum value load profile, the social acceptance model input variables range have been doubled to fit the case study in this scenario.

## 7.2.6 Design constraint

Similar to chapter six energy management strategy, abundant power generated from PV-WT PGS is considered uneconomic; therefore, this quantity should be minimized. This technical constraint is included in the following analysis by limiting the total energy lost during the period  $T$  (8760 hours) under a specific threshold  $THR$ . This constraint is the same as described in section 6.3.

## 7.3 Proposed Optimal Sizing of PV-WT grid connected PGSs Approach

As mentioned before in chapter three, MCDM algorithms deals with decision making problems under the presence of a number of criteria. In this chapter, Multi Objective Genetic Algorithm (MOGA) and Multi Criteria Decision Making (MCDM) optimization algorithms have been considered in defining the PV-WT PGS optimization approach.

Basically, MOGA provides feasible PV-WT sizes and combinations that fits design constraints, indicated in the following with the vector  $A$ , consisting of two variables: installed PV power and installed WT power; this vector consists of PV-WT alternatives minimizing some objective functions simultaneously; in the following analysis, the goal is to maximize the amount of reduced polluted emissions, minimize estimated costs and maximize social acceptance simultaneously, satisfying the aforementioned design criteria TEL. Hence, the vector of objective function is given by (7.1):

$$OF = (-E_{mss}, EC, -SA) \quad (7.1)$$

These functions must be optimized simultaneously under constraints related to the energy losses (7.2) and PV-WT power limits (7.3)-(7.5):

$$0 < TEL < THR \quad (7.2)$$

$$P_{min PGS} \leq PV_{inst.} + WT_{inst.} \leq P_{max PGS} \quad (7.3)$$

$$P_{min PV} \leq PV_{inst.} \leq P_{max PV} \quad (7.4)$$

$$P_{min WT} \leq WT_{inst.} \leq P_{max WT} \quad (7.5)$$

In general, the elements of vector  $A$  cannot minimize all the objective functions simultaneously in order to reach its global optimal value. So, the concept of Pareto optimum solution is used (section 3.3.5).

A feasible solution  $A_i$  is called Pareto optimal if there exists no other feasible solution  $A_j$  such that  $OF(A_j) \leq OF(A_i)$  with  $OF(A_j) < OF(A_i)$  for at least one objective function. In other words, a feasible vector  $A_i$  is called Pareto optimal when there is no other feasible solution  $A_j$  that would reduce one or more objective functions without causing a simultaneous increase in at least one other objective function.

The tracking of the optimal Pareto set is practically achieved in this study by means of MOGA, where the optimization problem starts with a random generated population of PV-WT combinations. Each nominated solution  $A_i$  in the population is evaluated by means of the objective functions. The reproduction, crossover, and mutation processes are iterated in order to evaluate a wide area of alternatives  $A_i$ . The procedure continues through several generations until the convergence criterion is satisfied and Pareto set is defined.

This algorithm usually provides a restricted number of feasible candidates to the optimal sizing and sharing PV-WT alternative, but all of them are considered with the same value.

The proposed approach can be summarized by the flowchart of Fig. 7.1, where the research of solar radiation, wind speed and load historical data is performed in the first step. The previous data can be also modified in this step in order to perform uncertainty analysis of the results. Moreover, objective functions, constraints, and system analytical model are developed, also including technical specifications of PV and WT PGSSs.

The next step to follow is the determination of the Pareto set by means of the MOGA algorithm; here, the system model is iteratively simulated in order to identify all alternatives considered valid candidate to become the optimal PV-WT PGS under the defined constraints.

The last step is to analyze the Pareto set with objective functions preference weights (sensitivity analysis) by using PROMETHEE MCDM algorithm (section 3.2); the scores achieved by applying this PROMETHEE method will help decision makers to establish which solution among Pareto set is the best one fulfilling all requirements.

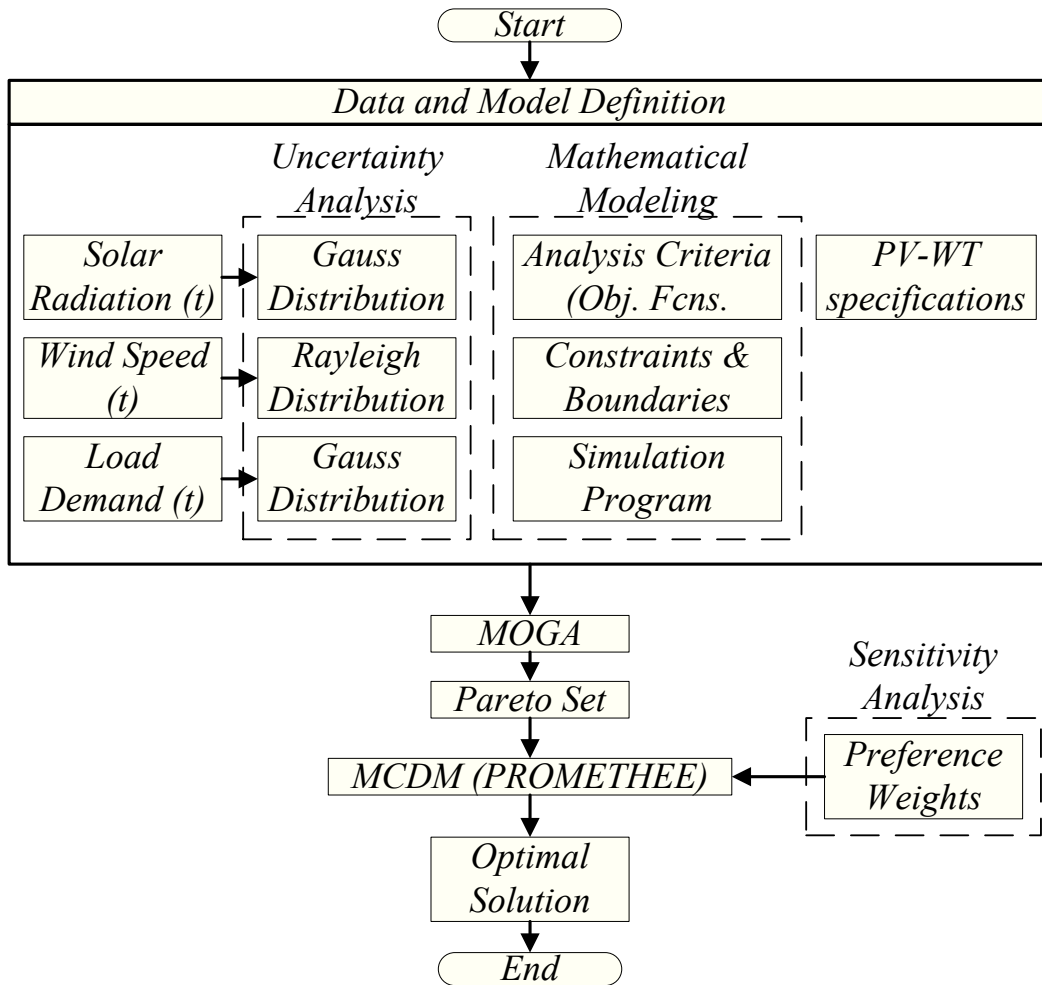


Fig. 7.1 Flowchart of the proposed optimal sizing method.

#### 7.4 Results of Applying the Proposed Approach to Case Studies

The proposed optimal sizing approach has been applied to two different scenarios. In both scenarios PV modules and WTs technical specifications are the same used in previous chapter (Tab. 6.3), while environmental and economic data are presented in (Tab. 6.4). Solar radiation, wind speed and load profiles according to both scenarios are displayed in Fig. 7.2; Moreover, as these profiles are yearly variable quantities, it could be advisable to carry out uncertainty analysis. In this work uncertainty analysis is performed by considering three additional profile sets, created by modifying the historical data through a stochastic approach; in this way, the new data set keeps the same trend (mean value and seasonality characteristics).



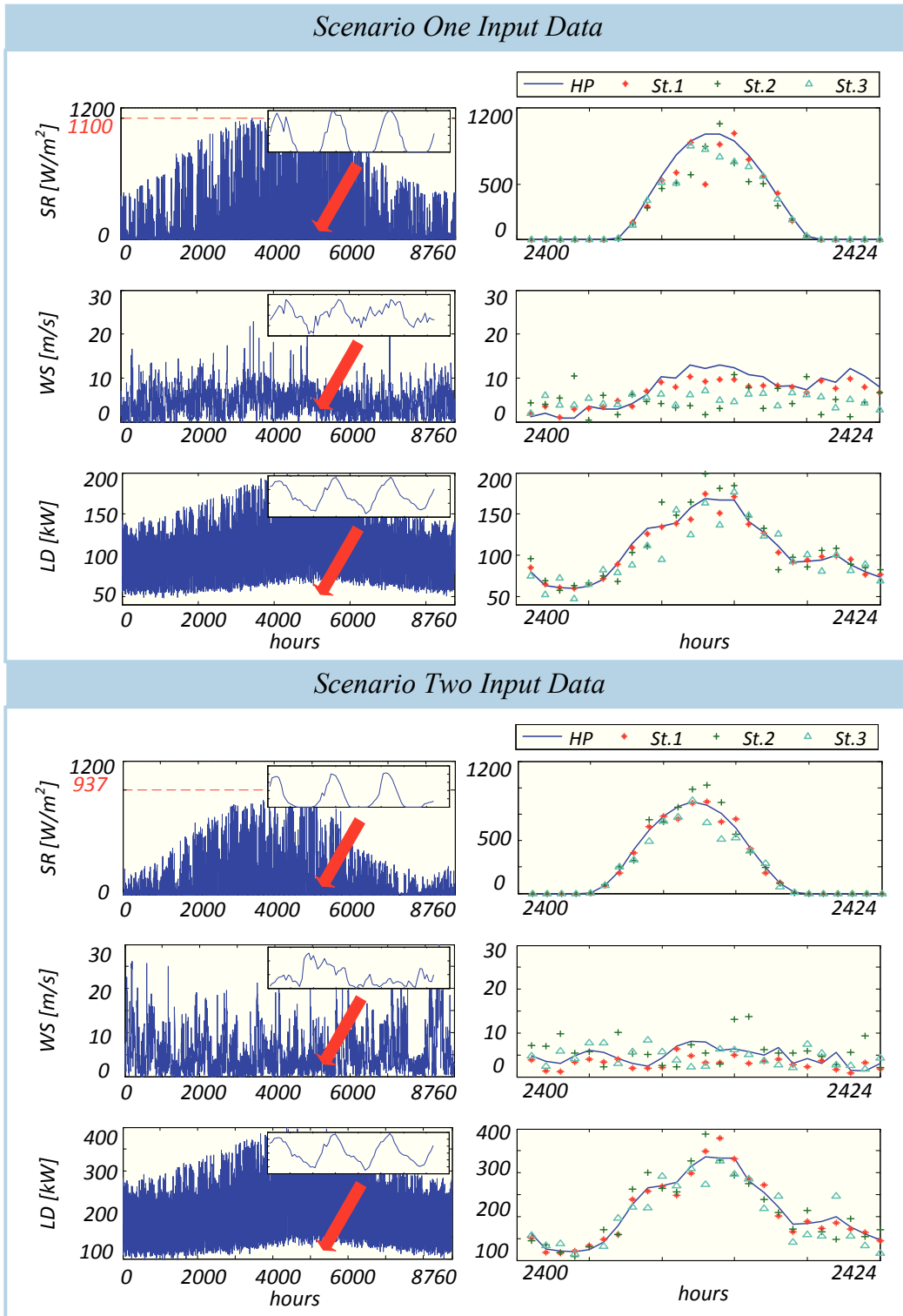


Fig. 7.2 Solar radiation, wind speed, load historical measurement & stochastically generated profiles.

Such disturbance terms are superimposed to the initial historical data set by applying a random generating number function based on Gauss probability distribution in case of the solar radiation and load profiles, while a random generating number function based on Rayleigh probability distribution is applied to the wind speed profile. A zoomed sample of the new profiles are also shown on the right hand side of Fig. 7.2, where HP is the historical measured profiles and St.1, St.2, and St.3 are the stochastic built profiles.

As previously stated, MOGA is used to select alternatives PV-WT maximizing the amount of reduced polluted emissions and social acceptance, minimizing estimated costs, and satisfying the design criteria TEL. This searching algorithm is here assumed to be subjected to the following constraints:

$$0 < TEL < 500kWh \quad (7.6)$$

$$PGS_{min kW} \leq PV_{inst.} + WT_{inst.} \leq PGS_{max kW} \quad (7.7)$$

$$PV_{min kW} \leq PV_{inst.} \leq PV_{max kW} \quad (7.8)$$

$$WT_{min kW} \leq WT_{inst.} \leq WT_{max kW} \quad (7.9)$$

where  $PGS_{min kW}$  and  $PGS_{max kW}$  are the minimum and maximum limits of installed PGS capacity respectively,  $PV_{min kW}$  and  $PV_{max kW}$  are the minimum and maximum limits of installed power of PVs;  $WT_{min kW}$  and  $WT_{max kW}$  are the minimum and maximum limits of installed power of WTs. Vector  $(PGS_{min kW}, PGS_{max kW}, PV_{min kW}, PV_{max kW}, WT_{min kW}, WT_{max kW})$  is equals to  $(30, 200, 0, 200, 0, 200)$  in case of the first scenario, while coincides with  $(60, 400, 0, 400, 0, 400)$  for the second scenario.

Relationships (7.6)-(7.9) establish the maximum energy losses and installed power range for PV and WT PGSs. Such limits are established by the decision makers on the basis of maximum investment costs and profitability. MOGA is parameterized as indicated in Tab. 7.1.

Results of the proposed procedure are presented hereafter for both scenarios. Uncertainty analysis has been carried out by considering the stochastic profiles variations indicated in Fig.7.2; in addition, a new set of solar radiation and wind speed profiles are considered, where the average values of the profiles reported in HP are modified.

Tab 7.1. Parameterization used in MOOGA.

<i>Population Size</i>	<i>20 individuals</i>
<i>algorithm</i>	<i>NSGA II</i>
<i>max. number of generations</i>	<i>400</i>
<i>Selection function</i>	<i>Tournament (tournament size = 2)</i>
<i>Crossover function</i>	<i>Intermediate (ratio = 1)</i>
<i>Mutation function</i>	<i>Adaptive feasible</i>

#### 7.4.1 Scenario one:

The results carried out from MOGA are shown in Fig. 7.3, where the upper chart presents the Pareto sets achieved by considering the input data that indicated in Fig.7.2, HP indicates the solar radiation, wind speed, and load demand measured historical data, St.1, St.2, and St.3 indicate the stochastic uncertainty analysis, while the lower one shows Pareto sets when increments of 10% and decrements of 10% of the average values of solar radiation and wind speed historical data sets are included. According to Pareto optimality principle, the PV-WT solutions related to data sets are represented in the objective functions (design criteria) space. In other words, Fig. 7.3 displays all possible alternatives using MOGA for each data set of the aforementioned input data. However, comparing alternatives performances with respect to design criteria, it could be noticed that PV-WT nominated solutions are placed in a restricted areas which are the frontiers of the feasible solutions spaces.

According to the proposed approach, PV-WT alternatives achieved through MOGA must now be submitted to PROMETHEE MCDM algorithm in order to define the best alternative among each Pareto set. Tab. 7.2 summarizes the results obtained by MOGA for the first data set HP. It shows the ration between installed PV power to WT power as a ration, and the total expected energy output from each alternative during one year operation. MCDM will be applied to the performance matrix  $X$  consisting of the last three columns of Tab. 7.2.

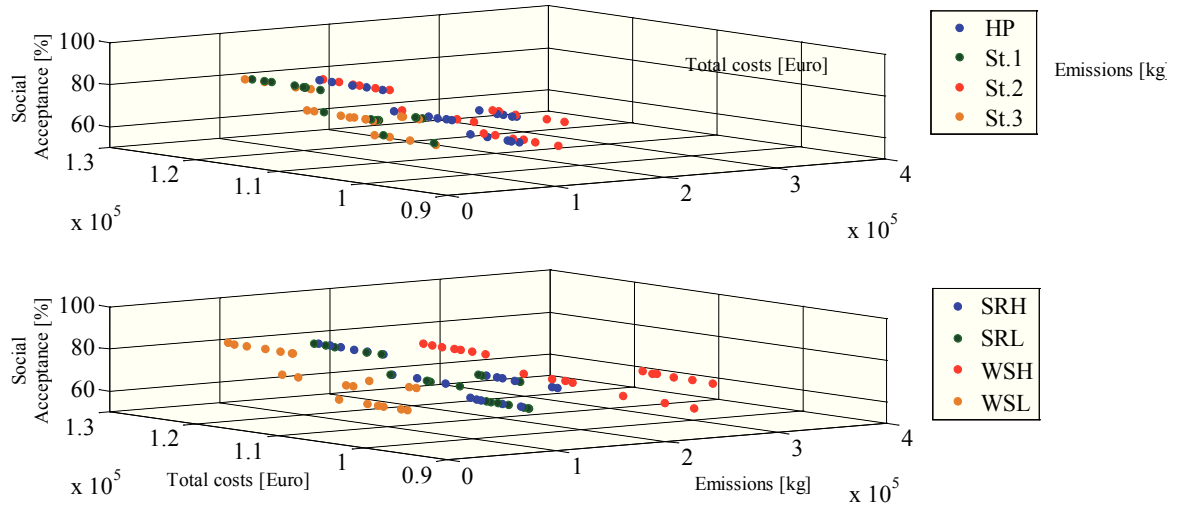


Fig. 7.3 Pareto sets, scenario 1.

Tab. 7.2: Pareto PV-WT results related to the first data set, scenario 1.

A	PV	WT50	$E_{PGS}$ kWh	$P_{PV}/P_{WT}$ ratio	Emss. [kg]	EC [Euro]	SA [%]
		WT30					
<b>A</b>	<b>188</b>	<b>2,1,0</b>	<b>280294</b>	<b>0.27</b>	<b>207970</b>	<b>108845</b>	<b>68</b>
B	180	2,0,2	274251	0.28	201737	107642	56
<b>C</b>	<b>202</b>	<b>2,1,0</b>	<b>285655</b>	<b>0.29</b>	<b>208493</b>	<b>109402</b>	<b>68</b>
D	190	2,0,1	253016	0.30	157044	109902	68
E	210	2,0,2	285472	0.31	202818	108756	56
F	230	2,1,0	296266	0.32	209532	110626	68
G	219	2,0,2	289071	0.32	203165	109299	56
H	245	2,1,0	301870	0.33	210082	111450	68
I	211	2,0,1	261083	0.33	157730	110628	68
J	209	2,0,0	235532	0.33	118217	113101	82
K	231	2,0,1	268704	0.35	158379	111763	68
L	248	2,0,1	274962	0.35	158912	112892	68
M	270	2,0,2	307827	0.36	204980	111893	56
N	299	2,1,0	321909	0.37	212053	113782	68
O	265	2,0,0	256278	0.40	119749	115147	82
P	230	2,0,2	330363	0.42	207171	114251	56
Q	300	2,0,0	269637	0.42	120741	117027	82
R	361	2,0,1	317322	0.46	162549	117472	68
S	364	2,0,0	293420	0.48	122517	119679	82
T	394	2,0,0	304649	0.49	123360	121190	82

The aim of PROMETHEE algorithm here is to support the choice of preference weights associated to the environmental, economic and social criteria; for this purpose, equal weights vector  $EW$  has been applied as default weighting technique. Moreover, in order to explore how sensitive the optimal size and share PV-WT results are to the weights and criteria (objective function), other three systematic weighting vectors have been considered. Basically, a weight of 50% has been assumed to each criteria, while a weight equal to 25% is associated to the remaining two criteria. Tab. 7.3 shows the four weight vectors.

Tab. 7.3: Applied weights according to sensitivity analysis

weighting vector	criteria		
	Emms.	EC	SA
EW	0,33	0,33	0,33
Emms. 50%	0,50	0,25	0,25
EC 50%	0,25	0,50	0,25
SA 50%	0,25	0,25	0,50

In order to define the optimal PV-WT solution, PROMETHEE MCDM algorithm has been applied to objective functions scores subjected to the preference weighting vectors of Tab. 7.3.

Results provided by MCDM analyzing the first data set (HP) are displayed in Fig. 7.4; alternatives A and C give the highest scores with all weighting vectors; in fact, by looking at Tab. 7.2, it is notable that SA performance is not the maximum for both of A and C, but, it is within the average with respect to Pareto set nominated solutions. Moreover, its Emissions and total estimated costs performances are very high and very close to the best ones. Comparing alternatives A and C against each other, it can be noticed from table 7.2 that both alternatives are identical from SA point of view and almost identical from reduced emissions and estimated costs point of view. Independently on the weighting methods, alternative A consists of 2 wind turbines of 50kW, one wind turbine of 30kW, and 188 PV modules, while alternative C consists of 2 wind turbines of 50kW, one wind turbine of 30kW, and 202 PV modules, though, both alternatives A and C can be considered an optimal design compromise.

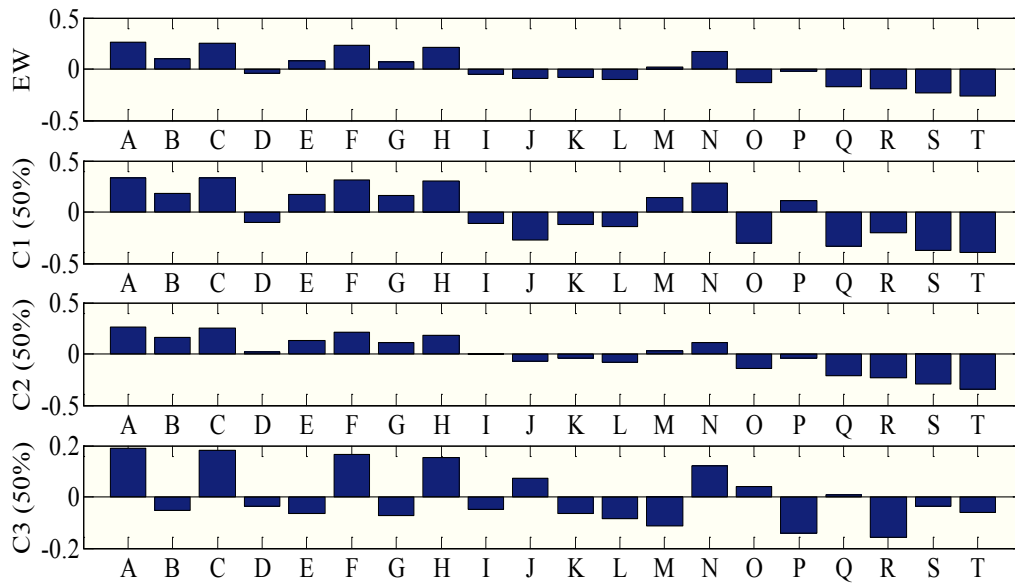


Fig. 7.4: PROMETHEE scores according to the first data set (HP), scenario 1.

Now, to accomplish an important goal of the proposed approach which is defining the optimal solution under different uncertainty and sensitivity conditions, the same analytical procedure has been applied to the remaining data sets: the optimal solution achieved for each data set, after applying PROMETHEE algorithm is also indicated. Tables 7.4 – 7.6 show the Pareto sets data of applying the same MOGA analysis procedure to St.1, St.2, and St.3 data sets which displayed in figure 7.3 upper part, and figures 7.5 – 7.7 show the results of applying PROMETHEE MCDM algorithm to the achieved results from St.1, St.2, and St.3 respectively.

Tab. 7.4: Pareto PV-WT results related to the second data set (St.1), scenario 1.

A	PV	WT50	E <sub>PGS</sub> kWh	P <sub>PV</sub> /P <sub>WT</sub> ratio	Emss. [kg]	EC [Euro]	SA [%]
		WT30					
		WT10					
<b>A</b>	<b>191</b>	<b>2,1,0</b>	<b>281529</b>	<b>0.27</b>	<b>148976</b>	<b>112302</b>	<b>68</b>
B	190	2,0,2	277996	0.29	150483	111159	56
C	210	2,0,1	260703	0.29	149482	113191	68
<b>D</b>	<b>210</b>	<b>2,1,0</b>	<b>288636</b>	<b>0.29</b>	<b>149482</b>	<b>113099</b>	<b>68</b>
E	194	2,0,1	254784	0.31	114673	113160	68
F	201	2,0,1	257450	0.32	114840	113365	68
G	201	2,0,1	257163	0.32	114822	113164	68
H	200	2,0,1	256729	0.32	114795	113031	68
I	209	2,0,0	235593	0.33	83937	115940	82
J	217	2,0,1	263313	0.33	115207	114021	68
K	252	2,0,0	251535	0.37	84791	117883	82
L	256	2,0,0	252846	0.38	84861	117994	82
M	259	2,0,0	254252	0.38	84936	118075	82
N	262	2,0,0	255215	0.39	84988	117915	82
O	338	2,0,2	333434	0.42	154474	117635	56
P	302	2,0,0	270225	0.44	85797	119292	82
Q	348	2,0,1	312461	0.44	118303	120067	68
R	348	2,0,0	287668	0.46	86742	122148	82
S	368	2,0,0	294967	0.47	87138	123080	82
T	418	2,0,0	313788	0.52	88166	124612	82

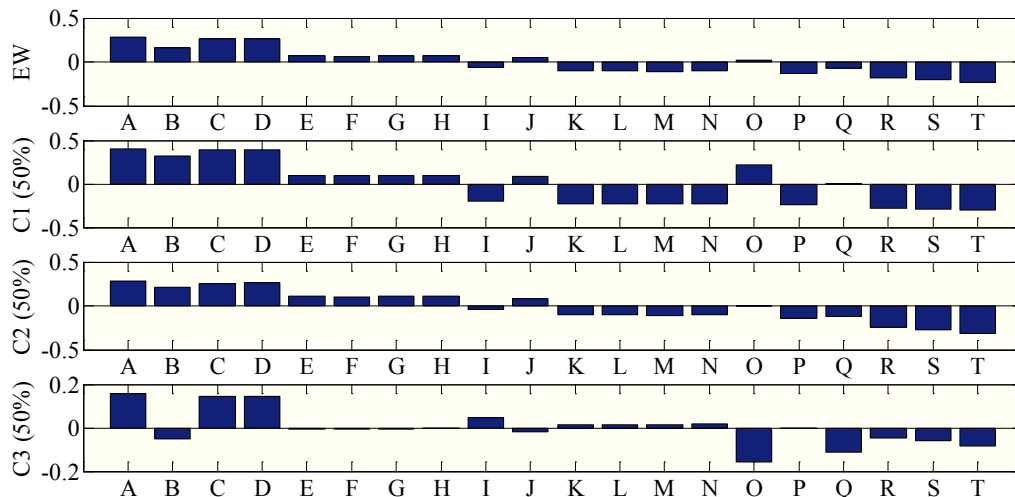


Fig. 7.5: PROMETHEE scores according to the second data set (St.1), scenario 1.

Tab. 7.5: Pareto PV-WT results related to the third data set (St.2), scenario 1.

A	PV	WT50	E <sub>PGS</sub> kWh	P <sub>PV</sub> /P <sub>WT</sub> ratio	Emss. [kg]	EC [Euro]	SA [%]
		WT30					
		WT10					
<b>A</b>	<b>92</b>	<b>2,1,0</b>	<b>244365</b>	<b>0.15</b>	<b>213956</b>	<b>103945</b>	<b>68</b>
B	109	2,0,2	247839	0.18	210893	104255	56
<b>C</b>	<b>142</b>	<b>2,1,0</b>	<b>263240</b>	<b>0.22</b>	<b>215562</b>	<b>106186</b>	<b>68</b>
D	152	2,0,1	238961	0.25	163650	108139	68
E	177	2,0,2	273199	0.26	213036	107287	56
F	210	2,0,2	285464	0.30	214076	108816	56
G	199	2,0,1	256640	0.30	164965	110313	68
H	229	2,1,0	295854	0.31	218350	110232	68
I	237	2,0,2	295748	0.32	214950	110199	56
J	210	2,0,0	235961	0.33	122768	112759	82
K	274	2,1,0	312501	0.35	219779	112445	68
L	289	2,0,2	315106	0.37	216600	112480	56
M	299	2,1,0	321995	0.37	220597	113304	68
N	259	2,0,0	254334	0.39	123952	114632	82
O	340	2,0,2	334096	0.42	218225	114033	56
P	306	2,0,0	271592	0.43	125070	116715	82
Q	228	2,0,0	280098	0.46	125623	117513	82
R	370	2,0,1	320665	0.46	169772	117451	68
S	362	2,0,0	292689	0.47	126443	119253	82
T	419	2,0,0	313997	0.52	127837	121377	82

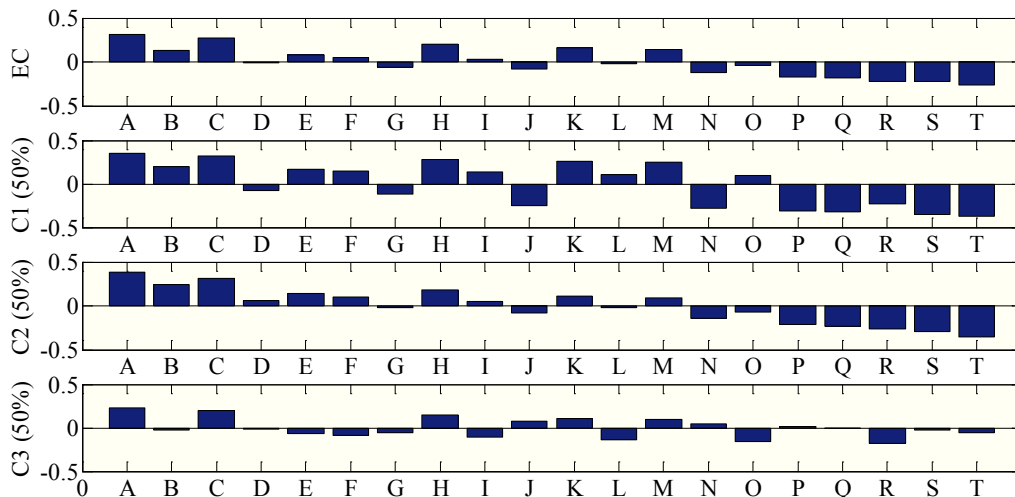


Fig. 7.6: PROMETHEE scores according to the third data set (St.2), scenario 1.



Tab. 7.6: Pareto PV-WT results related to the forth data set (St.3), scenario 1.

A	PV	WT50	E <sub>PGS</sub> kWh	P <sub>PV</sub> /P <sub>WT</sub> ratio	Emss. [kg]	EC [Euro]	SA [%]
		WT30					
		WT10					
<b>A</b>	<b>172</b>	<b>2,1,0</b>	<b>274532</b>	<b>0.26</b>	<b>142613</b>	<b>111959</b>	<b>68</b>
B	161	2,0,1	242314	0.26	109976	112683	68
C	166	2,0,2	269129	0.26	145616	110337	56
<b>D</b>	<b>212</b>	<b>2,1,0</b>	<b>289191</b>	<b>0.29</b>	<b>143634</b>	<b>114203</b>	<b>68</b>
E	182	2,0,1	250104	0.29	110452	113177	68
<b>F</b>	<b>217</b>	<b>2,1,0</b>	<b>291091</b>	<b>0.30</b>	<b>143766</b>	<b>113991</b>	<b>68</b>
G	196	2,0,1	255443	0.30	110779	114093	68
H	223	2,0,2	290233	0.31	147102	113605	56
I	213	2,0,1	261667	0.34	111160	114119	68
J	212	2,0,0	236628	0.34	80429	116709	82
K	235	2,0,1	270141	0.35	111681	115567	68
L	254	2,0,1	277053	0.37	112106	116126	68
M	269	2,0,1	282721	0.38	112456	117221	68
N	291	2,0,2	315788	0.38	148911	116192	56
O	262	2,0,0	255225	0.39	81402	118597	82
P	333	2,0,2	331484	0.42	150028	118113	56
Q	343	2,0,1	310457	0.43	114174	120683	68
R	346	2,0,0	286728	0.46	83065	122489	82
S	376	2,0,1	322954	0.47	114952	121612	68
T	413	2,0,0	311679	0.52	84393	125022	82

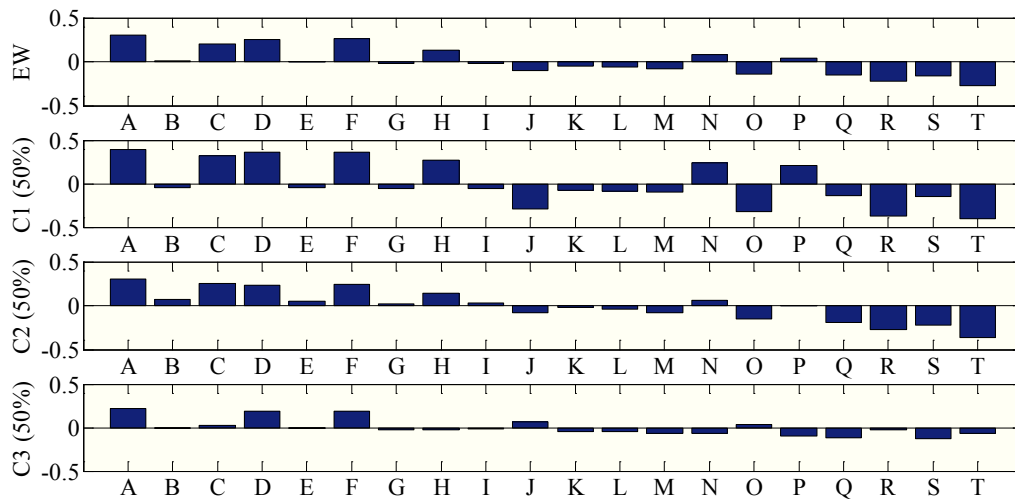


Fig. 7.7: PROMETHEE scores according to the forth data set (St.3), scenario 1.

Then, applying the same analytical procedure to the remaining SRH, SRL, WSH, and WSL data sets, tables 7.7 – 7.10 show Pareto set data obtained using MOGA algorithm. In addition, figures 7.8 – 7.11 show results of applying PROMETHEE MCDM algorithm to the Pareto sets results shown in the aforementioned tables 7.6 – 7.9.

Tab. 7.7: Pareto PV-WT results related to the fifth data set (SRH), scenario 1.

A	PV	WT50	E <sub>PGS</sub> kWh	P <sub>PV</sub> /P <sub>WT</sub> ratio	Emss. [kg]	EC [Euro]	SA [%]
		WT30					
		WT10					
<b>A</b>	<b>71</b>	<b>2,1,0</b>	<b>236667</b>	<b>0.12</b>	<b>203993</b>	<b>103588</b>	<b>68</b>
<b>B</b>	<b>81</b>	<b>2,1,0</b>	<b>240074</b>	<b>0.13</b>	<b>204356</b>	<b>104253</b>	<b>68</b>
C	175	2,0,2	272467	0.27	202209	107637	56
D	195	2,1,0	282808	0.27	208941	109262	68
E	220	2,0,2	289253	0.31	203994	110101	56
F	234	2,1,0	297646	0.32	210545	110932	68
G	213	2,0,1	261933	0.33	158496	110909	68
H	253	2,1,0	304863	0.33	211327	111704	68
I	213	2,0,0	236749	0.34	118905	113146	82
J	284	2,1,0	316329	0.36	212573	113116	68
K	287	2,0,2	314517	0.37	206696	112930	56
L	297	2,0,2	318093	0.37	207080	113585	56
M	259	2,0,0	254024	0.38	120315	115147	82
N	296	2,0,1	292745	0.40	161404	114630	68
O	336	2,0,2	332613	0.42	208642	114475	56
P	301	2,0,0	269995	0.42	121626	116929	82
Q	339	2,0,0	284257	0.45	122802	118652	82
R	378	2,0,1	323221	0.47	164307	118006	68
S	370	2,0,0	295782	0.48	123757	120021	82
T	417	2,0,0	313525	0.52	125235	121599	82

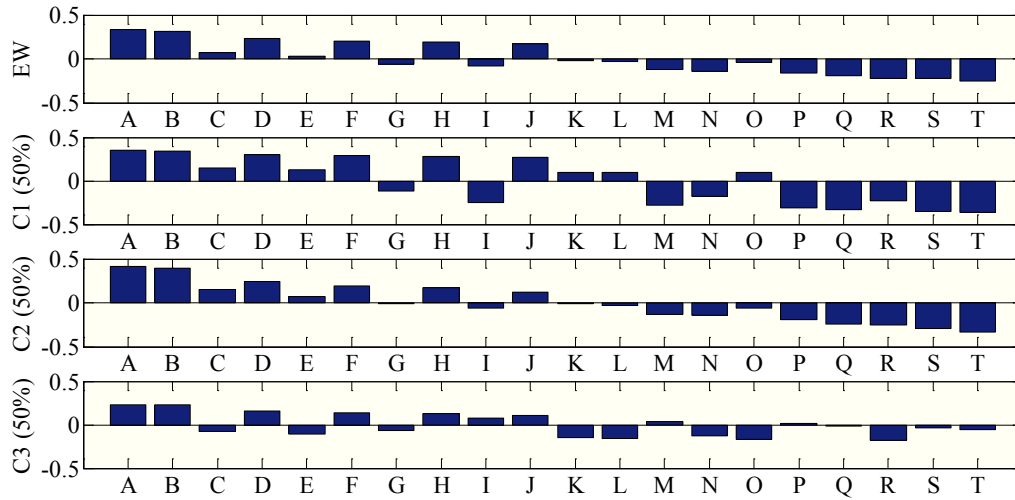


Fig. 7.8: PROMETHEE scores according to the fifth data set (SRH), scenario 1.

Tab. 7.8: Pareto PV-WT results related to the sixth data set (SRL), scenario 1.

A	PV	WT50	E <sub>PGS</sub> kWh	P <sub>PV</sub> /P <sub>WT</sub> ratio	E <sub>miss</sub> . [kg]	EC [Euro]	SA [%]
		WT30					
		WT10					
A	157	2,0,1	240973	0.26	155518	108882	68
B	160	2,0,2	266828	0.26	200440	106517	56
C	162	2,0,2	267466	0.26	200494	106584	56
<b>D</b>	<b>179</b>	<b>2,1,0</b>	<b>277085</b>	<b>0.26</b>	<b>206991</b>	<b>108389</b>	<b>68</b>
E	173	2,0,2	271747	0.27	200863	107162	56
F	205	2,0,2	283585	0.30	201885	109085	56
G	210	2,0,0	235916	0.33	117656	113187	82
H	254	2,0,2	301897	0.34	203470	111416	56
I	239	2,0,1	271427	0.34	157836	112636	68
J	246	2,0,2	298827	0.34	203204	110572	56
K	265	2,0,2	306040	0.35	203830	111994	56
L	287	2,1,0	317447	0.36	210537	113413	68
M	254	2,0,1	277175	0.37	158275	112972	68
N	300	2,1,0	322160	0.37	210954	113862	68
O	265	2,0,1	281155	0.38	158580	113175	68
P	261	2,0,0	254843	0.39	118908	115108	82
Q	343	2,0,0	285515	0.45	120950	119188	82
R	365	2,0,0	293710	0.46	161459	117803	68
S	376	2,0,0	297835	0.48	121776	120307	82
T	420	2,0,0	314589	0.52	122903	121848	82

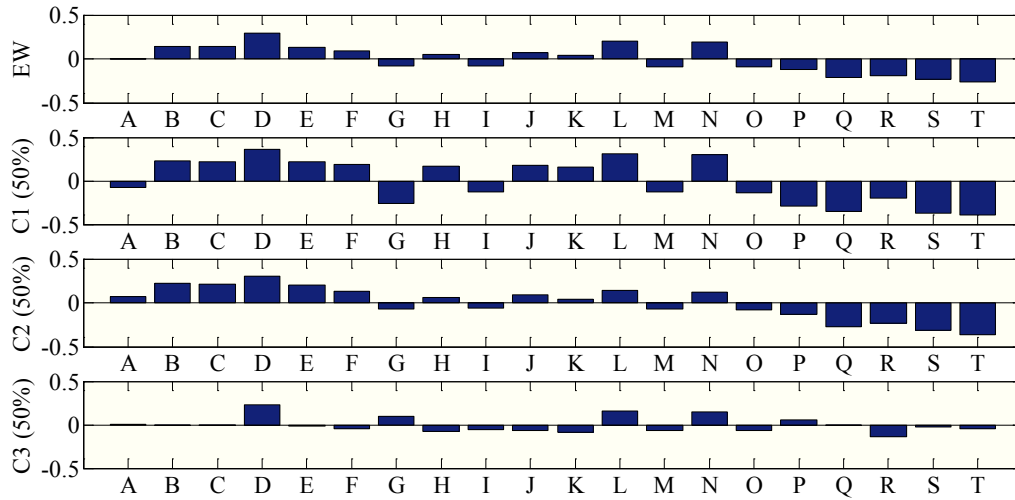


Fig. 7.9: PROMETHEE scores according to the sixth data set (SRL), scenario 1.

Tab. 7.9: Pareto PV-WT results related to the seventh data set (WSH), scenario 1.

A	PV	WT50	E <sub>PGS</sub> kWh	P <sub>PV</sub> /P <sub>WT</sub> ratio	E <sub>miss</sub> . [kg]	EC [Euro]	SA [%]
		WT30					
		WT10					
<b>A</b>	<b>81</b>	<b>2,1,0</b>	<b>240074</b>	<b>0.13</b>	<b>309296</b>	<b>98916</b>	<b>68</b>
B	94	2,0,2	241931	0.16	294998	99191	56
<b>C</b>	<b>148</b>	<b>2,1,0</b>	<b>265180</b>	<b>0.22</b>	<b>312293</b>	<b>101694</b>	<b>68</b>
D	187	2,0,2	276823	0.28	299070	103224	56
E	201	2,1,0	285080	0.28	314679	104208	68
F	203	2,0,1	257909	0.31	235563	105854	68
G	249	2,1,0	303212	0.33	316861	106501	68
H	213	2,0,0	237008	0.34	179447	108900	82
I	264	2,1,0	308698	0.34	317523	107066	68
J	229	2,0,1	267815	0.35	236594	106844	68
K	255	2,0,1	277581	0.36	237612	108609	68
L	300	2,1,0	322442	0.37	319183	108462	68
M	312	2,0,2	323861	0.39	304604	108865	56
N	262	2,0,0	255225	0.39	181103	110725	82
O	290	2,0,0	265715	0.41	182060	112217	82
P	316	2,0,0	275530	0.44	182958	113008	82
Q	339	2,0,0	283941	0.45	183729	114648	82
R	353	2,0,1	314095	0.45	241439	112473	68
S	369	2,0,0	295294	0.47	184773	115861	82
T	407	2,0,0	309551	0.51	186088	117117	82

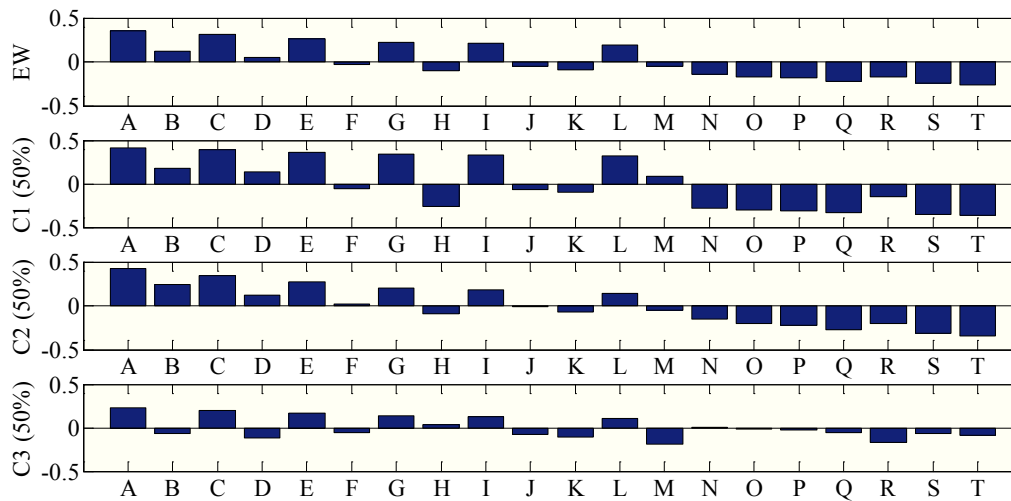


Fig. 7.10: PROMETHEE scores according to the seventh data set (WSH), scenario 1.

Tab. 7.10: Pareto PV-WT results related to the eight data set (WSL), scenario 1.

A	PV	WT50	E <sub>PGS</sub> kWh	P <sub>PV</sub> /P <sub>WT</sub> ratio	Emss. [kg]	EC [Euro]	SA [%]
		WT30					
		WT10					
<b>A</b>	<b>81</b>	<b>2,1,0</b>	<b>240074</b>	<b>0.13</b>	<b>122066</b>	<b>109586</b>	<b>68</b>
<b>B</b>	<b>111</b>	<b>2,1,0</b>	<b>251413</b>	<b>0.18</b>	<b>122915</b>	<b>110625</b>	<b>68</b>
C	124	2,0,2	253273	0.20	122829	110816	56
D	142	2,0,2	259925	0.22	123328	111634	56
E	161	2,0,1	242373	0.26	95044	113640	68
F	193	2,0,2	279252	0.28	124786	113935	56
G	179	2,0,1	248965	0.28	95480	114467	68
H	222	2,1,0	292992	0.30	126057	115715	68
I	213	2,0,2	286671	0.31	125348	114551	56
J	236	2,0,2	295169	0.32	125993	115964	56
K	222	2,0,0	240114	0.35	71311	117713	82
L	222	2,0,0	240285	0.35	71320	117702	82
M	260	2,0,0	254363	0.39	72128	119221	82
N	315	2,0,1	300140	0.41	98896	120612	68
O	336	2,0,2	332812	0.42	128871	119704	56
P	303	2,0,0	270505	0.43	73059	121163	82
Q	344	2,0,0	286047	0.45	73962	123429	82
R	377	2,0,1	323050	0.47	100445	122690	68
S	379	2,0,0	299190	0.48	74729	125036	82
T	418	2,0,0	313821	0.52	75588	125919	82

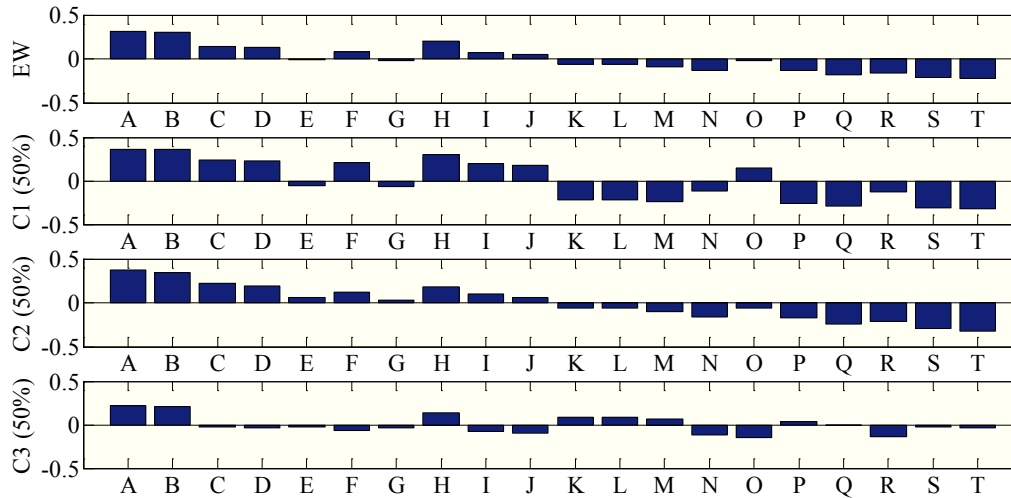


Fig. 7.11: PROMETHEE scores according to the eight data set (WSL), scenario 1.

It can be noticed that among all sensitivity and uncertainty data sets, the optimal design keeps to contain relatively low PV combined share (below 30%). All scenario one achieved optimal results with respect to all data sets are presented in table 7.11. It shows that WTs number has not been affected with different data sets uncertainty results, while PVs number has been changed significantly; it varies from 71 PV modules (17.75 kW) when considering SRH data set, to 217 modules (54.25 kW) when considering St.3 data set. By referring to table 7.2 and tables 7.4 – 7.10, for all optimal designs presented in table 7.11, SA performance equals to 68%, the only differences among all designs are between emissions reduction and estimated costs, where higher number of installed PVs increase the amount of reduced emissions but the system will cost more, and vice versa.

In this case, the designer could chose any of the optimal designs that meets his preference, either the one with the least estimated costs, maximum amount of reduced emissions, or a compromise by choosing the optimal design where the number of PVs is very close from the average number of PVs of all optimal designs presented in table 7.11, which equals to 149, so, alternative C from data set WSH will be the optimal.

Table 7.11: Optimal design summary for scenario 1 data sets.

Data set	Optimal design/s description				
	PV	WT50	WT30	WT10	Reference
HP	188	2	1	0	A from Tab. 7.2 and Fig. 7.4
	202	2	1	0	C from Tab. 7.2 and Fig. 7.4
St.1	191	2	1	0	A from Tab. 7.4 and Fig. 7.5
	210	2	1	0	D from Tab. 7.4 and Fig. 7.5
St.2	92	2	1	0	A from Tab. 7.5 and Fig. 7.6
	142	2	1	0	C from Tab. 7.5 and Fig. 7.6
St.3	172	2	1	0	A from Tab. 7.6 and Fig. 7.7
	212	2	1	0	D from Tab. 7.6 and Fig. 7.7
	217	2	1	0	F from Tab. 7.6 and Fig. 7.7
SRH	71	2	1	0	A from Tab. 7.7 and Fig. 7.8
	81	2	1	0	B from Tab. 7.7 and Fig. 7.8
SRL	179	2	1	0	D from Tab. 7.8 and Fig. 7.9
WSH	81	2	1	0	A from Tab. 7.9 and Fig. 7.10
	148	2	1	0	C from Tab. 7.9 and Fig. 7.10
WSL	81	2	1	0	A from Tab. 7.10 and Fig. 7.11
	111	2	1	0	A from Tab. 7.10 and Fig. 7.11

### 7.4.2 Scenario two

Here, the same methodology has been applied to a different solar radiation and wind speed profiles (figure 7.2 lower part), and by scaling up the load profile to 400 kW. Fig. 7.12 shows the Pareto sets achieved by applying MOGA to all pre-mentioned uncertainty scenarios. Similarly to Fig. 7.3, again, from objective functions performances point of views, PV-WT candidate solutions are placed in a very restricted area.

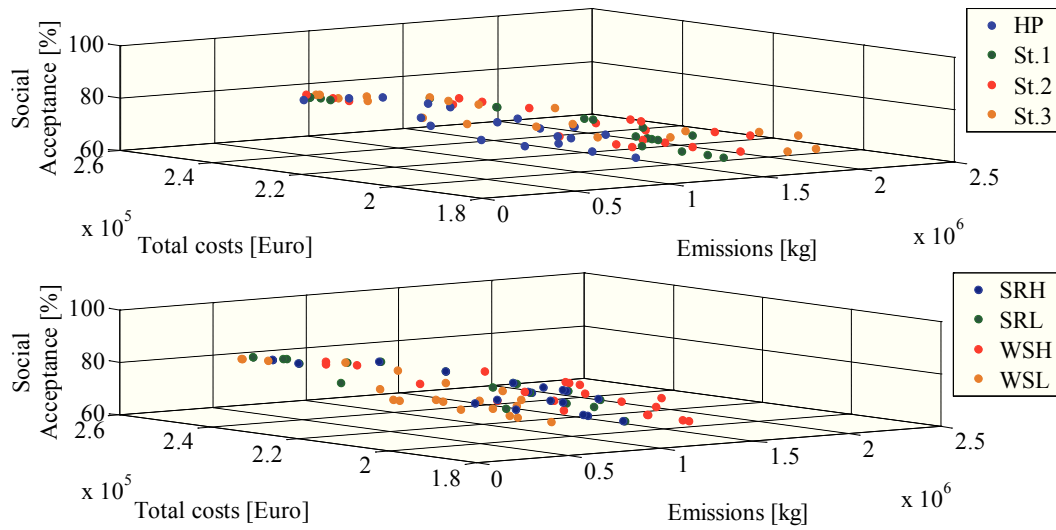


Fig. 7.12 Pareto sets, scenario 2.

Similarly to scenario number one analysis, PV-WT alternatives achieved through MOGA for all data sets presented in figure 7.12 have been submitted to PROMETHEE MCDM algorithm. For first data set (HP), the Pareto set and its related information is shown in Tab. 7.12.

Results achieved by applying PROMETHEE to HP are displayed in Fig. 7.13; in this case alternative A dominates all other alternatives in all cases except when giving 50% importance to the social acceptance criteria where alternative C becomes the optimal one. Alternative A consists of 5 wind turbine of 50kW, 2 wind turbine of 10kW, and 311 PV modules.



Tab. 7.12: Pareto PV-WT results related to the first data set (HP), scenario 2.

A	PV	WT50	E <sub>PGS</sub> kWh	P <sub>PV</sub> /P <sub>WT</sub> ratio	E <sub>miss</sub> . [kg]	EC [Euro]	SA [%]
		WT30					
		WT10					
<b>A</b>	<b>311</b>	<b>5,0,2</b>	<b>624305</b>	<b>0.23</b>	<b>1438841</b>	<b>206186</b>	<b>62</b>
B	318	5,0,0	573120	0.24	1181229	209086	74
<b>C</b>	<b>325</b>	<b>5,0,0</b>	<b>574625</b>	<b>0.25</b>	<b>1181583</b>	<b>208967</b>	<b>74</b>
D	322	4,1,0	537281	0.26	1016729	209599	74
E	374	4,1,1	574806	0.28	1136271	210494	68
F	364	4,0,2	534750	0.29	969324	211041	68
G	468	5,0,1	631715	0.31	1314964	215213	68
H	500	5,1,0	676501	0.31	1509522	215798	68
I	524	5,0,2	670100	0.33	1450667	216207	62
J	541	5,0,1	647410	0.34	1318853	218450	68
K	466	4,0,0	503990	0.36	763988	218885	82
L	536	4,1,0	583291	0.37	1026731	219606	74
M	599	5,0,0	633535	0.37	1195374	221972	74
N	570	4,0,2	579040	0.39	978755	220980	68
O	531	4,0,0	517965	0.40	728277	221801	74
P	583	4,0,0	529145	0.42	768746	224092	82
Q	750	4,0,1	591395	0.47	878045	230196	74
R	815	4,0,0	579025	0.51	778151	234465	82
S	810	3,1,1	567596	0.52	645501	236443	82
T	757	3,0,0	465605	0.55	441704	237959	82

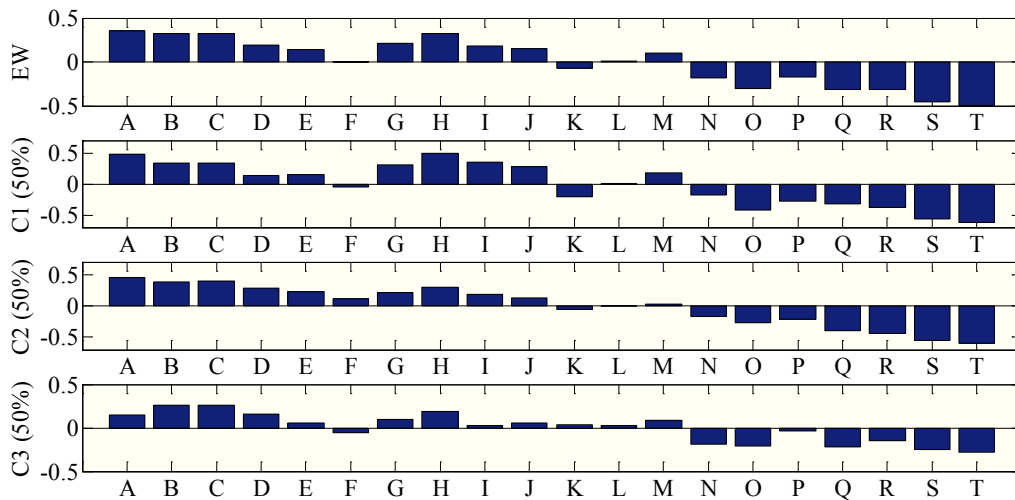


Fig. 7.13: PROMETHEE scores according to the first data set (HP), scenario 2.

Similar to the previous scenario, the same analytical procedure has been applied to the remaining data sets: the optimal solution achieved for each data set, after applying PROMETHEE algorithm is also indicated. Tables 7.13 – 7.15 show the Pareto sets data of applying the same MOGA analysis procedure to St.1, St.2, and St.3 data sets which displayed in figure 7.3 lower part, and figures 7.14 – 7.16 show the results of applying PROMETHEE MCDM algorithm to the achieved results from St.1, St.2, and St.3 respectively.

Tab. 7.13: Pareto PV-WT results related to the second data set (St.1), scenario 2.

A	PV	WT50	E <sub>PGS</sub> kWh	P <sub>PV</sub> /P <sub>WT</sub> ratio	Emss. [kg]	EC [Euro]	SA [%]
		WT30					
		WT10					
<b>A</b>	<b>304</b>	<b>5,0,2</b>	<b>622800</b>	<b>0.22</b>	<b>1723283</b>	<b>198544</b>	<b>62</b>
B	315	5,0,0	572475	0.24	1394477	202647	74
C	309	4,1,1	560831	0.25	1356238	201369	68
D	367	5,0,2	636345	0.25	1727109	202178	62
E	427	5,0,1	622900	0.29	1561278	206285	68
<b>F</b>	<b>488</b>	<b>5,1,0</b>	<b>673921</b>	<b>0.31</b>	<b>1789296</b>	<b>208152</b>	<b>68</b>
G	474	5,0,1	633005	0.31	1563999	208791	68
H	468	5,0,1	631715	0.31	1563662	207830	68
I	514	5,0,2	667950	0.33	1736037	208311	62
J	540	5,0,1	647195	0.34	1567819	211515	68
K	558	5,0,0	624720	0.36	1407751	214300	74
L	462	4,0,0	503130	0.36	901112	214416	82
M	465	4,0,0	503775	0.36	901244	214370	82
N	616	5,0,0	637190	0.38	1410892	216354	74
O	808	4,0,0	577520	0.51	916311	229757	82
P	773	3,0,0	469045	0.56	520453	235257	82
Q	823	3,0,0	479795	0.57	522107	237523	82
R	875	3,0,0	490975	0.59	523850	240003	82
S	876	3,0,0	491190	0.59	523899	239994	82
T	876	3,0,0	491190	0.59	523900	239913	82

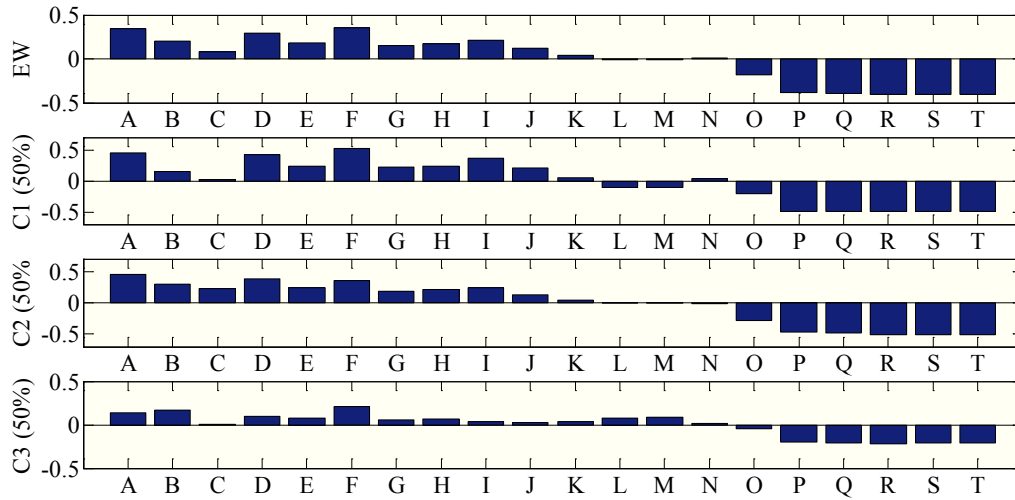


Fig. 7.14: PROMETHEE scores according to the second data set (St.1), scenario 2.

Tab. 7.14: Pareto PV-WT results related to the third data set (St.2), scenario 2.

A	PV	WT50	$E_{PGS}$ kWh	$P_{PV}/P_{WT}$ ratio	Emss. [kg]	EC [Euro]	SA [%]
		WT30					
		WT10					
<b>A</b>	<b>184</b>	<b>5,0,0</b>	<b>0.16</b>	<b>544310</b>	<b>1522823</b>	<b>192061</b>	<b>74</b>
B	300	4,1,1	0.24	558896	1506359	196404	68
C	315	4,1,0	0.26	535776	1331693	199458	74
D	362	4,0,2	0.29	534320	1298074	201025	68
E	426	4,1,1	0.30	585986	1513551	202809	68
F	500	5,1,0	0.31	676501	1972653	203083	68
G	521	5,0,2	0.33	669455	1929985	203509	62
H	446	4,0,2	0.34	552380	1302520	204667	68
I	551	5,0,0	0.35	623215	1543846	209338	74
J	450	4,0,0	0.35	500550	987941	210858	82
K	542	4,1,1	0.36	610926	1520151	207819	68
L	562	4,1,0	0.38	588881	1344879	211004	74
M	613	5,0,0	0.38	636545	1547445	211799	74
N	735	4,0,2	0.46	614515	1317821	218002	68
O	700	4,0,0	0.47	554300	999480	221815	82
P	649	3,1,0	0.48	506636	838104	221432	82
Q	817	4,0,0	0.51	579455	1004886	227050	82
R	769	3,0,0	0.56	468185	570160	233205	82
S	848	3,0,0	0.58	485170	572911	236957	82
T	979	3,0,0	0.62	513335	577532	242915	82

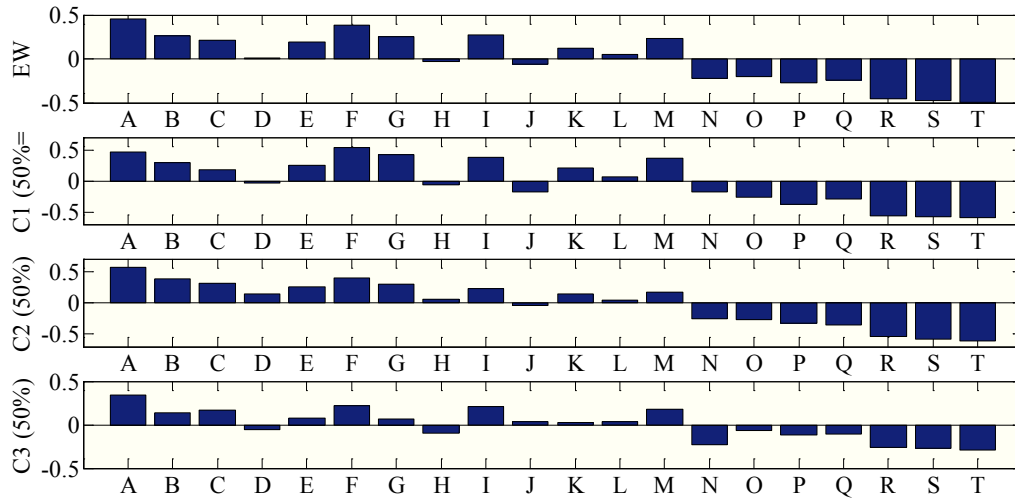


Fig. 7.15: PROMETHEE scores according to the third data set (St.2), scenario 2.

Tab. 7.15: Pareto PV-WT results related to the fourth data set (St.3), scenario 2.

A	PV	WT50	$E_{PGS}$ kWh	$P_{PV}/P_{WT}$ ratio	Ems. [kg]	EC [Euro]	SA [%]
		WT30					
		WT10					
<b>A</b>	<b>129</b>	<b>5,0,1</b>	<b>0.11</b>	<b>558830</b>	<b>1855865</b>	<b>183699</b>	<b>68</b>
<b>B</b>	<b>143</b>	<b>5,0,0</b>	<b>0.12</b>	<b>535495</b>	<b>1649414</b>	<b>187623</b>	<b>74</b>
C	275	4,1,0	0.23	527176	1443732	195246	74
D	499	5,1,0	0.31	676286	2141036	199412	68
E	538	5,0,2	0.34	673110	2102750	200181	62
F	457	4,0,0	0.36	502055	1071356	208646	82
G	609	4,1,1	0.39	625331	1657916	207554	68
H	611	4,0,1	0.43	561510	1247587	212061	74
I	573	3,1,1	0.44	516641	1061491	212283	74
J	718	4,0,2	0.45	610860	1434631	214400	68
K	637	3,1,0	0.47	504056	909044	218829	82
L	668	3,0,2	0.49	499160	883812	220162	74
M	788	3,1,0	0.52	536521	915679	225652	82
N	760	3,0,0	0.55	466250	617112	231009	82
O	881	3,1,0	0.55	556516	919781	230032	82
P	906	3,0,2	0.58	550330	894180	230553	74
Q	978	3,0,1	0.61	539465	755045	236969	82
R	915	2,1,1	0.62	489221	611071	237255	82
S	1017	3,0,0	0.64	521505	626482	242057	82
T	1033	2,1,1	0.65	514591	615332	242360	82

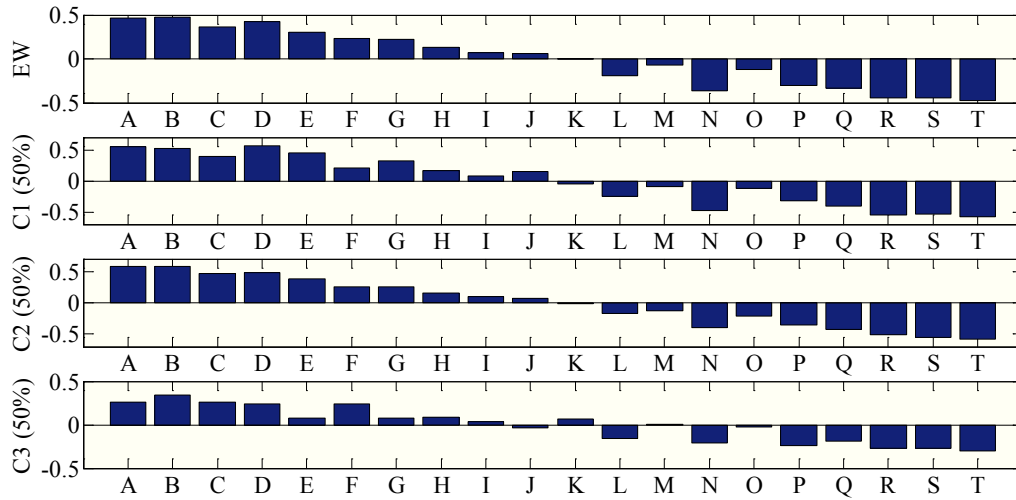


Fig. 7.16: PROMETHEE scores according to the forth data set (St.3), scenario 2.

Then, applying the same analytical procedure to the remaining SRH, SRL, WSH, and WSL data sets, tables 7.16 – 7.19 show Pareto set data obtained using MOGA algorithm. In addition, figures 7.17 – 7.20 show results of applying PROMETHEE MCDM algorithm to the Pareto sets results shown in the aforementioned tables 7.16 – 7.19.

Tab. 7.16: Pareto PV-WT results related to the fifth data set (SRH), scenario 2.

A	PV	WT50	E <sub>PGS</sub> kWh	P <sub>PV</sub> /P <sub>WT</sub> ratio	E <sub>miss</sub> . [kg]	EC [Euro]	SA [%]
		WT30					
		WT10					
<b>A</b>	<b>334</b>	<b>5,0,2</b>	<b>629250</b>	<b>0.24</b>	<b>1441966</b>	<b>207189</b>	<b>62</b>
B	334	5,0,0	576560	0.25	1183730	209861	74
C	336	5,0,0	576990	0.26	1183850	209227	74
D	340	4,1,0	541151	0.27	1019216	210853	74
E	337	4,1,0	540506	0.27	1019042	210045	74
F	435	5,0,0	598275	0.30	1189330	214491	74
<b>G</b>	<b>496</b>	<b>5,1,0</b>	<b>675641</b>	<b>0.31</b>	<b>1512190</b>	<b>215664</b>	<b>68</b>
H	389	4,0,2	540125	0.31	972288	211738	68
I	503	5,0,2	665585	0.32	1452360	215507	62
J	492	5,0,1	636875	0.32	1318910	215576	68
K	532	5,0,2	671820	0.33	1454145	216571	62
L	539	5,0,1	646980	0.34	1321661	218529	68
M	466	4,0,0	503990	0.36	765934	218841	82
N	604	5,0,0	634610	0.38	1198751	221790	74
O	590	4,0,2	583340	0.40	982397	221289	68
P	651	4,1,1	634361	0.41	1153249	223361	68
Q	815	4,0,0	579025	0.51	781531	234385	82
R	777	3,0,0	469905	0.56	444749	238502	82
S	910	3,0,0	498500	0.60	449296	244460	82
T	911	3,0,0	498715	0.60	449305	244459	82

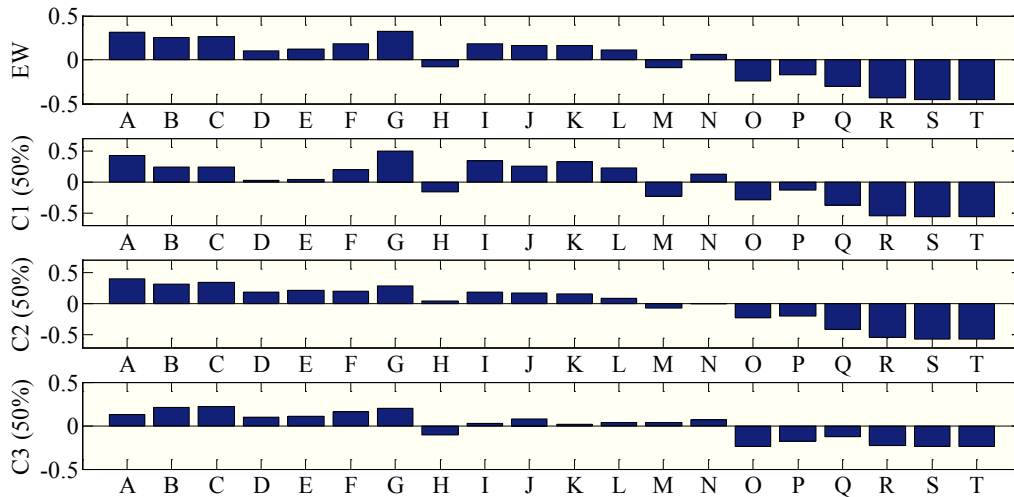


Fig. 7.17: PROMETHEE scores according to the fifth data set (SRH), scenario 2.

Tab. 7.17: Pareto PV-WT results related to the sixth data set (SRL), scenario 2.

A	PV	WT50	E <sub>PGS</sub> kWh	P <sub>PV</sub> /P <sub>WT</sub> ratio	E <sub>miss</sub> . [kg]	EC [Euro]	SA [%]
		WT30					
		WT10					
A	316	5,0,2	625380	0.23	1437334	206693	62
<b>B</b>	<b>316</b>	<b>5,0,2</b>	<b>625380</b>	<b>0.23</b>	<b>1437353</b>	<b>206567</b>	<b>62</b>
C	317	5,0,1	599250	0.23	1305260	208141	68
D	317	5,0,0	572905	0.24	1179529	208668	74
E	339	4,1,0	540936	0.27	1015917	210351	74
<b>F</b>	<b>475</b>	<b>5,1,0</b>	<b>671126</b>	<b>0.30</b>	<b>1505395</b>	<b>214988</b>	<b>68</b>
G	459	5,0,1	629780	0.31	1312015	214468	68
H	419	4,0,2	546575	0.32	969925	213805	68
I	456	4,0,0	501840	0.36	761736	218595	82
J	523	4,1,0	580496	0.36	1023643	219027	74
K	567	5,0,0	626655	0.36	1190841	220534	74
L	588	5,0,0	631170	0.37	1191775	221453	74
M	797	4,0,0	575155	0.50	774121	233713	82
N	797	3,1,0	538456	0.52	642003	235804	82
O	797	3,0,2	526895	0.54	602945	235634	74
P	759	3,0,0	466035	0.55	439400	238116	82
Q	943	3,0,1	531940	0.59	522885	244373	82
R	969	3,0,1	537530	0.61	523677	245213	82
S	993	3,0,0	516345	0.62	445865	248696	82
T	993	3,0,0	516345	0.62	445865	248696	82

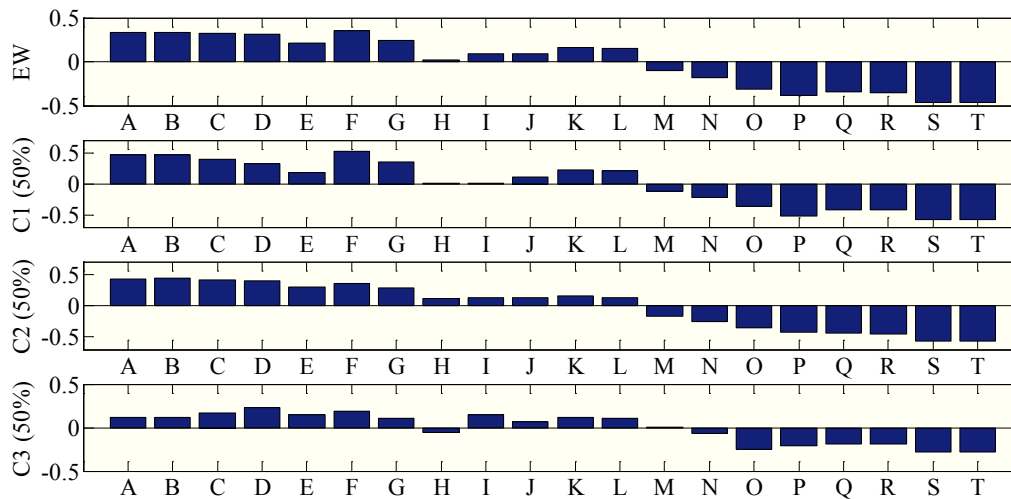


Fig. 7.18: PROMETHEE scores according to the sixth data set (SRL), scenario 2.

Tab. 7.18: Pareto PV-WT results related to the seventh data set (WSH), scenario 2.

A	PV	WT50	E <sub>PGS</sub> kWh	P <sub>PV</sub> /P <sub>WT</sub> ratio	E <sub>miss</sub> . [kg]	EC [Euro]	SA [%]
		WT30					
		WT10					
A	308	5,0,2	623660	0.22	1666171	201669	62
B	310	5,0,1	597745	0.23	1514624	202757	68
C	333	5,0,2	629035	0.24	1667687	203251	62
D	301	4,1,0	532766	0.25	1177551	204680	74
E	354	4,0,2	532600	0.28	1121313	207074	68
<b>F</b>	<b>499</b>	<b>5,1,0</b>	<b>676286</b>	<b>0.31</b>	<b>1749524</b>	<b>211364</b>	<b>68</b>
G	507	5,0,2	666445	0.32	1678079	211572	62
H	487	5,0,1	635800	0.32	1524712	211104	68
I	516	5,0,2	668380	0.33	1678593	211535	62
J	410	4,0,1	518295	0.33	1000086	210972	74
K	518	5,0,0	616120	0.34	1381412	214450	74
L	455	4,0,0	501625	0.36	885341	214963	82
M	575	5,0,0	628375	0.36	1384535	217034	74
N	608	5,0,0	635470	0.38	1386347	217811	74
O	627	4,1,1	629201	0.40	1329061	218069	68
P	698	4,0,2	606560	0.44	1138186	222718	68
Q	760	3,1,1	556846	0.50	851821	228243	74
R	755	3,0,1	491520	0.55	600723	231999	82
S	756	3,0,0	465390	0.55	511121	235147	82
T	907	3,0,1	524200	0.59	606177	239051	82

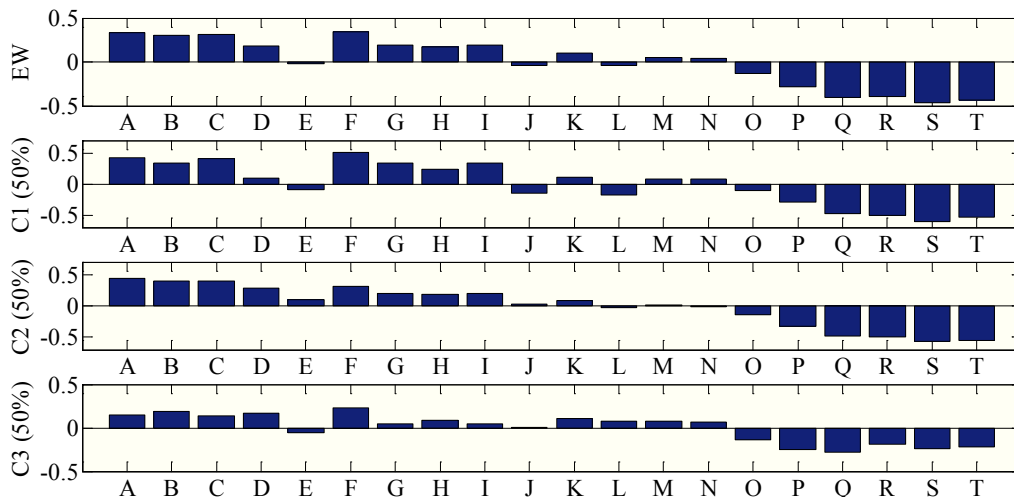


Fig. 7.19: PROMETHEE scores according to the seventh data set (WSH), scenario 2.



Tab. 7.19: Pareto PV-WT results related to the eight data set (WSL), scenario 2.

A	PV	WT50	E <sub>PGS</sub> kWh	P <sub>PV</sub> /P <sub>WT</sub> ratio	E <sub>miss</sub> . [kg]	EC [Euro]	SA [%]
		WT30					
		WT10					
<b>A</b>	<b>320</b>	<b>5,0,2</b>	<b>0.23</b>	<b>626240</b>	<b>1171792</b>	<b>212103</b>	<b>62</b>
B	326	5,0,0	0.25	574840	959511	214212	74
C	358	5,0,1	0.25	608065	1064646	215296	68
D	340	5,0,0	0.26	577850	923939	214825	68
E	364	4,0,2	0.29	534750	789988	216390	68
F	482	5,0,2	0.31	661070	1179871	219924	62
G	498	5,1,0	0.31	676071	1227671	221228	68
H	527	5,0,2	0.33	670745	1182160	221933	62
I	542	5,0,1	0.34	647625	1073437	224028	68
J	465	4,0,0	0.36	503775	621036	223581	82
K	608	5,0,0	0.38	635470	972288	227393	74
L	606	4,1,1	0.39	624686	935790	226607	68
M	643	4,1,1	0.40	632641	937423	228299	68
N	543	3,1,1	0.42	510191	594780	226415	74
O	692	4,0,2	0.44	605270	803514	230818	68
P	718	4,0,2	0.45	610860	804604	232176	68
Q	742	4,0,0	0.48	563330	631165	235800	82
R	872	3,0,1	0.58	516675	428123	244630	82
S	901	3,0,0	0.60	496565	364158	247927	82
T	901	3,0,0	0.60	496565	364158	247830	82

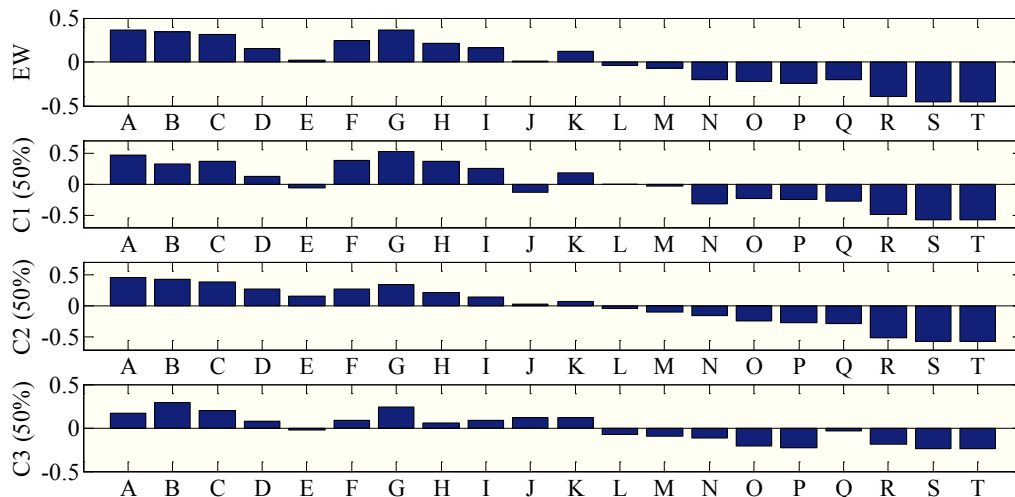


Fig. 7.20: PROMETHEE scores according to the eight data set (WSL), scenario 2.

It can be noticed that among all sensitivity and uncertainty data sets, the optimal design keeps to contain relatively low PV combined share (below 31%), which is similar to scenario number one, however, it does not mean that the proposed approach always leads to the same optimal solution, first of all, even if the optimal solution in both scenarios contains PV share equals or below 30%, the size (amount of installed power) of the PGS is different, moreover, analysis criteria in both scenarios are the same, and changing the analysis criteria will lead to different optimal solutions.

All scenario two achieved optimal results with respect to all data sets are presented in table 7.20. It shows that WTs number has been affected with different data sets uncertainty results, in all optimal solutions, five 50kW wind turbines were used, either alone or with different combinations of 30kW and 10kW WTs, however, the minimum optimal installed power in all data sets equals to 250 kW while the maximum equals to 280 kW. For PV modules, number of installed modules has been changed significantly; it varies from 129 PV modules (32.25 kW) when considering St.3 data set, to 499 modules (124.75 kW) when considering WSH data set. By referring to tables 7.12 – 7.19, for all optimal designs presented in table 7.20, C1, C2, and C3 performances are not fixed among all designs, in fact, there is slight variation between proposed designs.

The designer could chose any of the optimal designs that meets his preference, either the one with the least estimated costs, maximum amount of reduced emissions, best social acceptance index, or a compromise between all criteria. As an example, the designer could chose alternative A from HP data set which is the optimal design proposed in table 7.20, in this case, number of installed PV modules equals to 311 which is close to average number of all optimal designs presented in the aforementioned table which equals to 331, moreover, this solution considers installing five 50kW and two 10kW WTs, which is identical to five of the proposed optimal designs in table 7.20.

Table 7.20: Optimal design summary for scenario 2 data sets.

Data set	Optimal design/s description				
	PV	WT50	WT30	WT10	Reference
HP	311	5	0	2	A from Tab. 7.12 and Fig. 7.13
	325	5	0	0	C from Tab. 7.12 and Fig. 7.13
St.1	304	5	0	2	A from Tab. 7.13 and Fig. 7.14
	488	5	0	1	F from Tab. 7.13 and Fig. 7.14
St.2	184	5	0	0	A from Tab. 7.14 and Fig. 7.15
St.3	129	5	0	1	A from Tab. 7.15 and Fig. 7.16
	143	5	0	0	B from Tab. 7.15 and Fig. 7.16
SRH	334	5	0	2	A from Tab. 7.16 and Fig. 7.17
	469	5	1	0	G from Tab. 7.16 and Fig. 7.17
SRL	316	5	0	2	B from Tab. 7.17 and Fig. 7.18
	475	5	1	0	F from Tab. 7.17 and Fig. 7.18
WSH	499	5	1	0	F from Tab. 7.18 and Fig. 7.19
WSL	320	5	0	2	A from Tab. 7.19 and Fig. 7.20

## 7.5 Chapter Conclusions

Optimal sizing of PV-WT grid connected PGSs can be achieved by performing the proposed analysis, where MCDM algorithm based on MOGA – PROMETHEE methods have been applied. In comparison to the previous procedure proposed in chapter six, the new approach generates solutions more efficiently applying Pareto set principle, this advantage is necessary when the required PGS design is with relatively high installed power. In addition, the new procedure has more flexibility, it enable designers to include more input variables such as energy storage devices and technical, environmental, economic, and social constraints in a relatively easy way in comparison the previous approach. However, the drawback of this approach in comparison with the previous one is the required time for making analysis. If the required PGS design is quit simple from number of input variables and constraints, the previous approach (chapter six) is still valid as a good optimization tool, but if the considered case contains higher number of input variables and constraints, the new approach is more powerful and flexible to handle it efficiently.

## *Conclusions*

---

This research developed a Multi Criteria optimization approach to solve PV-WT PGS optimal design sources combination and system size problem. Different case studies have been applied, and results show that the MCDM algorithms can handle and solve the problem efficiently. The main conclusions of this research can be summarized as:

- Applying MCDM algorithms to the PGSs design process enables the designer to analyze multi criteria performance evaluation in simultaneously in order to define the optimal solution, thus, it is more practical in real life applications where different conflict criteria might be important in defining the optimal solution.
- It gives the user flexibility to simply interact with the analysis and modify it to fulfill his preferences and needs by introducing weighting vectors represents the importance of each criteria in defining the optimal solution.
- Defining vectors weights (criteria importance) is crucial and needs serious attention, in the analyzed case studies; it has been shown how changing these values can significantly affect final results.
- Sensitivity and uncertainty analysis are essential in the design process of PV-WT PGS; it gives deeper understanding of the results and shows the most critical parameters and variables.
- Larger PV-WT PGS are more sensitive, in which slight changes in any of the analysis inputs might change the optimal solution, and thus, more attention should be given to sensitivity and uncertainty analysis when carrying out the analysis of larger PGS.
- Social criteria is an important performance evaluation one. In the presented case studies, it has been shown that SA differences among feasible nominated alternatives can affect the final optimal solution significantly.

## References

- [1]. Abdul Rahman Mohamed, Keat Teong Lee. Energy for sustainable development in Malaysia: Energy policy and alternative energy. *Energy Policy Journal*, 2006, vol. 34, pp. 2388–2397.
- [2]. Noam Lior. Sustainable energy development: The present (2009) situation and possible paths to the future. *Energy Journal*, 2010, vol. 35, pp. 3976-3994.
- [3]. Robert A. Ristinen, Jack J. Kraushaar. *Energy and the Environment*. 1999. John Wiley & Sons, Inc.
- [4]. BP Energy Outlook 2030. Available at: <http://www.bp.com/sectiongenericarticle800.do?categoryId=9037134&contentId=7068677>. Access data: 22/10/2012.
- [5]. K. Bilena, O. Ozyurta, K. Bakırcıa, S. Karslıb, S. Erdoganc, M. Yılmaz, O. Comaklıa. Energy production, consumption, and environmental pollution for sustainable development: A case study in Turkey. *Renewable and Sustainable energy Reviews Journal*. 2008, vol. 12, pp. 1529–1561.
- [6]. The Organization of Economic Co-operation and Development (OECD). *Sustainable Development: Linking Economy, Society, and Environment*. 2008, OECD Insights.
- [7]. Y.P. Cai, G.H. Huang, Q.G. Lin, X.H. Nie, Q. Tan. An optimization-model-based interactive decision support system for regional energy management systems planning under uncertainty. *Expert systems with Applications Journal*, 2009, vol. 36, pp. 3470–3482.
- [8]. S.D. Pohekar , M. Ramachandran. Application of multi-criteria decision making to sustainable energy planning—A review. *Renewable and Sustainable energy Reviews Journal*, 2004, vol. 8, pp. 365–381.
- [9]. Theocharis Tsoutsos, Maria Drandaki, Niki Frantzeskaki, Eleftherios Iosifidis, Ioannis Kiosses. Sustainable energy planning by using multi-criteria analysis application in the island of Crete. *Energy Policy Journal*, 2009, vol. 37, pp. 1587–1600.
- [10]. Katharina Kowalski, Sigrid Stagl, Reinhard Madlener, Ines Omann. Sustainable energy futures: Methodological challenges in combining scenarios and participatory multi-

- criteria analysis. *European Journal of Operational Research*, 2009, vol. 197, pp. 1063–1074.
- [11]. Q.G. Lin, G.H. Huang. A dynamic inexact energy systems planning model for supporting greenhouse-gas emission management and sustainable renewable energy development under uncertainty—A case study for the City of Waterloo, Canada. *Renewable and Sustainable Energy Reviews Journal*, 2009, vol. 13, pp. 1836–1853.
- [12]. R. Sathiendrakumar. Greenhouse emission reduction and sustainable development. *International Journal of Social Economics*, 2003, vol. 30, pp.1233 - 1248.
- [13]. Abdeen Mustafa Omer. Energy, environment and sustainable development. *Renewable and sustainable energy Reviews Journal*, 2008, vol. 12, pp. 2265–2300 Ltd.
- [14]. Huang Liming, Emdad Haque, Stephan Barg. Public policy discourse, planning and measures toward sustainable energy strategies in Canada. *Renewable and Sustainable Energy Reviews*, 2008, vol. 12, pp. 91–115.
- [15]. V. Sánchez, J.M. Ramirez, G. Arriaga. Optimal sizing of a hybrid renewable system. *Proc. of Industrial Technology (ICIT)*, 2010. pp.: 949-954.
- [16]. Y. S. Zhao, J. Zhan, Y. Zhang, D. P. Wang and B. G. Zou. The Optimal Capacity Configuration of an Independent Wind/PV Hybrid Power Supply System Based on Improved PSO Algorithm. *Proc. of Advances in Power System Control Operation and Management APSCOM, 8th International Conference, Hong Kong, 2009*, pp. 1-7.
- [17]. Bashir M, Sadeh J. Optimal sizing of hybrid wind/photovoltaic/battery considering the uncertainty of wind and photovoltaic power using Monte Carlo. *Proc. of the 11th International Conference on Environment and Electrical Engineering (EEEIC)*, 2012. pp. 1081-1086.
- [18]. Víctor Sánchez, Juan M. Ramirez, and Gerardo Arriaga. Optimal sizing of a hybrid renewable system. *Proc. of Industrial Technology (ICIT)*, 2010. pp.: 949-954.
- [19]. Fatemeh Jahanbani Ardakani, Gholamhossein Riahy, Mehrdad Abedi. Design of an optimum hybrid renewable energy system considering reliability indices. *Proc. Of the 18<sup>th</sup> Iranian Conference on Electrical Engineering (ICEE)*, 2010, pp. 842 – 847.
- [20]. Tomonobu Senjyu, Daisuke Hayashi, Naomitsu Urasaki, Toshihisa Funabashi. Optimum Configuration for Renewable Generating Systems in Residence Using Genetic Algorithm. *IEEE Transaction on energy conversion*, 2006, vol. 21, pp. 459 - 466.

- [21]. Ying-Yi Hong, Ruo-Chen Lian, Optimal Sizing of Hybrid Wind/PV/Diesel Generation in a Stand-Alone Power System Using Markov-Based Genetic Algorithm. IEEE Transactions on power delivery, 2012, vol. 27, pp.: 640-647.
- [22]. Yang Hongxing, Zhou Wei, Lou Chengzhi. Optimal design and techno-economic analysis of a hybrid solar–wind power generation system. Applied Energy Journal vol. 86, 2009, pp. 163–169.
- [23]. Eftichios Koutroulis, Dionissia Kolokotsa, Antonis Potirakis, Kostas Kalaitzakis. Methodology for optimal sizing of stand-alone photovoltaic/wind-generator systems using genetic algorithms. Solar Energy Journal vol. 80, 2006, pp. 1072–1088.
- [24]. R. A. Gupta, Rajesh Kumar, Ajay Kumar Bansal. Economic Analysis and Design of Stand-Alone Wind/Photovoltaic Hybrid Energy System using Genetic Algorithm. Proc. of the International Conference of Computing, Communication and Applications (ICCCA), 2012, pp. 1-6.
- [25]. Hongxing Yang, Wei Zhou, Lin Lu, Zhaohong Fang. Optimal sizing method for stand-alone hybrid solar–wind system with LPSP technology by using genetic algorithm. Solar Energy journal, vol. 82, 2008, pp. 354–367.
- [26]. Y. M. Atwa, E. F. El-Saadany, M. M. A. Salama, R. Seethapathy. “Optimal Renewable Resources Mix for Distribution System Energy Loss Minimization”, IEEE Transaction on Power Systems, vol. 25, 2010. pp.: 360-370.
- [27]. Yiannis A. Katsigiannis, Pavlos S. Georgilakis, Emmanuel S. Karapidakis. “Hybrid Simulated Annealing–Tabu Search Method for Optimal Sizing of Autonomous Power Systems With Renewables”, IEEE Transaction on Sustainable Energy, vol. 3, 2012. pp.: 330-338.
- [28]. Giuseppe La Terra, Gagliano Salvina, Tina Giuseppe Marco. Optimal Sizing Procedure for Hybrid Solar Wind Power Systems by Fuzzy Logic. Proc. of the Mediterranean Electrotechnical Conference - IEEE, 2006. MELECON, pp. 865 – 868.
- [29]. M. Castañeda, L. M. Fernández, H. Sánchez, A. Cano, F. Jurado. Sizing methods for stand-alone hybrid systems based on renewable energies and hydrogen. Proc. of the Mediterranean Electrotechnical Conference (MELECON), 2012 16th IEEE, pp. 832 – 835.

- [30]. Tapas Kumar Saha, Debaprasad Kastha, “Design Optimization and Dynamic Performance Analysis of a Stand-Alone Hybrid Wind–Diesel Electrical Power Generation System”. *IEEE Transaction on Energy Conversion*, vol. 25, n° 4, 2010. pp.: 1209-1217.
- [31]. Rachid Belfkira, Cristian Nichita, Pascal Reghem, Georges Barakat. “Modeling and Optimal Sizing of Hybrid Renewable Energy System”, *proc. of Power Electronics and Motion Control Conference, EPE-PEMC 13th, Poznań, Poland, 2008* pp. 1834 – 1839.
- [32]. W.D. Kellogg, M.H. Nehrir, G. Venkataramanan, V. Gerez, “Generation Unit Sizing and Cost Analysis for Stand-Alone Wind, Photovoltaic, and Hybrid Wind/PV Systems”, *IEEE Trans. on Energy Conversion*, vol. 13, n° 1, 1998, pp. 70.
- [33]. R. Chedid, H. Akiki, Saifur Rahman, “A Decision Support Technique for the Design of Hybrid Solar –Wind Power Systems”, *IEEE Transactions on Energy Conversion*, vol. 13, n° 1, 1998, pp. 76 - 83.
- [34]. A. Kaabeche, M. Belhamel, R. Ibtouen. Sizing optimization of grid-independent hybrid photovoltaic/wind power generation system. *Energy Journal*. vol. 36, 2011, pp. 1214-1222.
- [35]. Rachid Belfkira, Lu Zhang, Georges Barakat. Optimal sizing study of hybrid wind/PV/diesel power generation unit. *Solar Energy Journal*. vol. 85, 2011, pp. 100–110.
- [36]. Fatih O. Hocaoglu, Omer N. Gerek, Mehmet Kurban. A novel hybrid (wind–photovoltaic) system sizing procedure. *Solar Energy Journal*, vol. 83, 2009, pp. 2019–2028.
- [37]. D.B. Nelson, M.H. Nehrir, C. Wang. Unit sizing and cost analysis of stand-alone hybrid wind/PV/fuel cell power generation systems. *Renewable Energy Journal*, vol. 31, 2006, pp. 1641–1656.
- [38]. G. Liu, M. G. Rasul, M. T. O. Amanullah, M. M. K. Khan. Economic and Environmental Modeling of a Photovoltaic-Wind-Grid Hybrid Power System in Hot Arid Australia. *International Journal of Thermal & Environmental Engineering*, vol. 1, No. 1, 2010, pp. 15-22.
- [39]. Ali Naci Celik. Techno-economic analysis of autonomous PV-wind hybrid energy systems using different sizing methods. *Energy Conversion and Management Journal*. vol. 44, 2003, pp. 1951–1968.



- [40]. R. Luna-Rubio, M. Trejo-Perea, D. Vargas-Va'zquez, G.J. Ri'os-Moreno. Optimal sizing of renewable hybrids energy systems: A review of methodologies. *Journal of Solar Energy*, vol. 86, issue 4, 2012, pp. 1077-1088.
- [41]. V. Lazarov, G. Notton, L. Stoyanov. Grid-Connected Multi-Source System Sizing. *Proc. of 8th International Symposium on Advanced Electromechanical Motion Systems & Electric Drives Joint Symposium, ELECTROMOTION*, 2009, pp. 1-5.
- [42]. S.C.Gupta, Y.Kumar, Gayatri Agnihotri. Optimal Sizing of Solar-Wind Hybrid System. *Proc. of IET-UK International Conference on Information and Communication Technology in Electrical Sciences (ICTES)*, 2007, pp. 282 - 287.
- [43]. M. Mousavi Badejani, M.A.S. Masoum and M. Kalanta. Optimal Design and Modeling of Stand-Alone Hybrid PV-Wind Systems. *Proc. of Australasian Universities Power Engineering Conference (AUPEC)*. 2007, pp. 1-6.
- [44]. W. Kellogg, M.H. Nehrir, G. Venkataramanan, V. Gerez. Optimal unit sizing for a hybrid wind/photovoltaic generating system. *Electric Power Systems Research journal*, vol. 39, 1996, pp. 35-38.
- [45]. M.H. Zamani, G.H. Riahy. Introducing a new method for optimal sizing of a hybrid (wind/PV/battery) system considering instantaneous wind speed variations. *energy for Sustainable Development Journal*, 2008, vol. 12, pp. 27–33.
- [46]. S. Diaf, D. Diaf, M. Belhamel, M. Haddadi, A. Louche. A methodology for optimal sizing of autonomous hybrid PV/wind system. *Energy Policy Journal*, vol. 35, 2007, pp. 5708–5718.
- [47]. Riad Chedid, Saifur Rahman. Unit sizing and Control of Hybrid Wind-Solar Power Systems. *IEEE Transactions on Energy Conversion*, Vol. 12, No. 1, 1997. pp. 70-85.
- [48]. Lingfeng Wang, Chanan Singh, “Multicriteria Design of Hybrid Power Generation Systems Based on a Modified Particle Swarm Optimization Algorithm”. *IEEE Transactions on Energy Conversion*, vol. 24, n° 1, March 2009.
- [49]. Y.A. Katsigiannis, P.S. Georgilakis, E.S. Karapidakis, “Multiobjective genetic algorithm solution to the optimum economic and environmental performance problem of small autonomous hybrid power system with renewable”, *IET Renewable Power Generation* 4 (5), 2010, pp. 404–419.
- [50]. Vaughn Nelson. *Introduction to Renewable Energy*. 2011. CRC press.

- [51]. Dictionary of Engineering. 2003. 2nd edition, McGRAW-HILL.
- [52]. IEEE Electrical Engineering Dictionary. 2000. CRC press LCC.
- [53]. Robert U Ayres, Robert Costanza, Jose Goldemberg, Marija D Ilic. Encyclopedia of Energy. 2004. Elsevier.
- [54]. Zekai Sen. Solar Energy Fundamentals and Modeling Techniques: Atmosphere, Environment, Climate Change and Renewable Energy. Springer. 2008.
- [55]. Volker Quaschnig. Understanding Renewable Energy Systems. 2005. Earthscan.
- [56]. US Department of Energy. Energy Efficiency and Renewable energy. Available at: [http://www.eere.energy.gov/basics/renewable\\_energy/pv\\_systems.html](http://www.eere.energy.gov/basics/renewable_energy/pv_systems.html). Last visit: 13/10/2012.
- [57]. US Department of Energy. Energy Efficiency and Renewable energy. Available at: <http://www.eere.energy.gov/basics/glossary.html>. Last visit: 13/10/2012.
- [58]. John Twiddel, Tony Weir. Renewable energy Resources, 2nd edition. 2006. Taylor and Francis.
- [59]. S.D. Pohekar, M. Ramachandran. Application of multi-criteria decision making to sustainable energy planning—A review. *Journal of Renewable and Sustainable Energy Reviews*. 2004, vol. 8, pp. 365–381.
- [60]. Edwards W, Barron FH, Smarts and smarter: improved simple methods for multi-attribute utility measurement. *Organizational Behavior and Human Decision Processes*. *Journal of Organizational Behavior and Human Decision Processes*, 1994, vol. 60, pp. 306–325.
- [61]. R. Venkata Rao, “Decision Making in the Manufacturing Environment: Using Graph Theory and Fuzzy Multiple Attribute Decision Making Methods”, 2007, Springer.
- [62]. Jovanovic M, Afgan N, Radovanovic P, Stevanovic V. Sustainable development of the Belgrade energy system. *Energy Journal*, 2009, vol. 34, pp. 532–539.
- [63]. Afgan NH, Carvalho MG. Multi-criteria assessment of new and renewable energy power plants. *Energy Journal*. 2002, vol. 27, pp. 739–755.
- [64]. Afgan NH, Carvalho MG. Sustainability assessment of hydrogen energy systems. *International Journal of Hydrogen*. *Energy Journal*. 2004, vol. 29, pp. 1327–1342.
- [65]. Afgan NH, Carvalho MG. Sustainability assessment of a hybrid energy system. *Energy Policy Journal*. 2008, vol. 36, pp. 2903–2910.

- [66]. Gwo-Hshiong Tzeng, Cheng-Wei Lin, Serafim Opricovic. Multi-criteria analysis of alternative-fuel buses for public transportation. *Energy Policy Journal*, 2005, vol. 33, pp. 1373-1383.
- [67]. Fausto Cavallaro. Fuzzy TOPSIS approach for assessing thermal-energy storage in concentrated solar power (CSP) systems. *Applied Energy Journal*, 2010, vol. 87, pp. 496-503.
- [68]. Goumas M, Lygerou V. An extension of the PROMETHEE method for decision making in fuzzy environment: Ranking of alternative energy exploitation projects. *European Journal of Operational Research*, 2000, vol. 123, pp. 606–13.
- [69]. Diakoulaki D, Karangelis F. Multi-criteria decision analysis and cost-benefit analysis of alternative scenarios for the power generation sector in Greece. *Renewable and Sustainable Energy Reviews Journal*, 2007, vol. 11, pp. 716–27.
- [70]. Madlener R, Kowalski K, Stagl S. New ways for the integrated appraisal of national energy scenarios: the case of renewable energy use in Austria. *Energy Policy Journal*, 2007, vol. 35, pp. 6060–74.
- [71]. Goumas MG, Lygerou VA, Papayannakis LE. Computational methods for planning and evaluating geothermal energy projects. *Energy Policy Journal*, 1999, vol. 27, pp. 147–54.
- [72]. Haralambopoulos DA, Polatidis H. Renewable energy projects: structuring a multi-criteria group decision-making framework. *Renewable Energy Journal*, 2003, vol. 28, pp. 961–73.
- [73]. Singiresu S. Rao. *Engineering Optimization Theory and Practice*. 4th edition. 2009. John Wiley & Sons, Inc.
- [74]. Edwin K. P. Chong. Stanislaw H. Zak. *An Introduction to Optimization*. 2nd edition. 2001. John Wiley & Sons, Inc.
- [75]. Mitsuo Gen, Runwei Cheng. *Genetic Algorithms and Engineering Optimization*. 2000, John Wiley & Sons, Inc.
- [76]. Yogesh Jalaria. *Design and Optimization of thermal systems*. Second edition. 2008. CRC Press. Taylor and Francis Group.
- [77]. Fausto Cavallaro, Luigi Cirraolob. A multicriteria approach to evaluate wind energy plants on an Italian island. *Energy Policy Journal*, vol. 33, 2005, pp. 235–244.

- [78]. Athanasios I. Chatzimouratidis, Petros A. Pilavachi. Multicriteria evaluation of power plants impact on the living standard using the analytic hierarchy process. *Energy Policy Journal*, vol. 36, 2008, pp. 1074–1089.
- [79]. Marko Liposcak, Naim H. Afgana, Neven Duic, Maria da Graca Carvalho. Sustainability assessment of cogeneration sector development in Croatia. *Energy journal*, vol. 31, 2006, pp. 2276–2284.
- [80]. Mousa S. Mohsen, Bilal A. Akash. Evaluation of Domestic Solar Water Heating System in Jordan Using Analytic Hierarchy Process. *Energy Conversion and Management Journal*, vol. 38, 1997, pp. 1851-1822.
- [81]. Rustom Mamlook, Bilal A. Akash, Salem Nijmeh. Fuzzy Sets Programming to Perform Evaluation of Solar Systems in Jordan. *Energy Conversion and Management Journal*, vol. 42, 2001, pp. 1717-1726.
- [82]. Jiang-Jiang Wang, You-Yin Jing, Chun-Fa Zhang, Guo-Hua Shi, Xu-Tao Zhang. A fuzzy multi-criteria decision-making model for tri-generation system. *Energy Policy Journal*, vol. 36, 2008, pp. 3823–3832.
- [83]. Jiang-Jiang Wang, You-Yin Jing, Chun-Fa Zhang, Xu-Tao Zhang, Guo-Hua Shi. Integrated evaluation of distributed triple-generation systems using improved grey incidence approach. *Energy Journal*, vol. 33, 2008, pp. 1427– 1437.
- [84]. P.A. Pilavachi, C.P. Roumpeas, S. Minett, N.H. Afgan. Multi-criteria evaluation for CHP system options. *Energy Conversion and Management Journal*, vol. 47, 2006, pp. 3519–3529.
- [85]. M. Beccali, M. Cellura, M. Ristretta. Decision-making in energy planning. Application of the Electre method at regional level for the diffusion of renewable energy technology. *Renewable Energy Journal*, vol. 28, 2003, pp. 2063–2087.
- [86]. Haris Ch. Doukas, Botsikas M. Andreas, John E. Psarras. Multi-criteria decision aid for the formulation of sustainable technological energy priorities using linguistic variables. *European Journal of Operational Research*, vol. 182, 2007, pp. 844–855.
- [87]. D.A. Haralambopoulos, H. Polatidis. Renewable energy projects: structuring a multi-criteria group decision-making framework. *Renewable Energy Journal*, vol. 28, 2003, pp. 961–973.

- [88]. Fajik Begic, Naim H. Afgan. Sustainability Assessment Tool for the Decision Making in Selection of Energy System—Bosnian case. *Energy Journal*, vol. 32, 2007, pp. 1979–1985.
- [89]. Timothy J. Ross. *Fuzzy Logic with Engineering Applications*. 2nd edition, 2004, John Wiley & Sons, Inc.
- [90]. F. Chevré, F. Guély. Cahier technique no 191: Fuzzy logic. 1998, Groupe Schneider. Available at: <http://mt.schneider-electric.be/Main/CT/ct191UK.pdf>, access date: 10/09/2012.
- [91]. A. Kornelakis E. Koutroulis. Methodology for the design optimization and the economic analysis of grid-connected photovoltaic systems. *IET Renewable Power Generation journal*, 2009, Vol. 3, pp. 476–492.
- [92]. The National Academies Press. *Environmental Impacts of Wind-Energy Projects*. 2007. Available at: [http://www.nap.edu/catalog.php?record\\_id=11935](http://www.nap.edu/catalog.php?record_id=11935).
- [93]. Danish Wind Industry Association. *Guided tour on Wind energy*. 2002. Available at: <http://www.heliosat3.de/e-learning/wind-energy/windpowr.pdf>.